European Journal of Taxonomy 835: 1–97
https://doi.org/10.5852/ejt.2022.835.1909
ISSN 2118-9773
www.europeanjournaloftaxonomy.eu
2022 · von Groll E. & Lopes-Andrade C.

Monograph

urn:lsid:zoobank.org:pub:8B8432B1-C714-4179-8687-66902F4CBF53

Contributions to the taxonomy of Neotropical *Cyparium* Erichson (Coleoptera: Staphylinidae: Scaphidiinae), with the description of five new species

Elisa VON GROLL [1,*] & Cristiano LOPES-ANDRADE [2]

[1,2] Programa de Pós-Graduação em Biologia Animal, Universidade Federal de Viçosa, Av. Peter Henry Rolfs, s/n, 36570-900, Viçosa, MG, Brasil.
[1,2] Laboratório de Sistemática e Biologia de Coleoptera, Departamento de Biologia Animal, Universidade Federal de Viçosa, Av. Peter Henry Rolfs, s/n, 36570-900, Viçosa, MG, Brasil.

*Corresponding author: elisavgroll@gmail.com
[2] Email: ciidae@gmail.com

[1] urn:lsid:zoobank.org:author:DC564233-82A9-4939-8B7A-F02C994BBA29
[2] urn:lsid:zoobank.org:author:525ABCB9-3334-407E-9084-F0784968D290

Abstract. The genus *Cyparium* Erichson, 1845 (Staphylinidae, Scaphidiinae, Cypariini) comprises 55 species, distributed mainly in the Neotropical and Oriental regions. Twenty-four species are known from the Neotropical region, but only eight species are reported from Brazil. In this paper we describe five new species and redescribe two species of Brazilian *Cyparium*, as follows: *Cyparium achardi* sp. nov., *C. lescheni* sp. nov., *C. loebli* sp. nov., *C. newtoni* sp. nov., *C. pici* sp. nov.; *Cyparium collare* Pic, 1920; and *Cyparium oberthueri* Pic, 1956. We provide images of adult males and females and their dissected parts, and information on host fungi whenever available. We also provide a comparative plate of dorsal colour patterns of Neotropical *Cyparium*.

Keywords. Insects, morphology, shining fungus beetles, Brazil, records.

von Groll E. & Lopes-Andrade C. 2022. Contributions to the taxonomy of Neotropical *Cyparium* Erichson (Coleoptera: Staphylinidae: Scaphidiinae), with the description of five new species. *European Journal of Taxonomy* 835: 1–97. https://doi.org/10.5852/ejt.2022.835.1909

Introduction

The shining fungus beetles (Coleoptera: Staphylinidae: Scaphidiinae Latreille, 1806) include over 1800 species and subspecies in 46 genera and four tribes: Cypariini Achard, 1924, Scaphiini Achard, 1924, Scaphidiini Latreille, 1806, and Scaphisomatini Casey, 1893 (Löbl 2018a). They are small beetles (≈ 0.84–14.0 mm long) (Tang *et al.* 2014; Löbl & Ogawa 2016), distributed worldwide, diverse and abundant in most terrestrial ecosystems, especially subtropical and tropical forests (Leschen & Löbl 1995). They are usually collected on fungi, slime moulds, by sifting litter or using flight intercept traps (Lawrence & Newton 1980; Newton 1984; Leschen 1994; Stephenson *et al.* 1994; Löbl & Leschen 2003; Tang *et al.* 2014; Löbl 2018a; Löbl *et al.* 2021).

The genus *Cyparium* Erichson, 1845 (Staphylinidae, Scaphidiinae, Cypariini), the only genus of Cypariini, comprises 55 species, distributed mainly in the Neotropical and Oriental regions (Leschen & Löbl 1995; Löbl 2018a). It is absent from oceanic islands, northern Africa, Australia, Europe, Madagascar, New Guinea and Chile (Leschen & Löbl 1995). Twenty-four species are known from the Neotropical region, but only eight species are reported from Brazil, as follows: *C. collare* Pic, 1920; *C. ferrugineum* Pic, 1920; *C. grilloi* Pic, 1920; *C. grouvellei* Pic, 1920; *C. oberthueri* Pic, 1956; *C. pygidiale* Achard, 1922; *C. ruficolle* Achard, 1922; and *C. rufohumerale* Pic, 1931.

Species of *Cyparium* are easily distinguished from other scaphidiines by their robust body, non-emarginate eyes, compact antennal club with only slightly flattened antennomeres, pronotum widest posteriorly, and spinose pro- and mesotibiae (Leschen & Löbl 1995; Newton *et al.* 2001). They are usually found in basidiomes of Agaricales Underw., 1899 (Newton 1984; Kompantsev & Pototskaya 1987), but there are also records from coral fungi (Clavaraceae (Chevall., 1826)) and tooth fungi (Hydnaceae Chevall., 1826) (Newton 1984; Leschen & Löbl 1995). As feeders on ephemeral gilled mushrooms, it is expected that *Cyparium* beetles will have a faster development than other scaphidiines (Ashe 1984).

The number of described Neotropical species of *Cyparium* is quite low, considering that they are probably easy to collect using SNV-FITs traps (Löbl *et al.* 2021) or manually (von Groll *et al.* 2021), and that the region has a vast territory and heterogeneity of tropical and subtropical terrestrial ecosystems. This low number may be due to actual low diversity, or a result of the few studies on the Neotropical Scaphidiinae. The second alternative is the most likely, considering that the faunas of some tropical and subtropical areas are virtually undescribed (Leschen & Löbl 1995), and that von Groll *et al.* (2021) were able to collect ten morphospecies and 192 individuals of *Cyparium* with low collection effort in two small forest remnants of the Brazilian Atlantic biome.

In the first detailed phylogenetic study including *Cyparium*, eight species from the Nearctic, Asian, Palearctic and Neotropical regions were examined (Leschen & Löbl 1995). *Cyparium* was recovered as monophyletic, supported by the prosternum in front of the procoxae reduced to a length less than that of the procoxa, the width of the mesoventral process more than that of the metacoxal process, abdominal sternite VIII with anteriorly projecting process, and the gonostyli long (Leschen & Löbl 1995). However, the position of Cypariini within Scaphidiinae was not well resolved. Sometimes it was placed as sister group of the remaining Scaphidiinae, or it formed a clade with Scaphiini Achard, 1924. They concluded that more data (from larvae and adults, based on better preserved specimens) were necessary to improve the results. Subsequent studies have faced the same problems. Grebennikov & Newton (2012), which included larvae and a member of Scaphiini, recovered *Cyparium* as sister to the remaining Scaphidiinae. On the other hand, McKenna *et al.* (2014) recovered *Cyparium* as the sister group of *Scaphidium* Olivier, 1790 (Scaphidiini), and them together as the sister group of *Scaphium* Kirby, 1837 (Scaphiini). When studying the phylogeny of Scaphisomatini (Scaphidiinae, Staphylinidae), Leschen & Löbl (2005) included both sexes of *Cyparium flavipes* LeConte, 1860 (synonym of *Cyparium concolor* (Fabricius, 1801)) as the outgroup. Their matrix included 110 characters and provided detailed information on the internal and external morphology of males and females of this genus.

Some of the original descriptions are remarkably complete (e.g., *Cyparium navarretei* Fierros-López, 2002), but most of them are too general and lack information necessary for accurate identifications (e.g., *C. nigronotatum* Pic, 1931 and *C. collare*), which can cause difficulties when studying these beetles, especially because it is not always easy to access type material (Löbl 2020). Regarding morphology, important contributions on coloration (Márquez 2007) and female terminalia (Ogawa & Sakai 2011) were made. Nonetheless, by studying specimens of *Cyparium*, we noticed that there are more structures to explore.

In this work we describe five new species of *Cyparium* and redescribe *C. collare* and *C. oberthueri*, all occurring in Brazil. We provide detailed morphological descriptions of adult males and females, including images of dissected structures, and host fungi data whenever possible. We also provide a comparative plate of dorsal colour patterns of Neotropical *Cyparium*.

Material and methods

Specimens collected in "Viçosa" were found at two Atlantic Forest remnants in Viçosa, state of Minas Gerais, Southeast Brazil: "Mata da Biologia" (20°45′32″ S, 42°51′49″ W), with 75 hectares and located within the campus of the Federal University of Viçosa; and "Estação de Pesquisa, Treinamento e Educação Ambiental Mata do Paraíso" (20°48′05″ S, 42°51′58″ W), with 194 hectares and located about 4 km south of the campus, but under the care of the university.

Specimens collected in 2019 followed the manual colleting method of von Groll *et al.* (2021). Fungi were photographed with a smartphone or a Nikon D810 camera, kept in a paper bag and dehydrated in a dry heat sterilizer. Beetles were kept in a freezer for a few hours and then mounted using double mounting.

For the dissections, beetles were boiled in water to soften the tissues. Then the larger parts were separated and boiled in saturated KOH solution for maceration of the tissues and cleaning. Then they were immersed in 10% acetic acid for a few minutes to neutralize any remaining KOH, and finally cleaned in water. More delicate structures were dissected after this process.

The structures were observed in glycerin and photographed in KY®. Male aedeagui were passed through a battery concentration until they were immersed in KY®: alcohol 40%, 70%, 80%; glycerin 40%, 70%, 100%; otherwise, the structure was crushed by the pressure of the 100% glycerin or KY®. Permanent slide preparations of hind wings were made using PVLG (polyvinyl alcohol-lactic acid-glycerol) (Omar *et al*. 1979). Photographs were taken using a Zeiss Discovery V20 stereo microscope equipped with a Zeiss AxioCam 506, a Zeiss AxioLab compound microscope equipped with a Zeiss AxioCam MRc or a Canon EOS 1000D digital camera; all photos were taken using the technique of focus-staking.

Antennomere measurements were taken using editing software. Body measurements were taken under a Zeiss Stemi 2000C stereo microscope equipped with a 2× objective lens and an ocular micrometer. Range, mean and standard deviation values were estimated using PAST. The following abbreviations are used for measurements (in mm):

EH = elytral height in lateral view (Fig. 1C)
EI = length of the inner margins of elytra; not including the scutellar shield (Fig. 1A)
EL = elytral length at the midline (Fig. 1A)
EW = greatest right elytron width (Fig. 1A)
HW = maximum width of the head including eyes (Fig. 1D)
IS = interocular space (Fig. 1D)
MB = mesothorax length between fore and middle legs (Fig. 1B)
MC = mesothorax length at the midline (Fig. 1B)
PA = pronotal width at the anterior margin (Fig. 1A)
PB = pronotal width at the posterior margin (Fig. 1A)
PL = pronotal length along the midline (Fig. 1A)
SL = scutellar shield length (Fig. 1A)
SW = scutellar shield width (Fig. 1A)
TL = total body length, not including head and abdomen (Fig. 1A)
VL = length of ventrite 1 in the midline (Fig. 1B)
WA = width between antennae (Fig. 1D)

To see if elytra were wider than long the following comparison was performed: EW*2 vs EL.

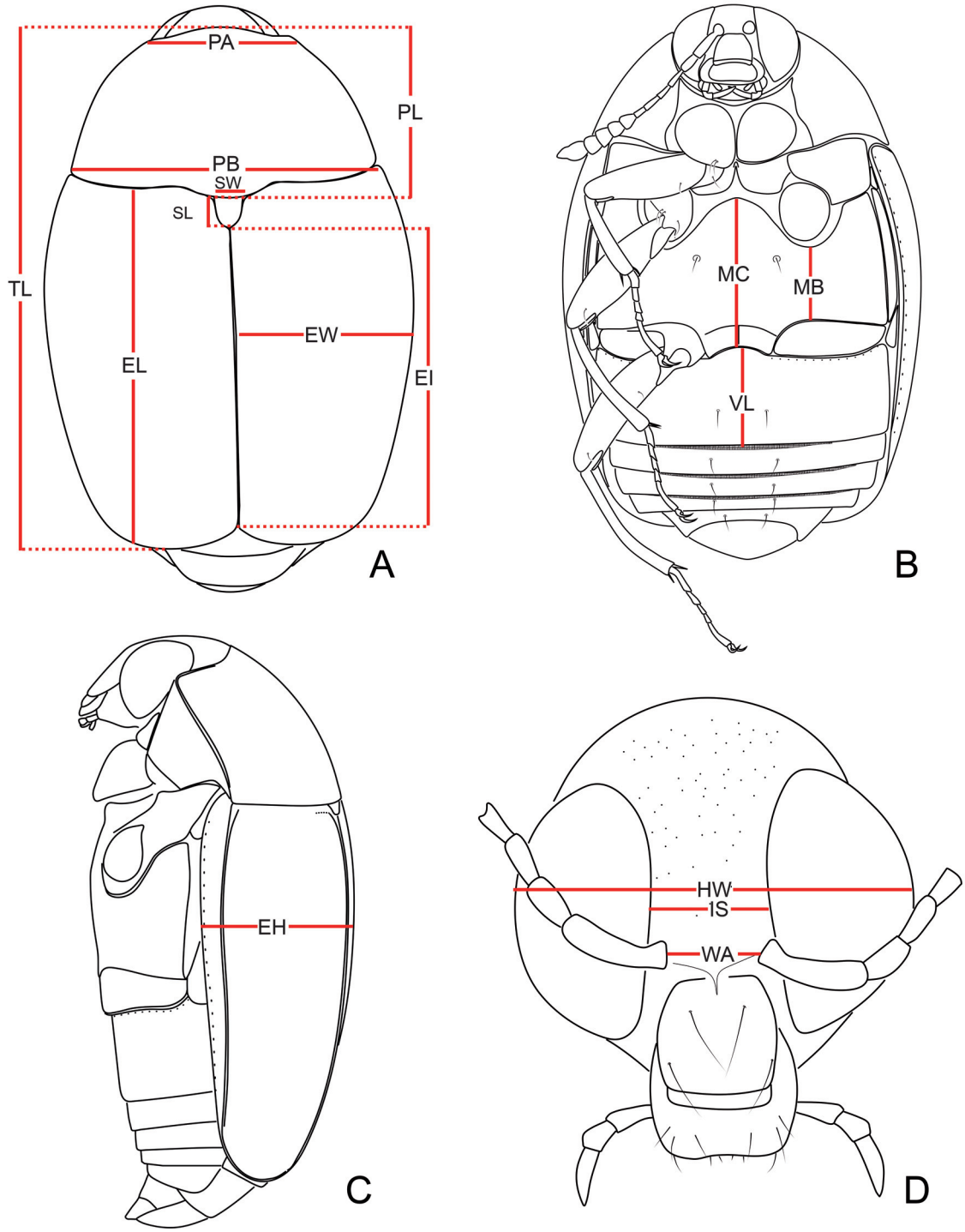

Fig. 1. *Cyparium collare* Pic, 1920. Measurements taken. **A**. Dorsal view. **B**. Ventral view. **C**. Lateral view. **D**. Head in frontal view. Abbreviations: EH = elytral height in lateral view; EI = length of the inner margins of elytra, not including the scutellar shield; EL = elytral length in the midline; EW = greatest right elytron width; HW = maximum width of the head including eyes; IS = interocular space; MB = mesothorax length between fore and middle legs; MC = mesothorax length in the midline; PA = pronotal width at the anterior margin; PB = pronotal width at the posterior margin; PL = pronotal length along the midline; SL = scutellar shield length; SW = scutellar shield width; TL = total body length, not including head and abdomen; VL = length of ventrite 1 in the midline; WA = width between antennae.

Unless otherwise specified, each description was based on the respective male holotype; descriptions of dissected parts were based on paratypes. Terminology follows Ogawa & Löbl (2013) for external morphology, and male and female terminalia; Naomi (1988a, 1988b), Leschen *et al*. (1990), Leschen & Löbl (2005) and Lawrence & Ślipiński (2013) for external morphology; Harris (1979) for microsculpture; Jałoszyński (2012) for the internal structure of the prothorax; Friedrich & Beutel (2006) for the mesonotum; Lawrence *et al.* (2021) for the hind wing venation; Crowson (1938), Naomi (1989a) and Hübler & Klass (2013) for the metendosternite; Naomi (1989b) for the abdominal segments; Naomi (1990) for male terminalia (Figs 2–3). Not all structures of scaphidiine metendosternites are well illustrated; therefore, at this moment, we adopted the term 'stalk ridge' for the suture present on the stalk

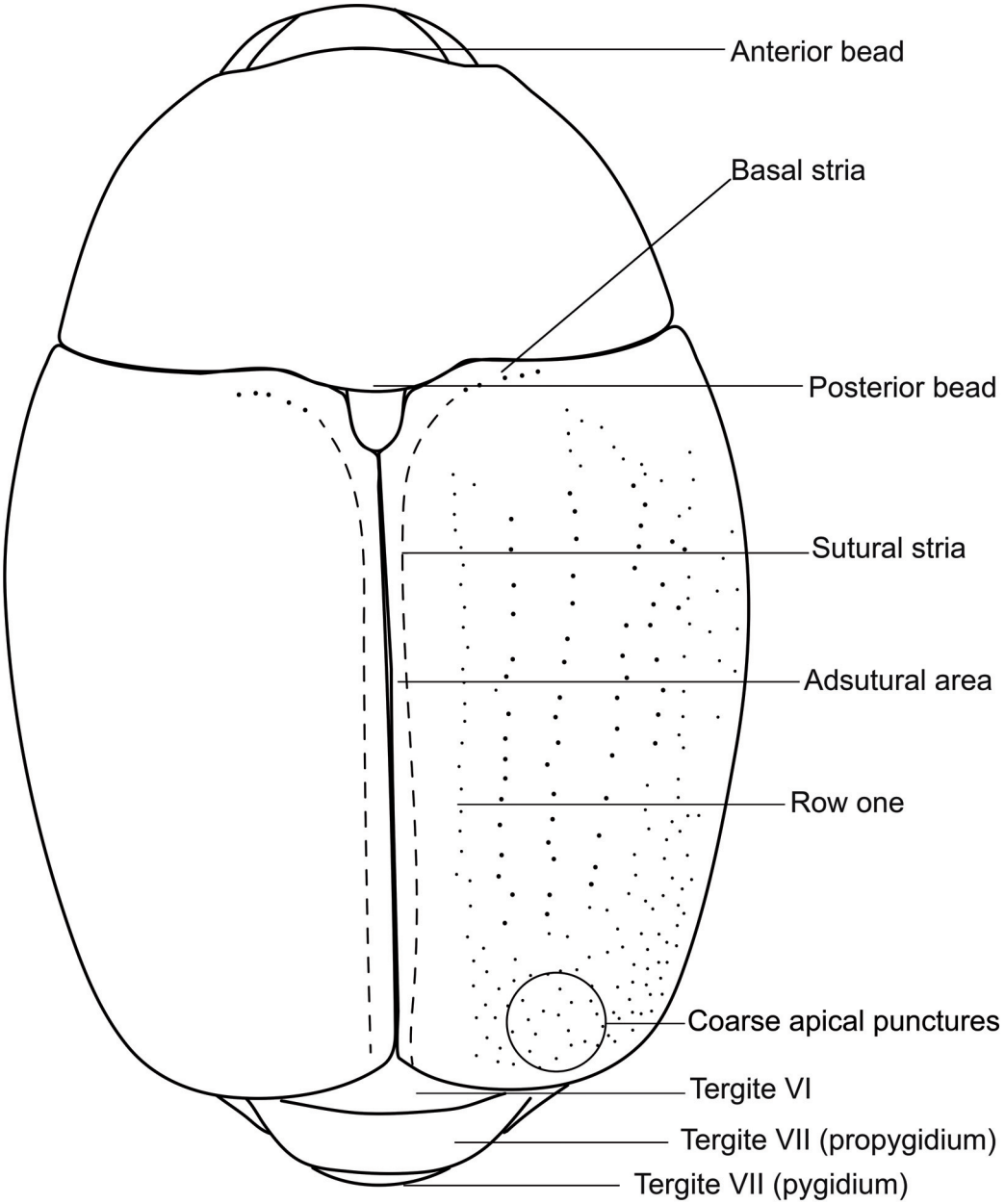

Fig. 2. Dorsal terminology. Model: *Cyparium collare* Pic, 1920.

(Fig. 10A). We call the parameral view of median lobe as 'ventral view' and the opposite view of it as 'dorsal view' even though the median lobe stays somewhat turned to the side when it is at rest.

Unless otherwise specified in the text (between square brackets), labels are printed on white paper. Each label is separated by a backslash. The number and gender of specimens bearing these labels are stated immediately before the label data.

Due to restrictions for loaning historical or type specimens to Brazilian researchers by a few museums, to the increasing Brazilian bureaucracy, risks for receiving and sending museum specimens, and high costs for visiting foreign museums, it was not possible to examine type series and historical

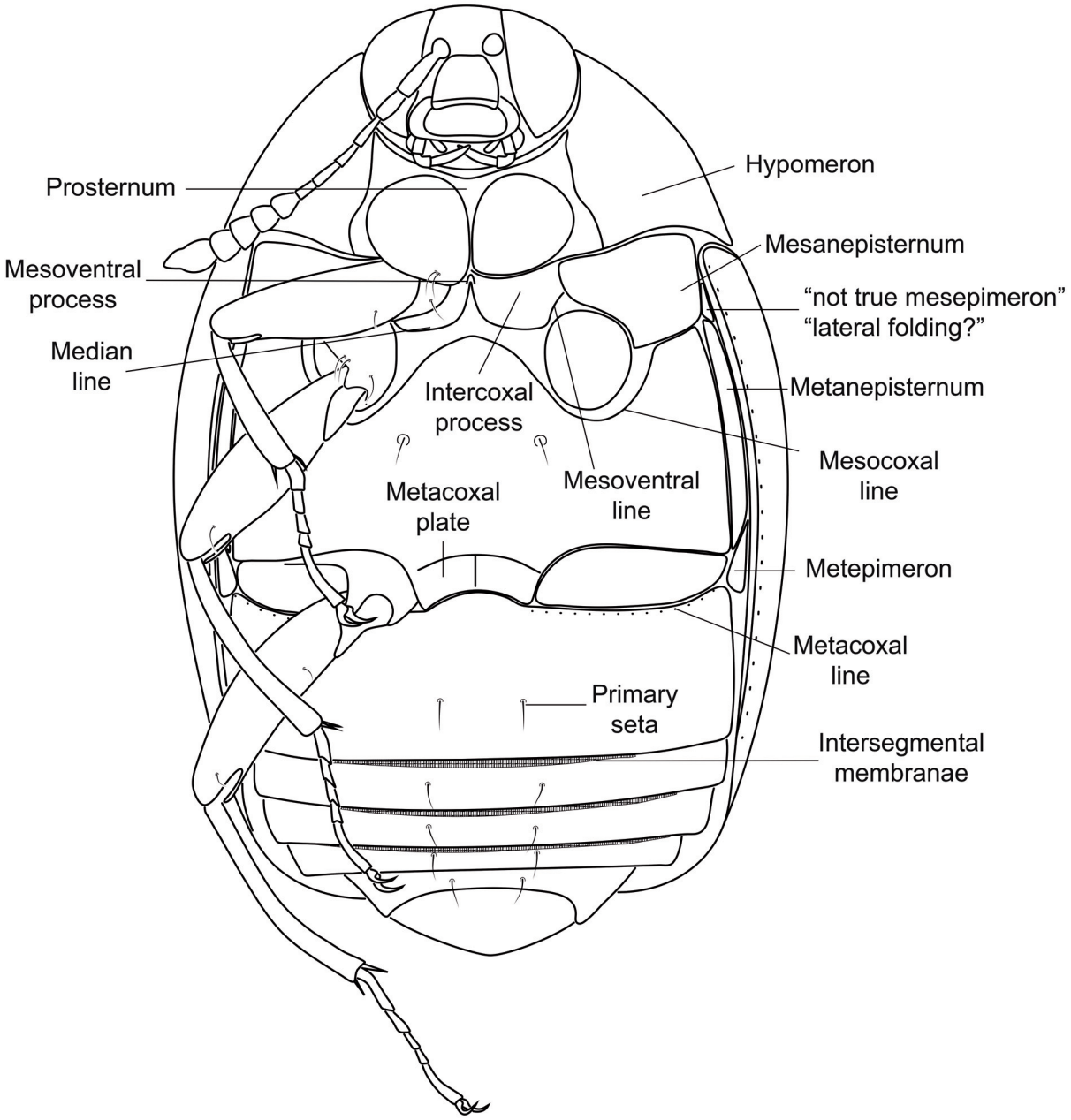

Fig. 3. Ventral terminology. Model: *Cyparium collare* Pic, 1920.

material of previously described species. Therefore, comparisons with previously described species and identification of specimens were made by consulting original descriptions, and by examining photographs kindly provided by the staff of the MNHN (Muséum national d'histoire naturelle, Paris) and the NMCZ (Natural History Museum, Prague).

Illustrations of the Neotropical species of *Cyparium* (Figs 4–5) were made using colour and length information extracted from the original descriptions, and the available photographs of type specimens (Fig. 6). Since the purpose was only to show the colour and length patterns, the shape does not represent the species. Species illustrations are displayed in alphabetical order and in proportional size (considering the anterior margin of the pronotum to elytral apex).

Supplementary material includes labels of the holotypes of the new species (Supp. file 1); figures of female terminalia of *C. lescheni* sp. nov. and *C. collare* (Supp. file 2B); and photos of habitus and male terminalia of *C. collare* from two different localities (Supp. file 3 (Figs 1A–4H)).

Acronyms of scientific collections:

CAMB = Coleção Ayr de Moura Bello, Rio de Janeiro, RJ, Brazil
CELC = Coleção Entomológica do Laboratório de Sistemática e Biologia de Coleoptera da UFV, Viçosa, MG, Brazil
CEMT = Seção de Entomologia da Coleção Zoológica, Departamento de Biologia e Zoologia, Instituto de Biociências, Universidade Federal de Mato Grosso, Cuiabá, MT, Brazil
CERPE = Coleção Entomológica da Universidade Federal Rural de Pernambuco, Recife, PE, Brazil
CZUG = Centro de Estudios Zoología, Universidad de Guadalajara, Jalisco, Mexico
FZCH = Fernando de Zayas Collection, Habana, Cuba
MCNZ = Museu de Ciências Naturais, Secretaria do Meio Ambiente e Infraestrutura, Porto Alegre, RS, Brazil
MCSN = Museo Civico di Storia Naturale, Genova, Italy
MNHN = Muséum national d'histoire naturelle, Paris, France
NHML = The Natural History Museum, London, UK (former British Museum (Natural History))
NMPC = Národní Muzeum, Entomologické oddělení, Praha, Czech Republic
SNSD = Senckenberg Naturhistorische Sammlungen Dresden, Dresden, Germany
ZMUB = Zoologisches Museum, Museum für Naturkunde, Berlin, Germany

As the diversity of Neotropical *Cyparium* is certainly much higher than we could access at this moment, providing a key to the described Brazilian or Neotropical species would not be useful here. Moreover, we have examined only photos of some species, which do not provide enough information for including them in an identification key.

Results

Catalogue of Neotropical species

The Neotropical *Cyparium* are barely studied and the species may have a much broader geographic distribution than currently known. At this moment we shall consider the possibility that any of the previously described Neotropical *Cyparium* may occur in Brazil. Because of this, and as a support for subsequent works, below we list all Neotropical *Cyparium* species and subspecies, based mostly on Löbl (2018a). In Figs 4–5 we provide a comparative plate of their dorsal colour patterns.

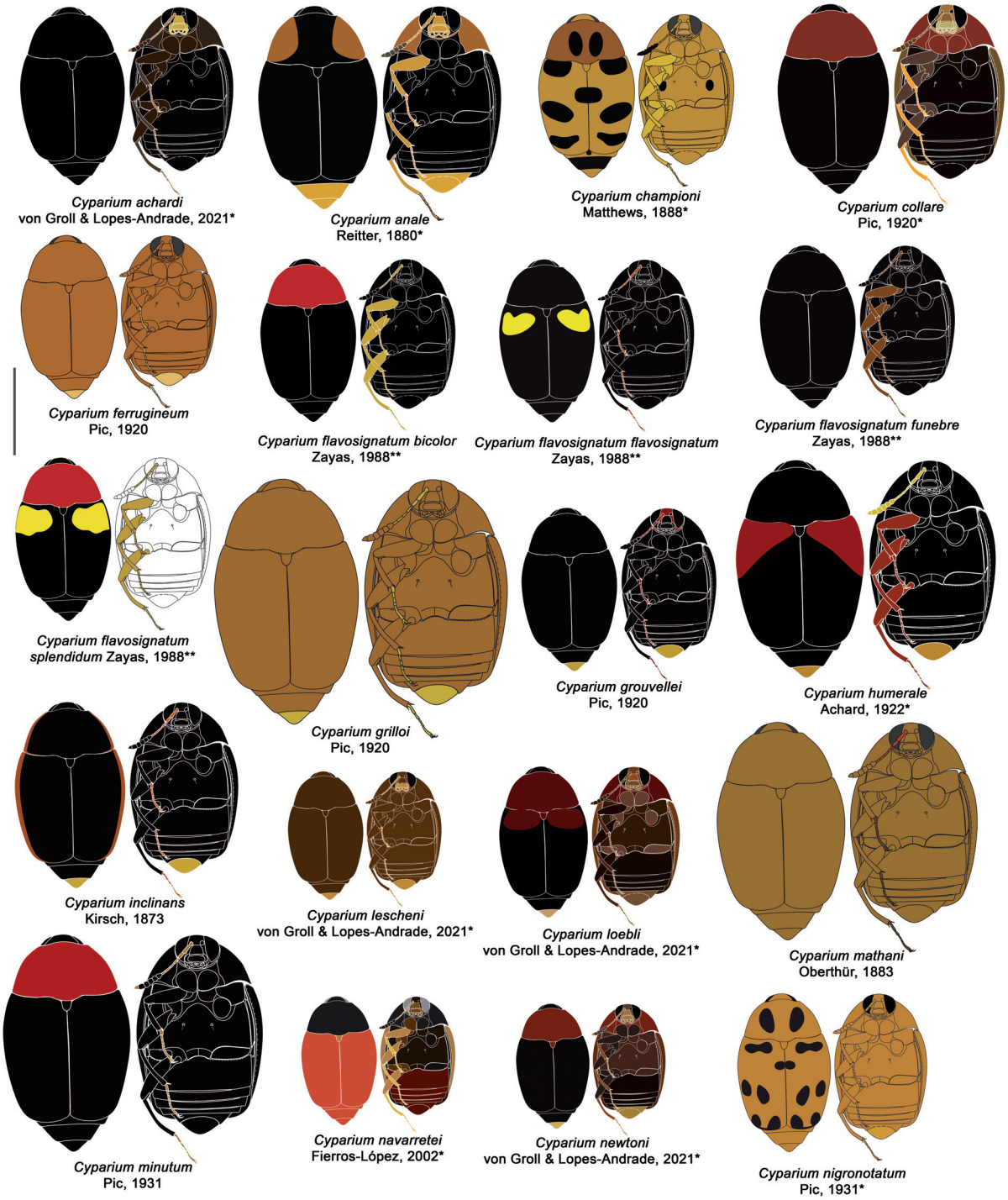

Fig. 4. *Cyparium* Erichson, 1845. Neotropical species. Illustrations based on the original descriptions. *Illustrations made based on photographs, specimens, or illustrations made by other authors; **size not provided in original description. Model: *Cyparium collare* Pic, 1920. Scale bar = 2 mm.

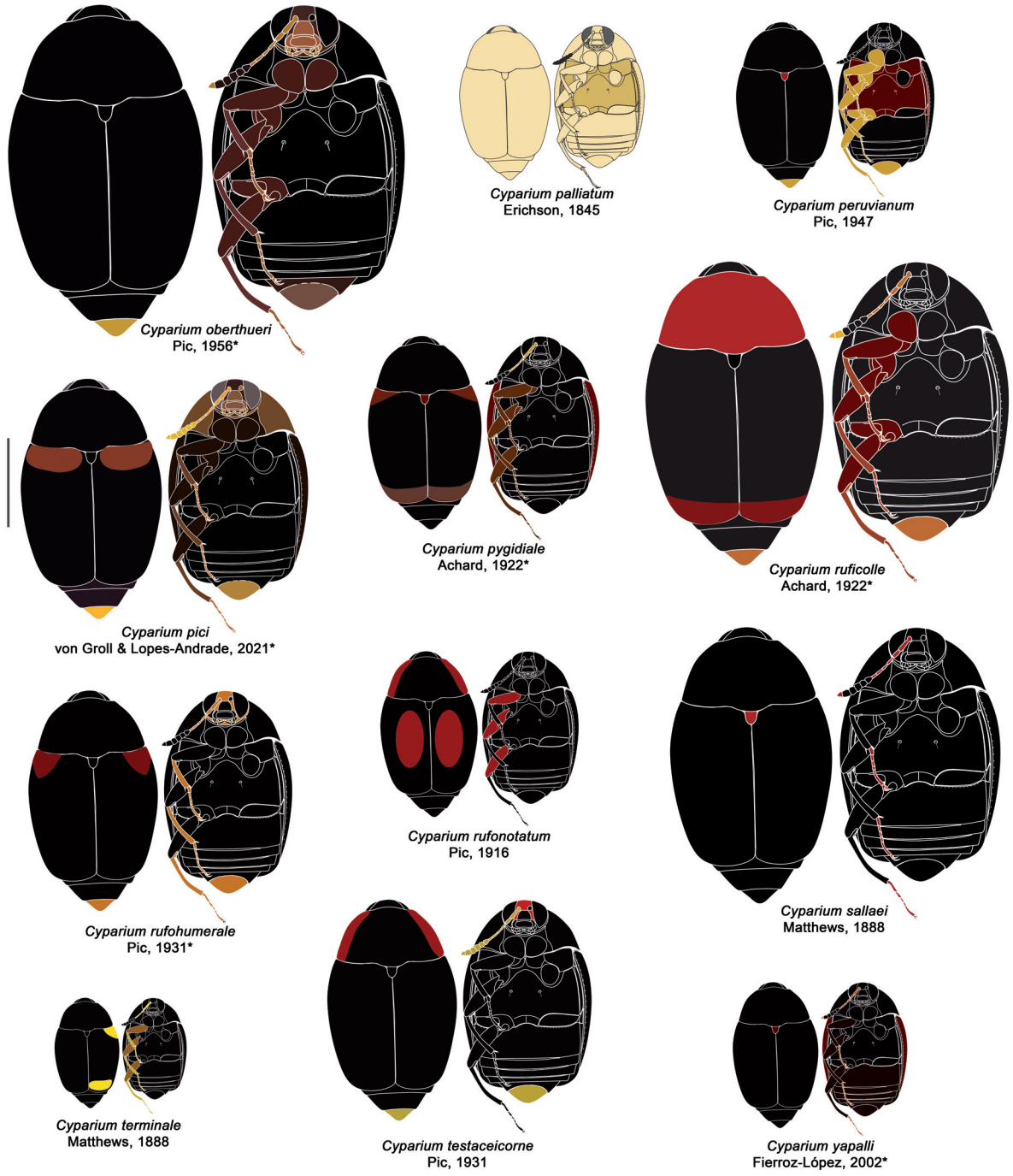

Fig. 5. *Cyparium* Erichson, 1845. Neotropical species. Illustrations based on the original descriptions. *Illustrations made based on photographs, specimens, or illustrations made by other authors. Model: *Cyparium collare* Pic, 1920. Scale bar = 2 mm.

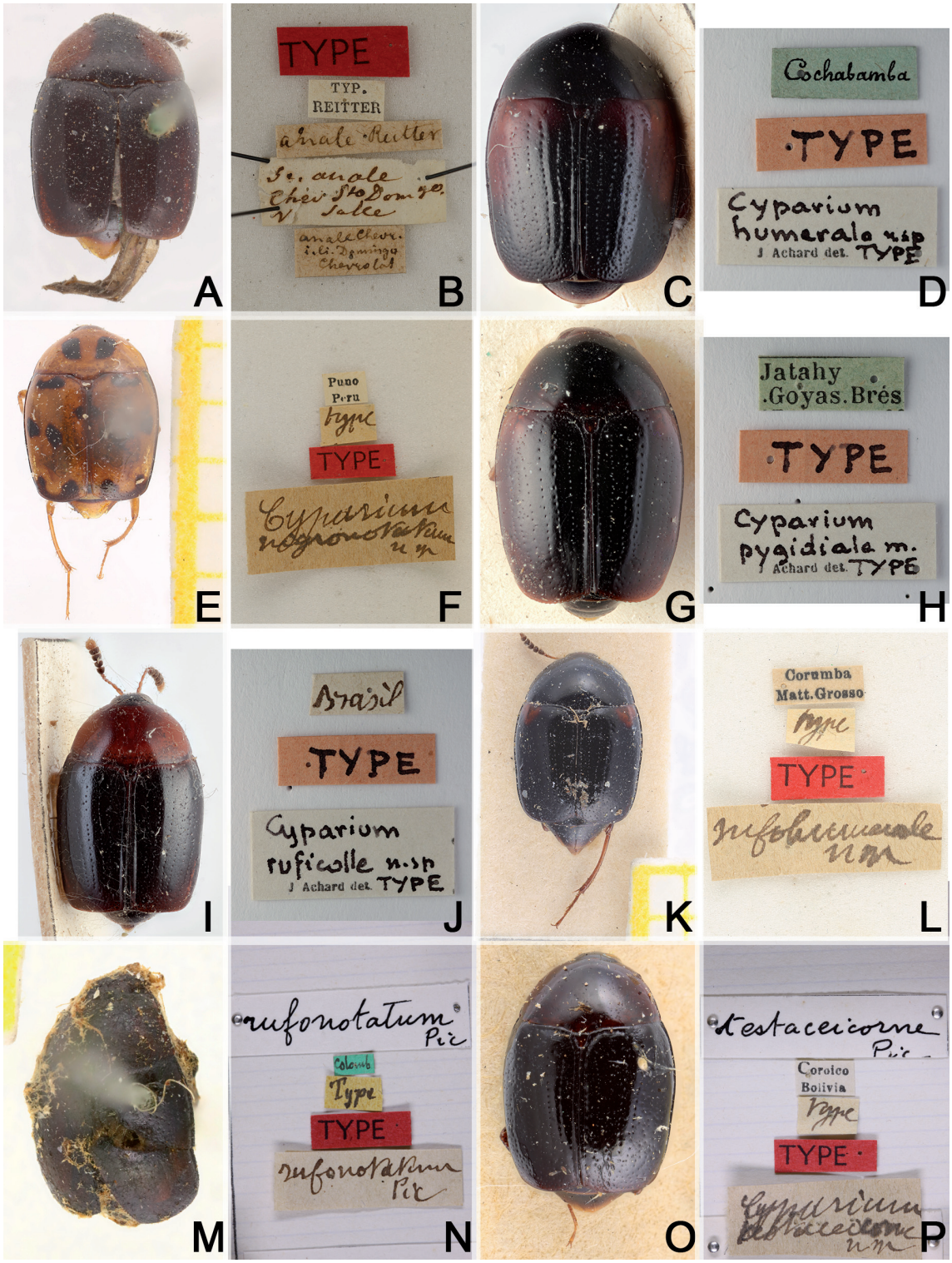

Fig. 6. Syntypes. **A–B**. *Cyparium anale* Reitter, 1880 (MNHN). **A**. Habitus. **B**. Labels. **C–D**. *C. humerale* Achard, 1992 (NMPC). **C**. Habitus. **D**. Labels. **E–F**. *C. nigronotatum* Pic, 1931 (MNHN). **E**. Habitus. **F**. Labels. **G–H**. *C. pygidiale* Achard, 1922 (NMPC collection-Prague). **G**. Habitus. **H**. Labels. **I–J**. *C. ruficolle* Achard, 1922 (NMPC). **I**. Habitus. **J**. Labels. **K–L**. *C. rufohumerale* Pic, 1931 (MNHN). **K**. Habitus. **L**. Labels. **M–N**. *C. rufonotatum* Pic, 1916 (MNHN). **M**. Habitus. **N**. Labels. **O–P**. *C. testaceicorne* Pic, 1931 (MNHN). **O**. Habitus. **P**. Labels.

Class Insecta Linnaeus, 1758
Order Coleoptera Linnaeus, 1758
Family Staphylinidae Latreille, 1802
Subfamily Scaphidiinae Latreille, 1806
Tribe Cypariini Achard, 1924
Genus *Cyparium* Erichson, 1845

Cyparium anale Reitter, 1880
Figs 4, 6A–B

Cyparium anale Reitter, 1880: 42. Syntypes, MNHN; type locality: St. Domingo.
Cyparium submetallicum Reitter, 1880: 43. Syntypes, MNHN; type locality: "India or.?". [syn.].

Cyparium anale – Achard, 1921: 86 (synonymy of *C. submetallicum* with *C. anale*).

Distribution

Dominican Republic.

Cyparium championi Matthews, 1888
Fig. 4

Cyparium championi Matthews, 1888: 167, pl. 4 fig. 9. Holotype, NHML; type locality: Panama: Bugaba.

Distribution

Bolivia; Costa Rica; Ecuador; Nicaragua; Panama; Suriname.

Cyparium collare Pic, 1920
Figs 4, 47–55, Supp. file 2B, Supp. file 3 (Figs 1A–4H)

Cyparium collare Pic, 1920a: 4. Syntypes, MNHN; type localities: "Brésil" [Matu Sinhos, Minas; Matto Grosso; Pery-Pery, Pernambuco; right bank of Parahyba].

Distribution

Brazil.

Cyparium ferrugineum Pic, 1920
Fig. 4

Cyparium ferrugineum Pic, 1920a: 5. Syntypes, MNHN; type locality: Brazil [Pery-Pery, Pernambuco, Matto Grosso].

Distribution

Brazil.

Cyparium flavosignatum Zayas, 1988
Cyparium flavosignatum flavosignatum Zayas, 1988
Fig. 4

Cyparium flavosignata Zayas, 1988: 23, fig. 13. Syntypes, FZCH; type locality: Cuba.

Distribution

Cuba.

Cyparium flavosignatum bicolor Zayas, 1988
Fig. 4

Cyparium flavosignata bicolor Zayas, 1988: 24, fig. 15. Syntypes, FZCH; type locality: Cuba.

Distribution

Cuba.

Cyparium flavosignatum funebre Zayas, 1988
Fig. 4

Cyparium flavosignata funebris Zayas, 1988: 24, fig. 14. Syntypes, FZCH; type locality: Cuba.

Distribution

Cuba.

Cyparium flavosignatum splendidum Zayas, 1988
Fig. 4

Cyparium flavosignata splendidum Zayas, 1988: 25, fig. 16. Syntypes, FZCH; type locality: Cuba.

Distribution

Cuba.

Cyparium grilloi Pic, 1920
Fig. 4

Cyparium grilloi Pic, 1920b: 94. Syntypes, MCSN; type locality: Brazil: Paranà, Palmeira.

Distribution

Brazil.

Cyparium grouvellei Pic, 1920
Fig. 4

Cyparium grouvellei Pic, 1920a: 5. Syntypes, MNHN; type locality: Brazil.

Distribution

Brazil.

Cyparium humerale Achard, 1922
Figs 4, 6C–D

Cyparium humerale Achard, 1922: 40. Syntypes, NMPC; type locality: Bolivia: Cochabamba.

Distribution

Bolivia.

Cyparium inclinans Kirsch, 1873
Fig. 4

Cyparium inclinans Kirsch, 1873: 135. Syntypes, SNSD; type locality: Peru.

Distribution

Peru.

Cyparium mathani Oberthür, 1883
Fig. 4

Cyparium mathani Oberthür, 1883: 12. Syntypes, MNHN; type localities: Peru: Iquitos and Amazones.

Distribution

Peru.

Cyparium minutum Pic, 1931
Fig. 4

Cyparium minutum Pic, 1931: 2. Syntypes, MNHN; type locality: Jamaica: Jackson Town.

Distribution

Jamaica.

Cyparium navarretei Fierros-López, 2002
Fig. 4

Cyparium navarretei Fierros-López, 2002: 8, figs 1, 3–5. Holotype male, CZUG; type locality: Mexico: Veracruz, Cerro Acatlán, Naolinco.

Distribution

Mexico.

Cyparium nigronotatum Pic, 1931
Figs 4, 6E–F

Cyparium nigronotatum Pic, 1931: 2. Syntypes, MNHN; type locality: Peru: [Puno].

Distribution

Peru.

Cyparium oberthueri Pic, 1856
Fig. 5, 56–64

Cyparium oberthüri Pic, 1956: 175. Syntypes, MNHN; type locality: Brazil: Matto Grosso.

Distribution

Brazil.

Cyparium palliatum Erichson, 1845
Fig. 5

Cyparium palliatum Erichson, 1845: 4. Syntypes ZMUB [single female, labelled as holotype]; type locality: Mexico.

Distribution

Mexico.

Cyparium peruvianum Pic, 1947
Fig. 5

Cyparium peruvianum Pic, 1947: 7. Syntypes, MNHN; type locality: Peru.

Distribution

Peru.

Cyparium pygidiale Achard, 1922
Figs 4, 6G–H

Cyparium pygidiale Achard, 1922: 40. Syntypes, NMPC; type localities: Brazil: Goyaz, Jatahy.

Distribution

Brazil.

Cyparium ruficolle Achard, 1922
Figs 4, 6I–J

Cyparium ruficolle Achard, 1922: 39. Syntypes, NMPC; type locality: Brazil [Corumba, Matto Grosso].

Distribution

Brazil.

Cyparium rufohumerale Pic, 1931
Figs 4, 6K–L

Cyparium rufohumerale Pic, 1931: 2. Syntypes, MNHN; type locality: Brazil.

Distribution

Brazil.

Cyparium rufonotatum Pic, 1916
Figs 5, 6M–N

Cyparium rufonotatum Pic, 1916: 18. Holotype, MNHN; type locality: Colombia.

Distribution

Colombia.

Cyparium sallaei Matthews, 1888
Fig. 5

Cyparium sallaei Matthews, 1888: 166, pl. 4 fig. 10. Syntypes, NHML; type locality: Mexico: Cordoba.

Distribution

Mexico.

Cyparium terminale Matthews, 1888
Fig. 5

Cyparium terminale Matthews, 1888: 167, pl. 4 fig. 9. Syntypes, NHML; type localities: Mexico: Jalapa, Cordoba; Guatemala, Zapote, Capetillo, San Juan in Vera Paz; Panama, Bugaba.

Distribution

Guatemala; Mexico; Panama.

Cyparium testaceicorne Pic, 1931
Figs 5, 6O–P

Cyparium testaceicorne Pic, 1931: 2. Syntypes, MNHN; type locality: Bolivia: [Coroico].

Distribution

Bolivia.

Remarks

We received photos of the dorsal view and labels of the type (MNHN), but the specimen shown in the photos does not match the original description. The pronotum of this specimen is entirely reddish brown and 3 mm long, while in the description Pic (1931) wrote "capite antice et thorace lateraliter rufis (…) Long. 4 mill. (…) Voisin de anale Reitt.". The specimen on the photo better fits the description of *C. collare*, by its coloration (pronotum reddish brown) and length of 3 mm. We could not locate the syntypes of *C. collare*. The illustration of *C. testaceicorne* (Fig. 5) provided here was based on the original description and not on the specimen shown in the available photos (Fig. 6O).

Cyparium yapalli Fierros-López, 2002
Fig. 5

Cyparium yapalli Fierros-López, 2002: 9, figs 2, 6–7, 9, 11. Holotype male, CZUG; type locality: Mexico: Oaxaca, Km 164 carr. Sola de Vega-Puerto Escondido.

Distribution

Mexico.

Descriptions of new species

Cyparium achardi sp. nov.
urn:lsid:zoobank.org:act:ABFE4E1F-DB31-46C1-BDC7-BDD1C4FF81E3
Figs 4, 7–13, 46; Supp. file 1A

Diagnosis

TL: 3.00–3.28 mm in males and 3.32–3.40 mm in females. Entirely black, with lateral areas of some ventral sclerites lighter (Fig. 7A–C). Eyes long (Fig. 7D). Hypomeron and metaventrite smooth. Metanepisternum and metepimeron with imbricate microsculpture. Tergite VIII of males coarsely punctate (Fig. 11D). Aedeagus strongly sclerotized (Fig. 12A–C); apex and parameres short (Fig. 12A). Distal gonocoxites of females straight and thick (Fig. 13C, E).

Etymology

In homage to the entomologist Julien Achard (1881–1925) for his significant contribution on the Neotropical Scaphidiinae.

Material examined

Holotype

BRAZIL • ♂; Minas Gerais, Viçosa, EPTEA Mata do Paraíso; 19 Nov. 2019; LabCol leg.; "Fungo 27 \\ Em *Leucoagaricus* sp. \\ *Cyparium achardi* von Groll & Lopes-Andrade HOLOTYPUS" [red paper]; CELC. (Supp. file1A).

Paratypes

BRAZIL • 3 ♂♂, 1 ♀ (1 ♂ entirely dissected, preserved in glycerin); same collection data as for holotype; "T. do Pesquisador"; 8 Nov. 2016; C. Lopes-Andrade *et al.* leg.; "\\ Em *Marasmiellus volvatus*"; CELC • 2 ♀♀ (1 ♀, abdomen dissected, preserved in glycerin); same collection data as for holotype; 14 Nov. 2019; "Fungo 22 \\ Em *Marasmiellus* sp."; CELC • 1 ♀; same collection data as for holotype; "Fungo 26 \\ Em *Hygrocybe* sp."; CELC • 1 ♂; same collection data as for holotype; "Fungo 28 \\ Em *Leucocoprinus ianthinus*"; CELC • 1 ♂; same collection data as for holotype; "Fungo 12 \\ Em *Marasmius haematocephalus*"; CELC • 1 ♀; same collection data as for holotype; 26 Nov. 2019; LabCol leg.; "Fungo 53 \\ Em *Leucocoprinus* sp."; CELC • 1 spec.; Viçosa, Recanto das Cigarras, Mata da Biol.; 20 Nov. 2019; LabCol leg; "Fungo 19 \\ Em *Leucocoprinus cepistipes*"; CELC.

All paratypes additionally labelled "*Cyparium achardi* von Groll & Lopes-Andrade PARATYPUS [yellow paper]".

Description

Measurements (holotype, in mm). TL 3.12, PL 1.31, PA 0.80, PB 1.90, EW 1.20, EL 2.17, IS 0.18, HW 0.80.

Coloration. Black; iridescent (Fig. 7A–C). Clypeus yellowish-brown; mouth parts yellowish (Fig. 7D); antennomeres I–VI and apical half of XI yellow; VII–X dark yellow (Fig. 7D–F). Hypomeron, epipleuron, and metepimeron brown to black, lighter laterally (Fig. 7B). Thorax and abdomen brown to black, lighter laterally (Fig. 7B). Coxae and femora light to chestnut brown, lighter posteriorly in some specimens; tibiae light to dark brown; tarsi yellow (Fig. 7B–C).

Head. Punctation dense, fine (Fig. 7D). Eyes tapered apically (Fig. 7D). Labrum transverse; lateral areas rounded, smoothly delimited apically; central margin slightly curved; sclerotized portion rounded with a row of short setae; lateral setae slightly exceeding margins of labrum; slightly porose centrally (Fig. 7G). Mandibles curved, subapical serrations on left mandible conspicuous (Fig. 7H–I). Maxillae with palpomere II thickened; galea and lacinia densely pubescent, narrow (Fig. 7J). Mentum with sides distinctly angulated, curved apically (Fig. 8A). Setae of labial palpomere II exceeding palpomere III; palpomere III thick, with long apical setae (Fig. 8A). Hypopharynx with sclerotized plate cup-shaped (Fig. 8A–B). Postgena with strigulate microsculpture; gular pores sparse; gula small and rounded at anterior region (Fig. 7C). Antennae variable in size between males and females (Fig. 7E–F).

Prothorax. Pronotum smooth, shining; punctation somewhat dense, fine; pubescence short, fine (Fig. 8D–E); somewhat squared, lateral areas curved, forming an obtuse angle at lateral areas of posterior margin (Fig. 8E). Hypomeron smooth (Fig. 8F). Notosternal suture straight, inward-directed (Fig. 8F). Profurca elongated, exceeding half of foramen (Fig. 8G). Prosternal process acute apically (Fig. 9A).

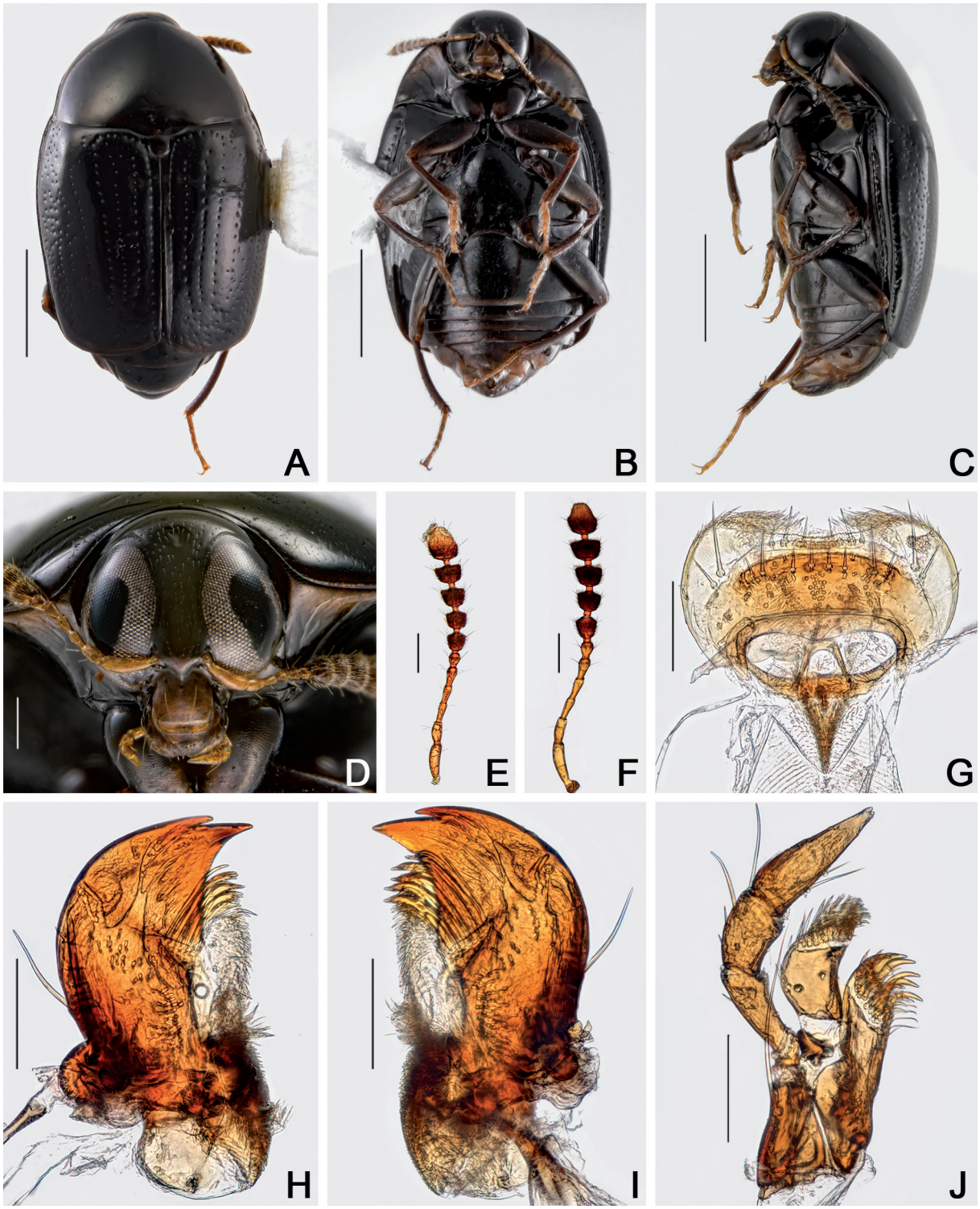

Fig. 7. *Cyparium achardi* sp. nov. **A–D**. Holotype, ♂ (CELC). **A**. Dorsal view. **B**. Ventral view. **C**. Lateral view. **D**. Frontal view. **E–F**. Antennae, paratype, ♂ (CELC) (E) and paratype, ♀ (CELC) (F). **G–J**. Paratype, ♂ (CELC). **G**. Labrum. **H–I**. Mandible. **H**. Left. **I**. Right. **J**. Maxilla. Specimens collected at Mata do Paraíso, Viçosa (MG, Brazil). Scale bars: A–C = 1.0 mm; D–F = 0.2 mm; G–J = 0.1.

Mesothorax. Mesonotum with prescutellar suture (= scutellar lines, Leschen & Löbl, 2005) almost straight (Fig. 9B). Scutellum rounded posteriorly (Fig. 9B). Anterior phragma wide, slightly curved (Fig. 9C). Mesanepisternum smooth (Fig. 9D). Procoxal rest rounded, curved posteriorly (Fig. 9D). Mesoventral line rounded; median line moderately curved; area between median line and mesocoxal line longer laterally (Fig. 9D). Mesoventral process large and straight at base in lateral view (Fig. 9E).

Metathorax. Metanotum with wide alacrista, rounded and somewhat turned to the posterior end; scutoscutellar suture slightly straight; median membranous area wide and very short (Fig. 9F). Metaventrite smooth; punctation sparse, fine; some specimens with faint lateral imbricate microsculpture (Fig. 9D). Mesocoxal line forming an open angle next to each coxal cavity and finely punctate under coxal cavity (Fig. 9D). Metanepisternum and metepimeron (Figs 7B–C, 9D) with imbricate microsculpture, but almost inconspicuous in some specimens. Intercoxal plates smooth (Fig. 7B). Metendosternite with straight furcal arms; 'stalk ridge' not exceeding half of stalk length (Fig. 10A); ventral longitudinal flange flat in lateral view (Fig. 10B).

Wings. Elytra slightly longer than wide, partially covering tergite VI (Fig. 7A); basal and lateral lines punctate (Fig. 8D); sutural line dashed; adsutural area with a row of short setae (Fig. 7A); six rows of coarse punctures (not including sutural line), but row 5 and 6 somewhat intermixed (Figs 7A, 10C); apical coarse punctation moderately sparse; apical serrations moderately large, well visible (Fig. 10D); pubescence short, fine, denser on disc. Epipleuron with a row of punctures (poorly marked in some specimens). Hind wings fully developed (Fig. 10E).

Legs. Pro-, meso- and metacoxae, and femora with strigulate microsculpture. Pro- and mesofemora somewhat fusiform (Fig. 10F–G); punctation moderately sparse and coarse. Metafemora straight, finely punctate (Fig. 10H). Mesotibiae densely spinose, spines fine (Fig. 10G). Metatibiae sparsely spinose, spines fine (Fig. 10H).

Abdomen. Tergites VI–VIII with imbricate microsculpture (Fig. 11A). Tergite VII trapezoidal; punctation dense, coarse; pubescence sparse, fine (Fig. 11A). Ventrite 1 sparsely and coarsely punctate; pubescence sparse, fine; strigulate microsculpture (Fig. 11B–C). Metacoxal lines finely punctate. Ventrites 2–5 sparsely and finely punctate; pubescence sparse, fine; imbricate microsculpture anteriorly and with strigulate microsculpture middle-posteriorly.

Males

Measurements (n = 1, paratype; in mm). Antennomeres (length(width)): 0.18(0.06), 0.11(0.05), 0.10(0.04), 0.09(0.04), 0.10(0.05), 0.07(0.06), 0.09(0.10), 0.09(0.11), 0.10(0.12), 0.10(0.13), 0.17(0.14); (n = 5, including the holotype; in mm): TL 3.00–3.28 (mean = 3.14, standard deviation ± 0.10), PL 1.20–1.31 (1.25 ± 0.04), PA 0.80–0.97 (0.89 ± 0.06), PB 1.72–2.07 (1.93 ± 0.13), SL 0.13–0.17 (0.14 ± 0.01), SW 0.15–0.20 (0.18 ± 0.02), EI 1.72–1.92 (1.81 ± 0.07), EL 2.07–2.32 (2.18 ± 0.09), EW 1.07–1.25 (1.19 ± 0.07), EH 0.70–0.80 (0.75 ± 0.05), HW 0.74–0.83 (0.78 ± 0.03), IS 0.15–0.24 (0.17 ± 0.03), WA 0.14–0.17 (0.16 ± 0.01), MC 0.72–0.92 (0.81 ± 0.08), MB 0.42–0.50 (0.46 ± 0.04), VL 0.62–0.70 (0.64 ± 0.03).

Antennae almost reaching level of mesanepisternum, smaller than in females (Fig. 7E). Pro- and mesotarsomeres I–III enlarged, with tenent setae (Fig. 10F). Tergite VIII triangular; punctation dense, coarse, subglabrous (Fig. 11D). Tergite IX with rectangular ventral struts (Fig. 11E,F). Sternite VIII rectangular, longish; finely punctate and with strigulate microsculpture (Fig. 11G). Sternite IX thicker posteriorly and triangular anteriorly (Fig. 11F). Aedeagus strongly sclerotized, enlarged and darker basely and narrowed apically, apex of median lobe short (Fig. 12A,B); openings in dorsal view somewhat enlarged, forming an acute angle (Fig. 12C); internal sac with irregular sclerites, with two hooks (Fig. 12D,E), parameres short, somewhat enlarged apically (Fig. 12A).

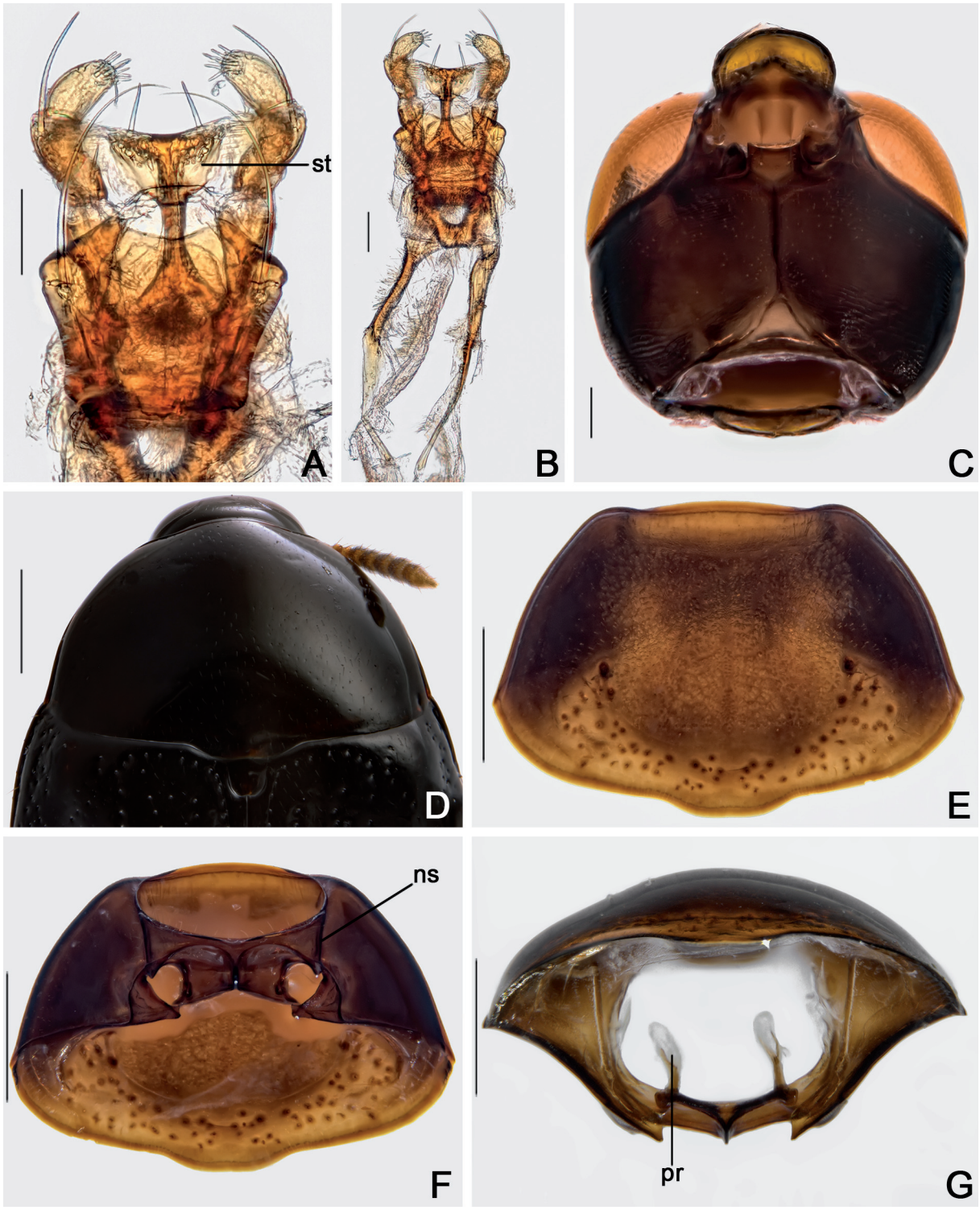

Fig. 8. *Cyparium achardi* sp. nov. **A–C.** Paratype, ♂ (CELC). **A**. Labium. **B**. Hypopharynx. **C**. Head, ventral view. **D**. Holotype, ♂ (CELC), pronotum, dorsal view. **E–G**. Paratype, ♂ (CELC), prothorax. **E**. Frontal view. **F**. Ventral view. **G**. Inner view. Specimens collected at Mata do Paraíso, Viçosa (MG, Brazil). Abbreviations: ns = notosternal suture; pr = profurca; st = sclerotized plate. Scale bars: A–B = 0.05 mm; C = 0.1 mm; D–G = 0.5 mm.

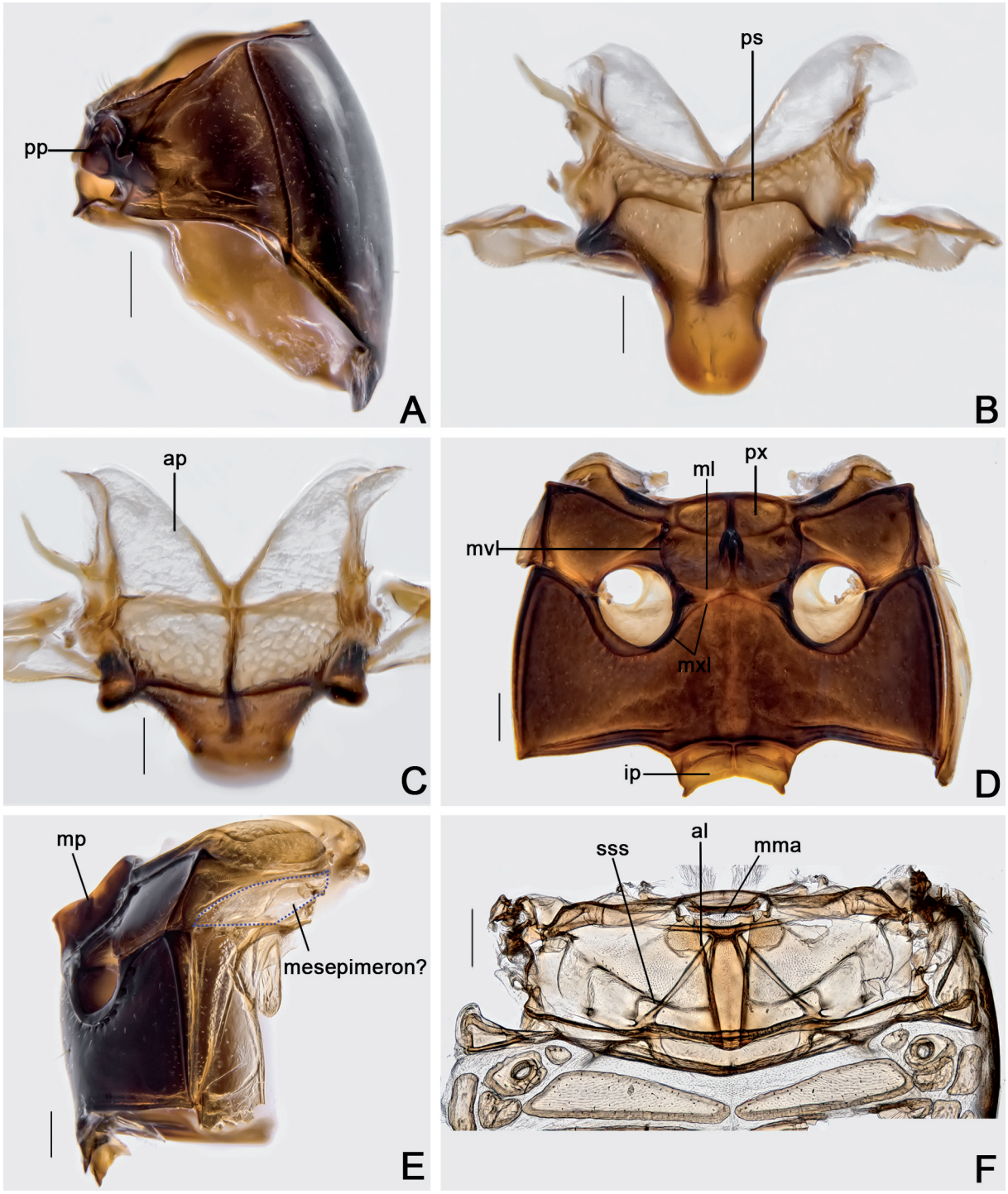

Fig. 9. *Cyparium achardi* sp. nov., paratype, ♂ (CELC). **A**. Prothorax, lateral view. **B–C**. Scutellar plate. **B**. Dorsal view. **C**. Apically slanted view. **D–E**. Meso- and metathorax. **D**. Ventral view. **E**. Lateral view. **F**. Metanotum. Specimen collected at Mata do Paraíso, Viçosa (MG, Brazil). Abbreviations: al = alacrista; ap = anterior phragma; ip = intercoxal plate; ml = median line; mma = median membranous area; mp = mesoventral process; mvl = mesoventral line; mxl = mesocoxal line; pp = prosternal process; ps = prescutellar line; px = procoxal rest; sss = scutoscutellar suture. Scale bars: A, D–F = 0.2 mm; B–C = 0.1 mm.

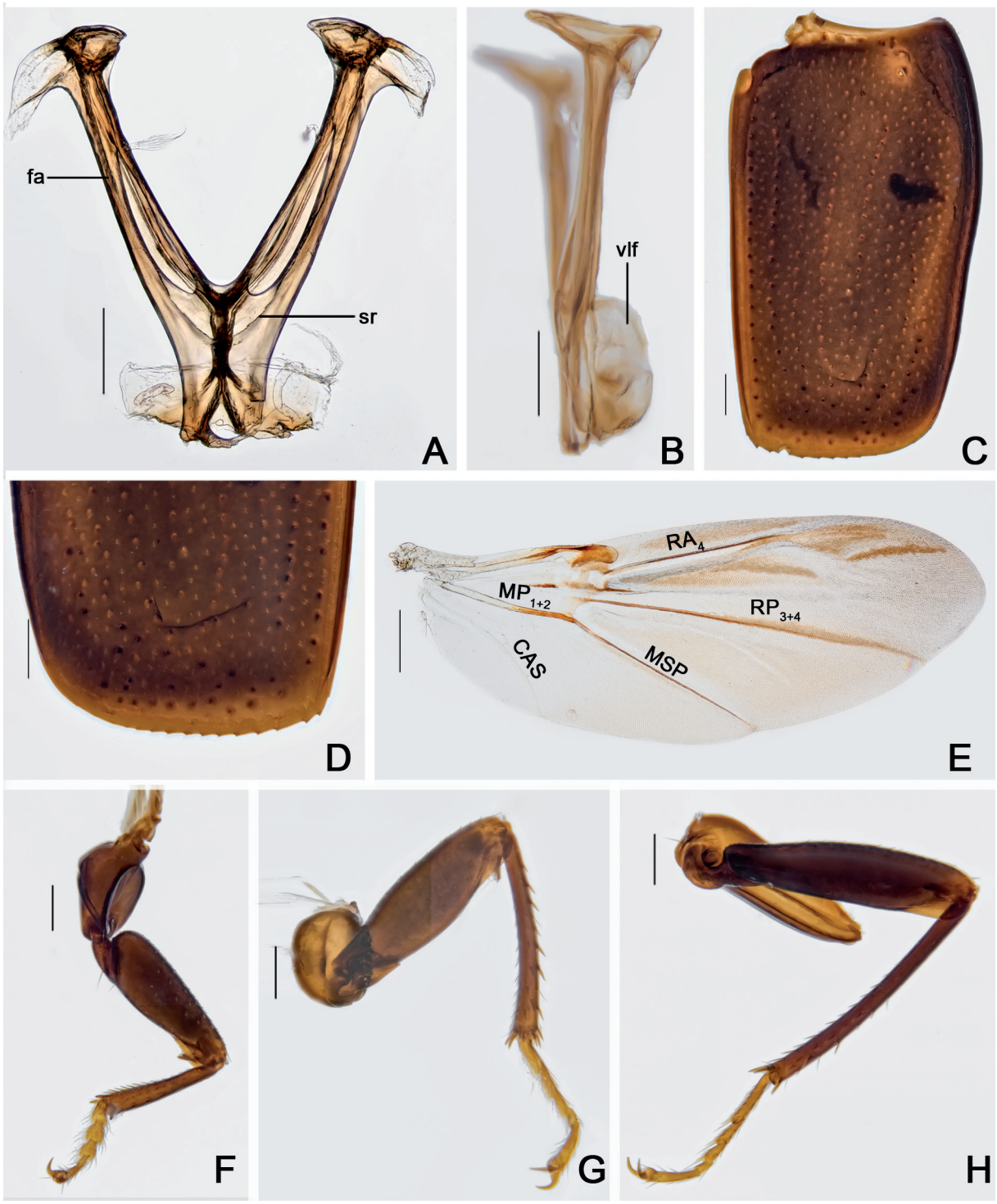

Fig. 10. *Cyparium achardi* sp. nov., paratype, ♂ (CELC). **A–B**. Metendosternite. **A**. Dorsal view. **B**. Lateral view. **C–D**. Elytron. **C**. Entire. **D**. Apex. **E**. Hind wing. **F–H**. Legs. **F**. Fore. **G**. Middle. **H**. Hind. Specimen collected at Mata do Paraíso, Viçosa (MG, Brazil). Abbreviations: CAS = cubitoanal strut; fa = furcal arms; MP_{1+2} = medial field; MSP = medial spur; RA_4 = radius anterior; RP_{3+4} = radius posterior; sr = 'stalk ridge'; vlf = ventral longitudinal flange. Scale bars: A–D, F–H = 0.2 mm; E = 0.5 mm.

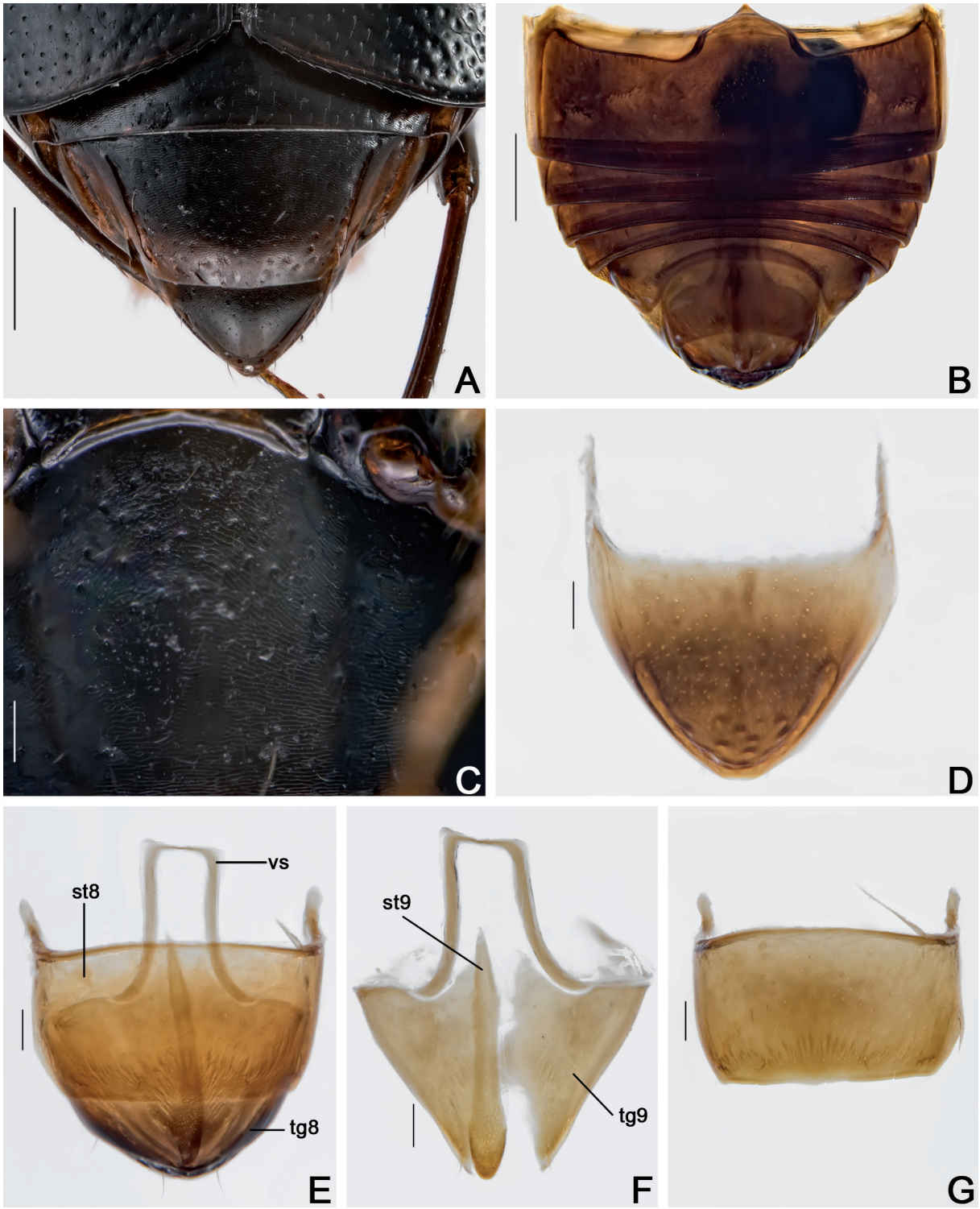

Fig. 11. *Cyparium achardi* sp. nov. **A, C**. Holotype, ♂ (CELC). **B, D–G**. Paratype ♂ (CELC). **A–B**. Abdomen, dorsal view (A) and ventral view (B). **C**. Ventrite 1. **D**. Tergite VIII. **E**. Terminalia. **F**. Tergite IX. **G**. Sternite VIII. Specimens collected at Mata do Paraíso, Viçosa (MG, Brazil). Abbreviations: st = sternite; tg = tergite; vs = ventral strut. Scale bars: A–B = 0.4 mm; C–G = 0.1 mm.

Fig. 12. *Cyparium achardi* sp. nov., paratype, ♂ (CELC): aedeagi. **A**. Lateral view. **B**. Frontal view. **C**. Dorsal view. **D**. Internal sac, frontal view. **E**. Internal sac, dorsal view. Specimen collected at Mata do Paraíso, Viçosa (MG, Brazil). Abbreviations: hk = hook; op = opening; pa = parameres. Scale bars = 0.2 mm.

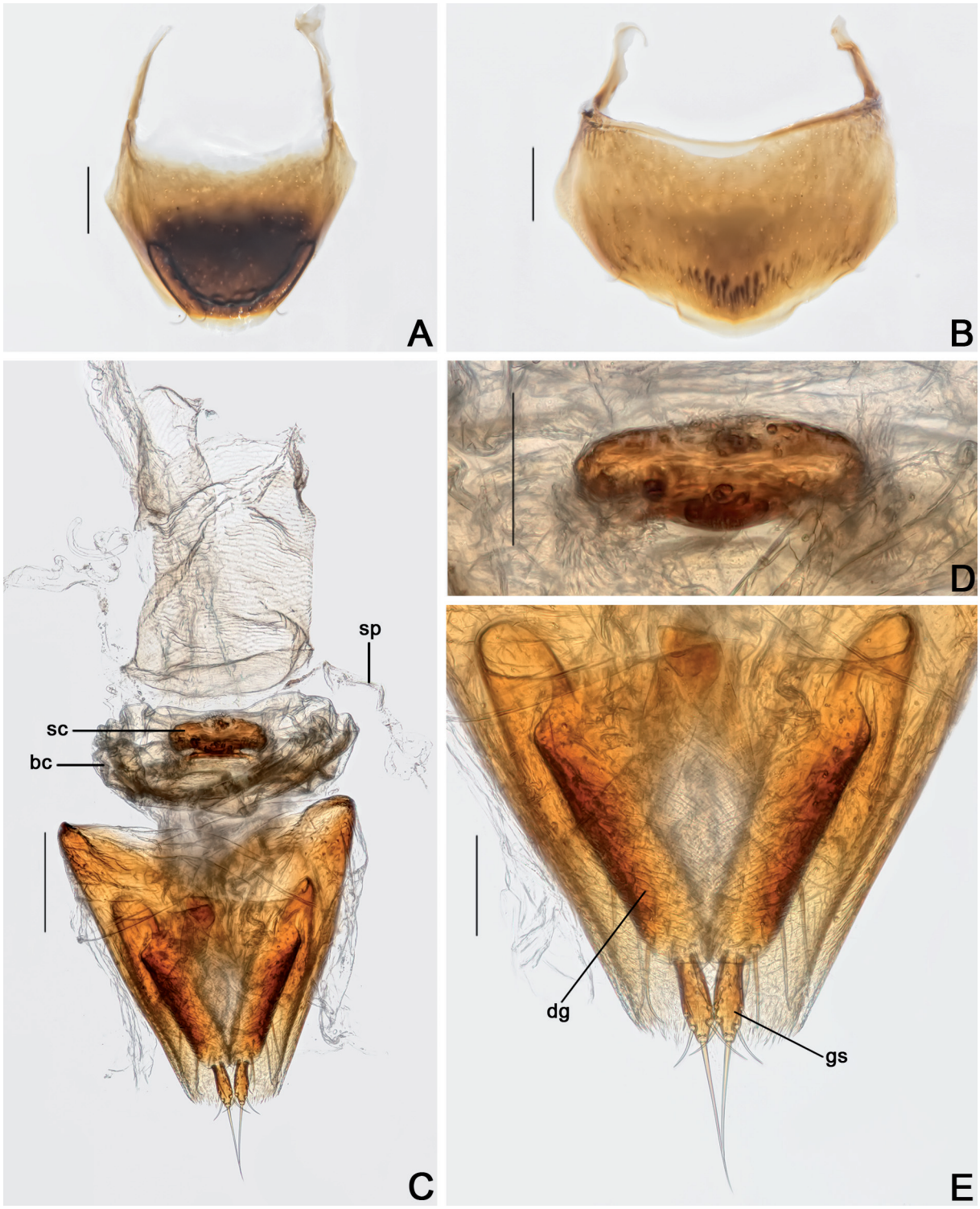

Fig. 13. *Cyparium achardi* sp. nov., paratype, ♀ (CELC). **A**. Tergite VIII. **B**. Sternite VIII. **C**. Terminalia. **D**. Sclerite of vaginal plate. **E**. Ovipositor. Specimen collected at Mata do Paraíso, Viçosa (MG, Brazil). Abbreviations: bc = bursa copulatrix; dg = distal gonocoxites; gs = gonostyli; sc = sclerite; sp = spermatheca. Scale bars: A–C = 0.2 mm; D–E = 0.1 mm.

Females

Measurements (n = 1, paratype; in mm). Antennomeres (length(width)): 0.20(0.06), 0.13(0.05), 0.11(0.04), 0.12(0.05), 0.11(0.06), 0.08(0.07), 0.11(0.11), 0.10(0.13), 0.11(0.14), 0.10(0.16), 0.16(0.15); (n = 4, paratype; in mm): TL 3.32–3.40 (mean = 3.37, standard deviation ± 0.04), PL 1.23–1.39 (1.33 ± 0.07), PA 0.97–1.05 (1.01 ± 0.04), PB 2.05–2.17 (2.10 ± 0.05), SL 0.18–0.21 (0.19 ± 0.01), SW 0.17–0.20 (0.19 ± 0.01), EI 1.90–2.00 (1.94 ± 0.05), EL 2.27–2.40 (2.35 ± 0.05), EW 1.25–1.27 (1.25 ± 0.01), EH 0.80–1.00 (0.88 ± 0.09), HW 0.81–0.84 (0.84 ±0.02), IS 0.16–0.25 (0.20 ±0.04), WA 0.15–0.21 (0.18 ± 0.02), MC 0.87–0.95 (0.90 ± 0.03), MB 0.42–0.52 (0.46 ± 0.04), VL 0.67–0.75 (0.71 ± 0.03).

Antennae longer than in males, surpassing mesanepisternum (Fig. 7F). Tergite VIII triangular, rounded posteriorly; punctation dense, coarse (inconspicuous in some specimens); subglabrous (Fig. 13A). Sternite VIII rectangular with strigulate microsculpture (Fig. 13B). Vagina and bursa copulatrix membranous; vaginal plate with an apical sclerite and a pair of spermatheca at base of oviduct (Fig. 13C–D). Distal gonocoxites parallel, straight and thick; gonostyli larger at apex (Figs 13C, E).

Host fungi

Adults were collected from *Marasmiellus volvatus* Singer (Agaricales, Omphalotaceae) (1 record, 4 individuals), *Marasmiellus* sp. Murrill (1, 2), *Marasmius haematocephalus* (Mont.) Fr. (Agaricales, Marasmiaceae) (1, 1), *Leucocoprinus ianthinus* (Sacc.) P.Mohr (Agaricales, Agaricaceae) (1, 1), *L. cepistipes* (Sowerby) Pat. (1, 1), *Leucoprinus* sp. (1, 1), *Hygrocybe* sp. (Agaricales, Hygrophoraceae) (1, 1), *Leucoagaricus* sp. (Agaricales, Agaricaceae) (1, 1).

Remarks

Similar to *C. pygidiale*, which occurs in Jataí, Goiás, Brazil (1174 km from the collection site of *C. achardi* sp. nov.), but they differ in the humeral and apical region of the elytra, and in the scutellar shield (blackish in *C. achardi* and reddish in *C. pygidiale*); elytral punctation is also different: rows 1–3 are coarser in *C. pygidiale* and the remainder are coarser in *C. achardi*; furthermore, rows 1–3 are somewhat outward directed, while they are inward directed in *C. pygidiale*.

Distribution

Known only from Mata da Biologia, campus of the Universidade Federal de Viçosa, Viçosa, state of Minas Gerais, Southeast Brazil (Fig. 46).

Cyparium lescheni sp. nov.
urn:lsid:zoobank.org:act:8A653AB2-6DEF-4FA6-A885-438BDAF11D5F
Figs 4, 14–21, 46; Supp. file 1B, Supp. file 2A

Diagnosis

TL: 2.07–2.25 mm in males and 2.10–2.35 mm in females. Brown (Fig. 14A). Hypomeron, metaventrite and intercoxal plates with strigulate microsculpture. Metaventrite coarsely punctate above intercoxal plates (Figs 14B, 17D). Tergite VIII in males triangular (Fig. 19D). Openings of aedeagus in dorsal view forming an acute angle (Fig. 20C); internal sac with drop-like sclerites (Fig. 20D–E). Tergite VIII of females with a posterior invagination (Fig. 21A).

Etymology

In homage to Dr Richard A.B. Leschen (New Zealand Arthropod Collection) for his great contributions to the systematics of Coleoptera, especially regarding Scaphidiinae.

Material examined

Holotype

BRAZIL • ♂; Minas Gerais, Viçosa, EPTEA Mata do Paraíso; 19 Nov. 2019; LabCol leg.; "Fungo 30 \\ em *Agaricus sylvaticus* \\ *Cyparium lescheni* von Groll & Lopes-Andrade HOLOTYPUS" [red paper]; CELC. (Supp. file 1B)

Paratypes

BRAZIL • 1 ♂, 4 ♀♀; same collection data as for holotype, "T. dos Gigantes"; 15 Feb. 2015; S. Aloquio, A. Orsetti and M. Bento leg.; CELC • 1 ♀; same collection data as for holotype, "T. da Madeira"; 27 Feb. 2015; I.S.C. Pecci-Maddalena *et al.* leg.; CELC • 1 ♂; same collection data as for holotype; 13 Mar. 2015; S. Aloquio, A. Orsetti, C. Lopes-Andrade and M. Bento leg.; CELC • 1 ♂; same collection data as for holotype; 9 Nov. 2016; I. Pecci-Maddalena and C. Lopes-Andrade leg.; "\\ ex *Psathyrella candolleana*"; CELC • 5 ♂♂, 7 ♀♀ (2 ♂♂, 1 ♀, entirely dissected, preserved in glycerin; 1 ♂, 2 ♀♀, abdomen dissected, preserved in glycerin); same collection data as for holotype; CELC • 1 ♂; 1 ♀; same collection data as for holotype; CAMB • 1 ♂; 1 ♀; same collection data as for holotype; CERPE • 2 ♂♂; 1 ♀, 1 spec.; same collection data as for holotype; 21 Nov. 2019; LabCol leg.; "Fungo 06 \\ Em *Agaricus dulcidulus* e *Leucocoprinus brebissoni*"; CELC • 2 ♀♀; Viçosa, Recanto das Cigarras, Mata da Biol.; 20 Nov. 2019; LabCol leg.; "Fungo 29 \\ Em *Entoloma* (*Inocephalus*) sp."; CELC • 8 ♂♂, 3 ♀♀ (1 ♂, entirely dissected, preserved in glycerin; 2 ♂♂, 1 ♀, abdomen dissected, preserved in glycerin); same collection data as for preceding; "Fungo 08; CELC \\ Em *Psathyrella* sp."; CELC • 6 ♂♂, 11 ♀♀, 1 spec.; Viçosa, Mata da Biologia; 15 Oct. 2021; E. von Groll and A. Orsetti leg.; "Fungo 20 \\ Em *Agaricus* sp."; CELC.

All paratypes additionally labelled "*Cyparium lescheni* von Groll & Lopes-Andrade PARATYPUS [yellow paper]".

Description

Measurements (holotype, in mm). TL 2.32, PL 0.76, PA 0.70, PB 1.40, EW 0.86, EL 1.62, IS 0.20, HW 0.62.

Coloration. Iridescent. Brown; antennomeres I–VI, clypeus, mouthparts, tarsi yellow (Figs 14A, 15A). Variation: few paratypes with pronotum and hypomeron reddish brown (Fig. 14D–F); scutellum reddish brown or black (Fig. 14D); meso- and metathorax reddish brown, each sclerite lighter laterally (Fig. 14E); elytra blackish (Fig. 14D); epipleuron dark ochre; coxae and trochanters dark ochre; femora dark ochre, apex lighter; tibiae dark ochre, lighter anteriorly and posteriorly; tarsi yellow (Fig. 14E); tergite VI and VII blackish; tergite VIII yellow; ventrite 1 dark ochre, 2–4 dark yellow, 5 and 6 yellow (Fig. 14E).

Head. Punctation dense, fine (Fig. 15A). Eyes long (Fig. 15A). Labrum sub-rectangular, lateral margins smoothly rounded, not well delimited apically; central margin sub-straight; sclerotized portion inwardly curved; lateral setae considerably extending from the margins of the labrum; densely porose centrally (Fig. 15D). Mandibles strongly curved; subapical serrations on left mandible conspicuous (Fig. 15E–F). Maxillary palps, galea and lacinia moderate pubescent, elongated (Fig. 15G). Mentum straight apically and rounded laterally; sides well delimited (Fig. 16A). Setae of labial palpomere II extending palpomere III; palpomere III longish with long apical setae (Fig. 16A). Hypopharynx with narrow and rounded sclerotized-plate (Fig. 16A–B). Post gena microsculptured with transversal lines; gular pores sparse; gula long and sharp (Fig. 16C). Antennal club very distinct; antennomere XI longish, hexagonal, more or less rounded apically; remarkably different between sexes (Fig. 15B–C).

Prothorax. Pronotum smooth, shining; punctuation dense, fine; pubescence short, fine (Fig. 16D–E); transverse, sub-straight laterally, forming an obtuse angle at lateral areas of posterior margin (Fig. 16E). Hypomeron with strigulate microsculpture. Notosternal suture straight, inward directed (Fig. 16F). Profurca somewhat thick and elongated, slightly extending half length of foramen (Fig. 16G). Prosternal process acuminated (Fig. 17A).

Mesothorax. Mesonotum with prescutellar suture (= scutellar lines, Leschen & Löbl 2005) strongly wavy (Fig. 17B). Anterior phragma large and straight (Fig. 17C). Mesanepisternum with strigulate microsculpture. Procoxal rests triangular; slightly curved posteriorly (Fig. 17D). Mesoventral lines wavy and obtuse; median lines moderately wavy; area between median and mesoventral lines thin (Fig. 17D). Mesoventral process long, slightly curved at top and base, forming a not well marked ridge (Fig. 17E).

Fig. 14. *Cyparium lescheni* sp. nov. **A–C**. Holotype, ♂ (CELC). **D–F**. Paratype, ♂ (CELC). **A**. Dorsal view. **B**. Ventral view. **C**. Lateral view. **D**. Dorsal view. **E**. Ventral view. **F**. Lateral view. Specimens collected at Mata do Paraíso, Viçosa (MG, Brazil). Scale bars = 1.0 mm.

Metathorax. Metanotum with alacrista somewhat enlarged anteriorly and turned to anterior portion; scutoscutellar suture very strongly curved; median membranous area remarkably wide, and short (Fig. 17F). Metaventrite with strigulate microsculpture; punctuation sparse, fine; coarsely punctate above intercoxal plates (Fig. 17D). Mesocoxal line forming a smooth angle between coxal cavities (Fig. 17D). Metanepisternum and metepimeron with imbricate microsculpture. Intercoxal plates with strigulate microsculpture. Metendosternite with curved furcal arms; 'stalk ridge' exceeding half length of stalk (Fig. 18A); ventral longitudinal flange long and narrow in lateral view (Fig. 18B).

Wings. Elytra slightly wider than long, partially covering tergite VI (Fig 14A); basal and lateral lines punctate (Fig. 16D); sutural lines dashed; adsutural area with a row of setae; six rows of coarse punctures (not including sutural line) (Figs 14A, D, 18C); apical coarse punctation sparse; apical fine punctation dense (Fig. 18D); apical serrations almost inconspicuous (Fig. 18D); pubescence short and fine. Epipleuron with a line of coarse punctures. Hind wings fully developed (Fig. 18E).

Legs. Pro-, meso- and metacoxae, and femora with strigulate microsculpture. Femora strongly fusiform (Fig. 18F–H). Profemora with inconspicuous punctuation; mesofemora with sparse and coarse punctuation; metafemora with fine and shallow punctuation. Mesotibiae densely spinose, spines fine; metatibiae sparsely spinose, spines fine.

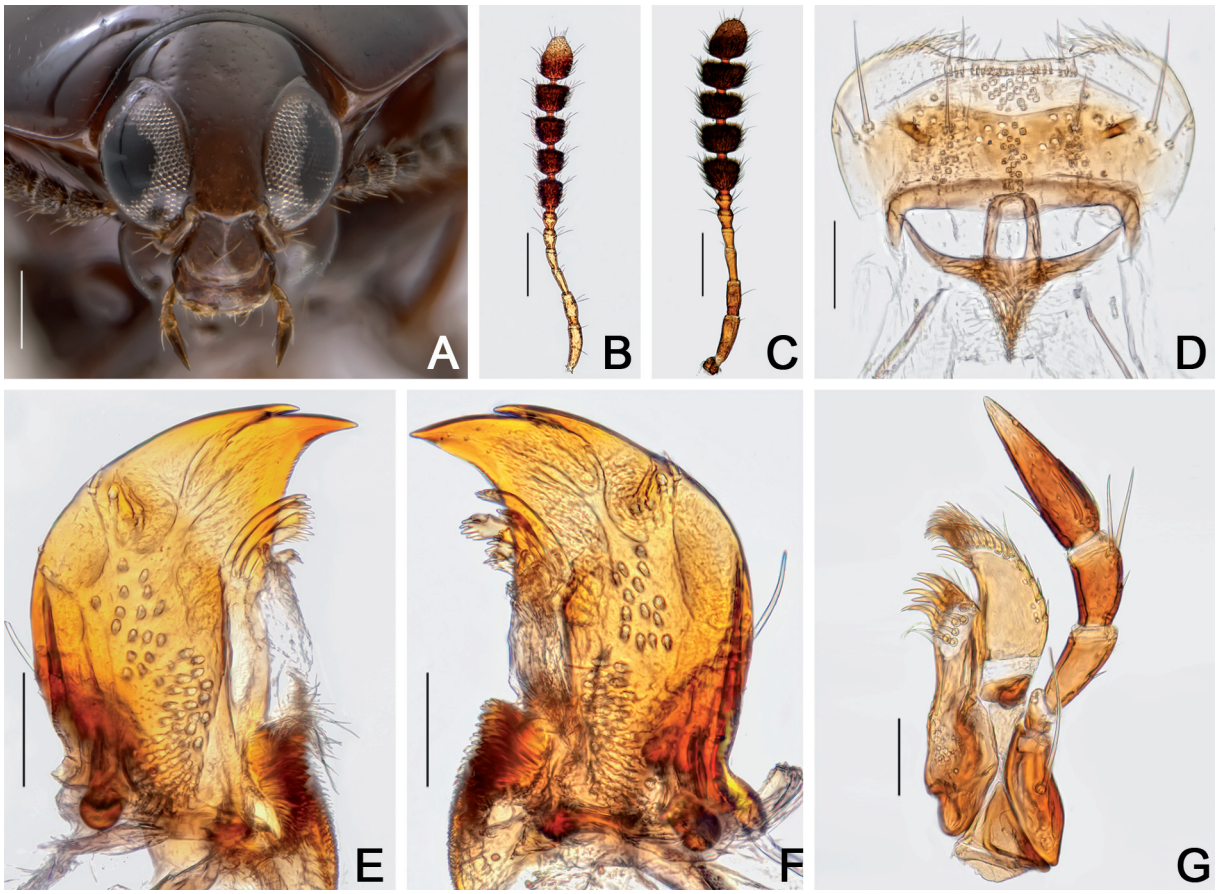

Fig. 15. *Cyparium lescheni* sp. nov. **A**. Holotype, ♂ (CELC), frontal view. **B**. Paratype, ♂ (CELC), antennae. **C**. Paratype, ♀ (CELC), antennae. **D–G**. Paratype, ♂ (CELC). **D**. Labrum. **E**. Left mandible. **F**. Right mandible. **G**. Maxilla. Specimens collected at Mata do Paraíso, Viçosa (MG, Brazil). Scale bars: A–C = 0.2 mm; D–G = 0.05 mm.

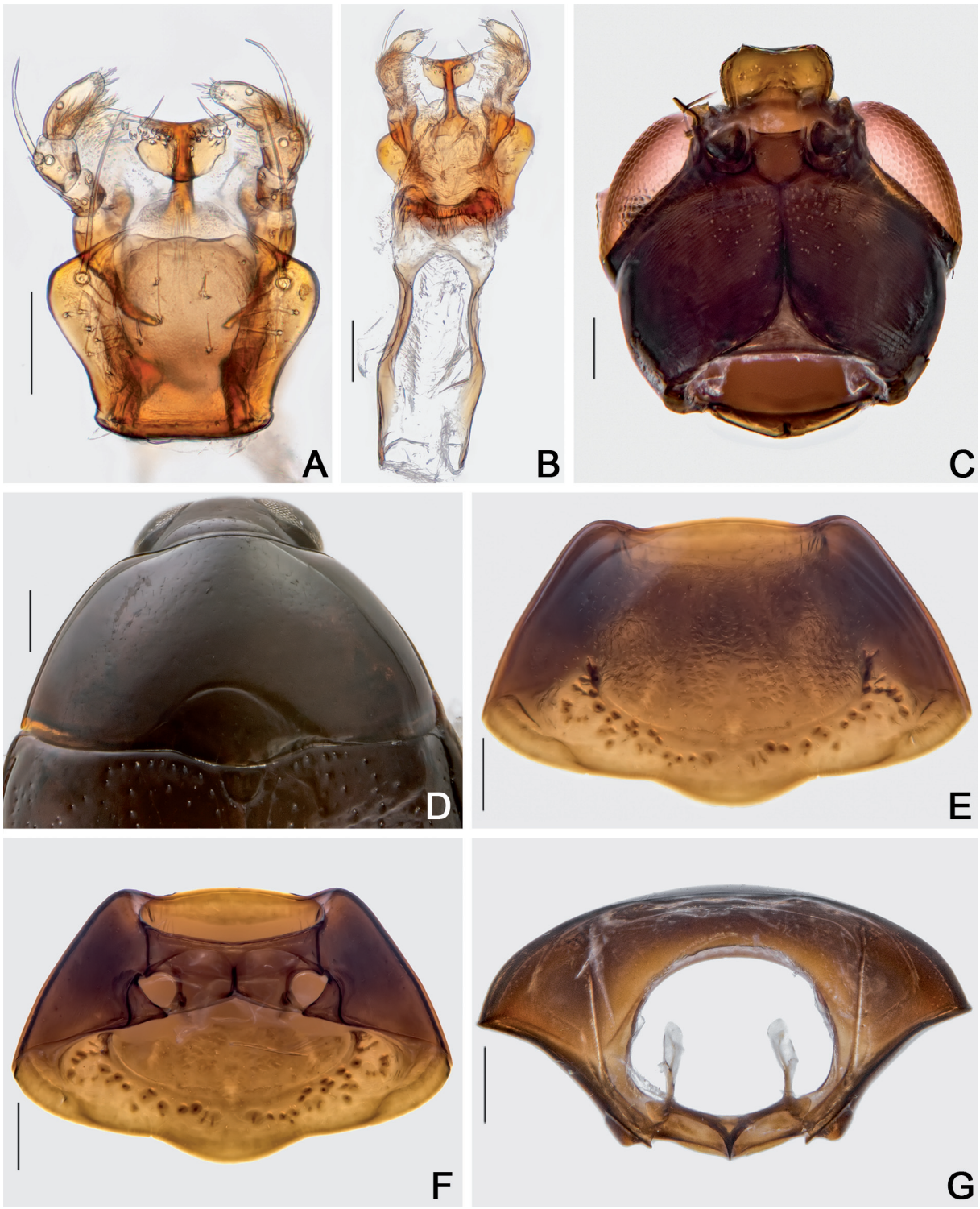

Fig. 16. *Cyparium lescheni* sp. nov. **A–C**. Paratype, ♂ (CELC). **A**. Labium. **B**. Hypopharynx. **C**. Head, ventral view. **D–E**. Pronotum, dorsal view. **D**. Holotype, ♂ (CELC). **E**. Paratype, ♂ (CELC). **F–G**. Paratype, ♂ (CELC), prothorax. **F**. Ventral view. **G**. Inner view. Specimens collected at Mata do Paraíso, Viçosa (MG, Brazil). Scale bars: A–B = 0.05 mm; C = 0.1 mm; D–G = 0.2 mm.

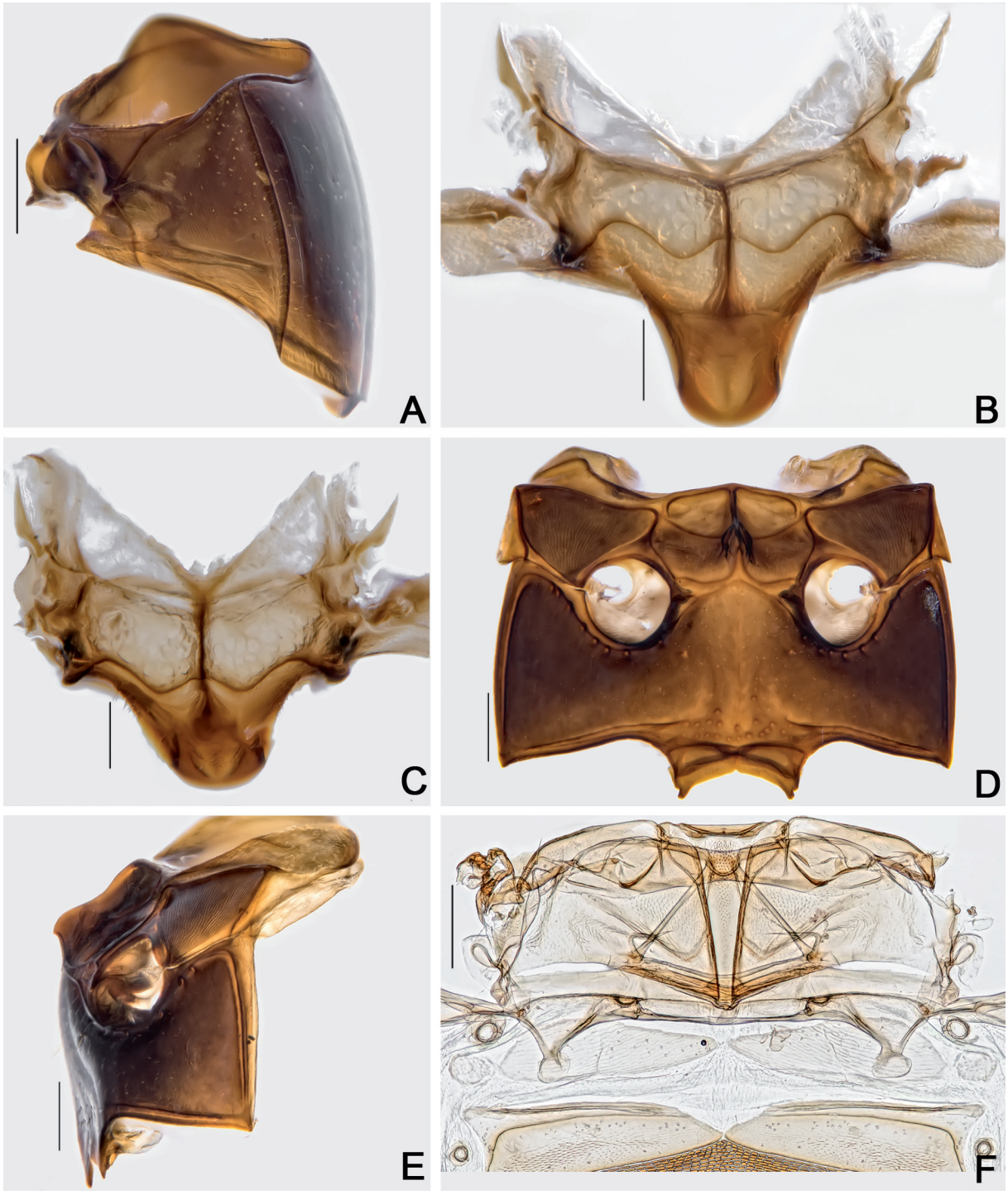

Fig. 17. *Cyparium lescheni* sp. nov., paratypes, ♂ (CELC). **A**. Prothorax, lateral view **B–C**. Scutellar plate. **B**. Dorsal view. **C**. Apically slanted view. **D–E**. Meso- and metathorax. **D**. Ventral view. **E**. Lateral view. **F**. Metanotum. Specimens collected at Mata do Paraíso, Viçosa (A–E) and Mata da Biologia (F), Viçosa (MG, Brazil). Scale bars: A, D–F = 0.2 mm; B–C = 0.1 mm.

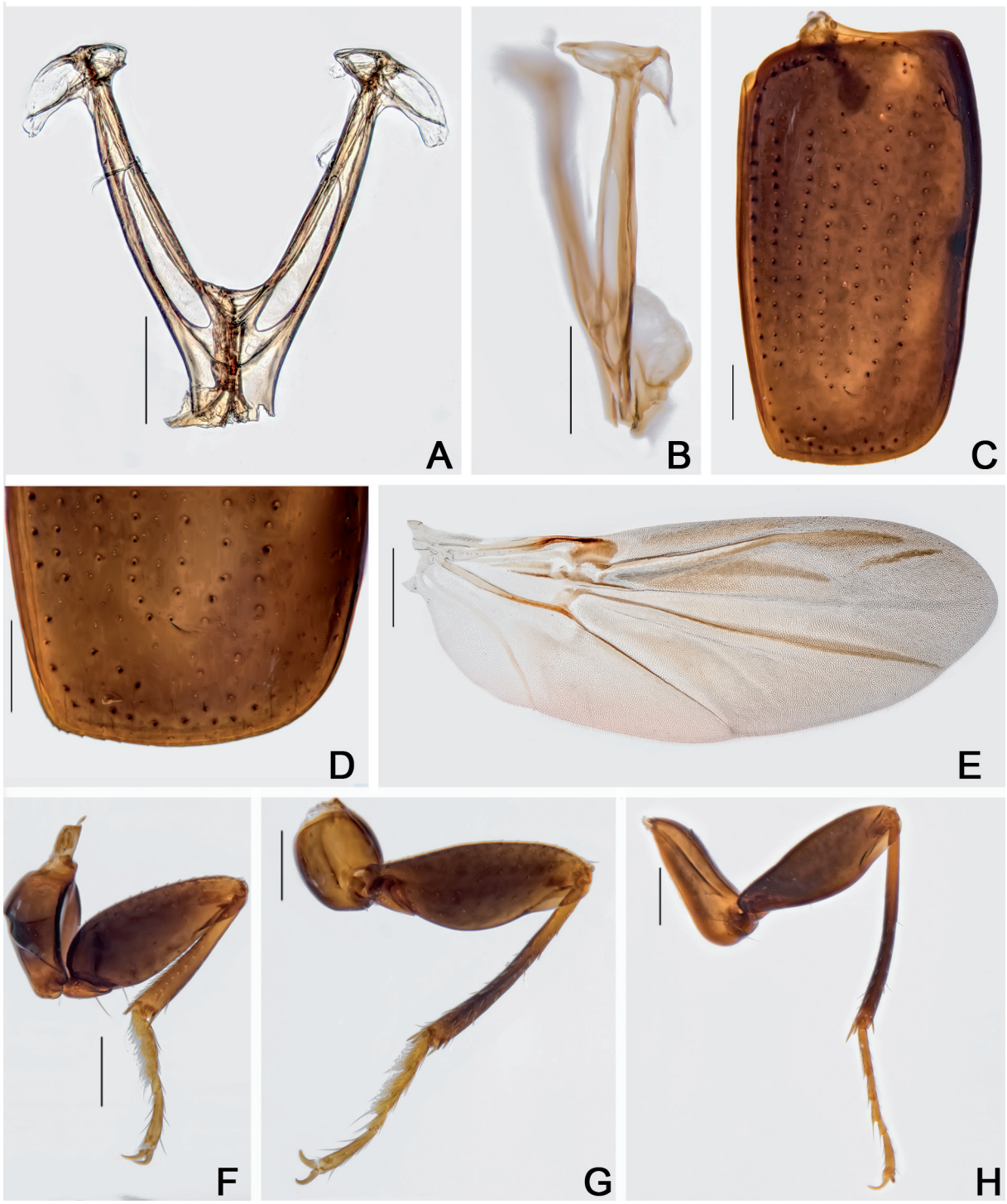

Fig. 18. *Cyparium lescheni* sp. nov., paratype, ♂ (CELC). **A–B**. Metendosternite. **A**. Dorsal view. **B**. Lateral view. **C–D**. Elytron. **C**. Entire. **D**. Apex. **E**. Hind wing. **F–H**. Legs. **F**. Fore. **G**. Middle. **H**. Hind. Specimen collected at Mata do Paraíso, Viçosa (MG, Brazil). Scale bars: A–D, F–H = 0.2 mm; E = 0.5 mm.

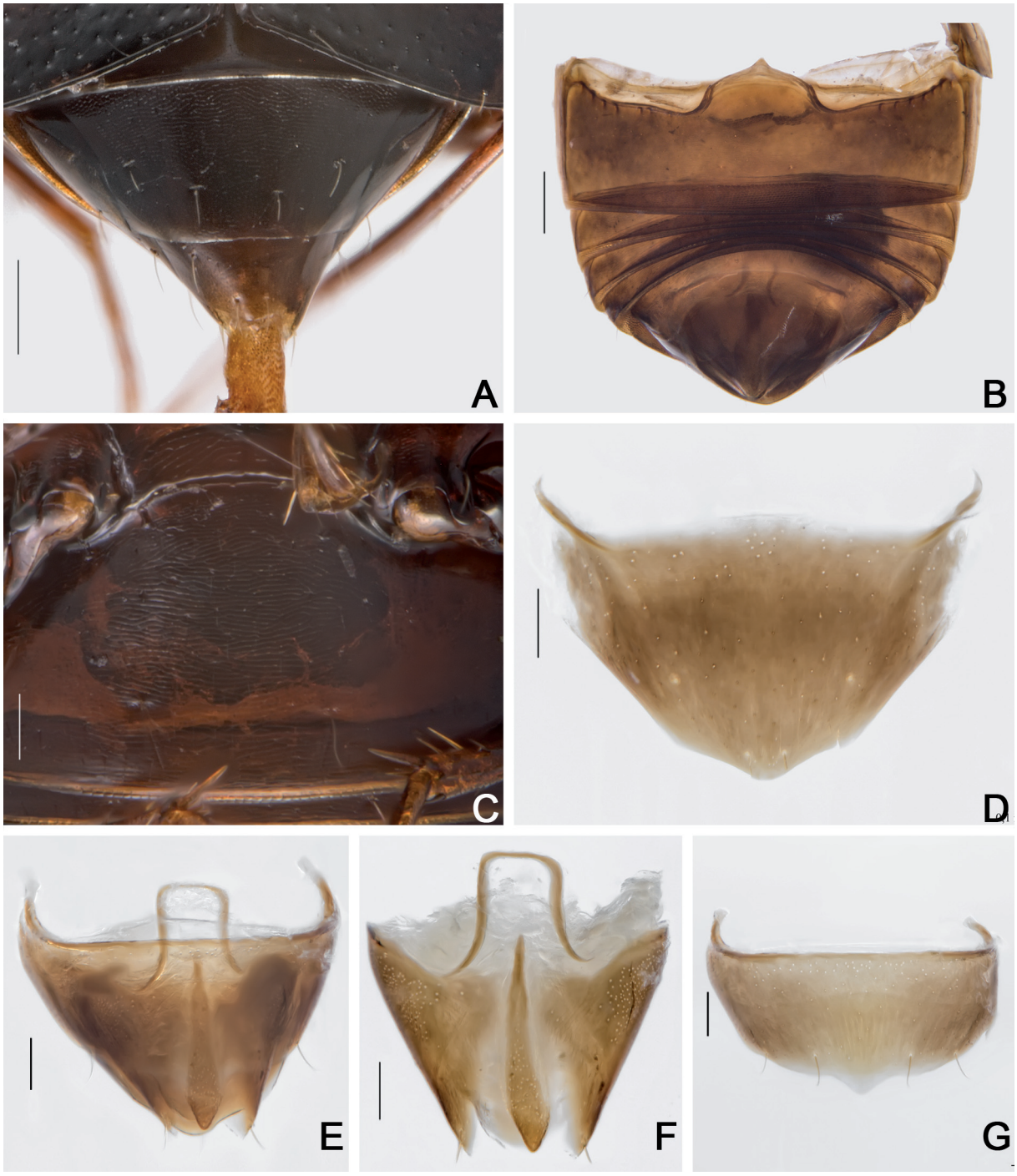

Fig. 19. *Cyparium lescheni* sp. nov. **A–C**. Holotype, ♂ (CELC). **D–G**. Paratype ♂ (CELC). **A**. Abdomen, dorsal view. **B**. Abdomen, ventral view. **C**. Ventrite 1. **D**. Tergite VIII. **E**. Terminalia. **F**. Tergite IX. **G**. Sternite VIII. Specimens collected at Mata do Paraíso, Viçosa (A–C) and Mata da Biologia (D–G), Viçosa (MG, Brazil). Scale bars: A–B = 0.2 mm; C–G = 0.1 mm.

Fig. 20. *Cyparium lescheni* sp. nov., paratype, ♂ (CELC). **A–C**. Aedeagi. **A**. Lateral view. **B**. Frontal view. **C**. Dorsal view. **D–E**. Internal sac. **D**. Frontal view. **E**. Dorsal view. Specimen collected at Mata da Biologia, Viçosa (MG, Brazil). Scale bars = 0.1 mm.

Abdomen. Tergite VI and VII with imbricate microsculpture (Fig. 19A). Tergite VII trapezoidal (Fig. 19A), triangular in some paratypes with tergite VIII not exposed; punctation sparse, fine; pubescence sparse, fine. Ventrites 1–5 sparsely and finely punctate; pubescence sparse, fine; with strigulate microsculpture (Fig. 19B–C). Metacoxal lines finely punctate.

Males

Measurements (n = 1, paratype; in mm). Antennomeres (length(width)): 0.14(0.05), 0.10(0.04), 0.08(0.03), 0.07(0.04), 0.06(0.04), 0.06(0.05), 0.09(0.08), 0.08(0.08), 0.09(0.10), 0.09(0.11), 0.14(0.10); (n = 8, including the holotype, unless otherwise specified; in mm): TL 2.07–2.32 (mean = 2.18, standard deviation ± 0.08), PL 0.74–0.80 (0.78 ± 0.02), PA 0.66–0.70 (0.69 ± 0.02), PB 1.30–1.40 (1.36 ± 0.04), SL (n = 7) 0.07–0.15 (0.11 ± 0.02), SW (n = 7) 0.09–0.14 (0.11 ± 0.02), EI 1.24–1.36 (1.30 ± 0.04), EL 1.44–1.62 (1.53 ± 0.08), EW 0.76–0.86 (0.81 ± 0.03), EH 0.50–0.62 (0.55 ± 0.04), HW 0.59–0.65 (0.62 ± 0.02), IS 0.15–0.20 (0.17 ± 0.02), WA 0.12–0.19 (0.14 ± 0.02), MC 0.55–0.64 (0.60 ± 0.03), MB 0.23–0.30 (0.27 ± 0.02), VL 0.40–0.49 (0.45 ± 0.03).

Antennae shorter than in females; club less distinct than in females (Fig. 15B). Pro- and mesotarsomeres I–III enlarged, with tenet setae (Fig. 18F–G). Tergite VIII heptagonal, acuminated posteriorly; punctuation inconspicuous; subglabrous (Fig. 19D). Tergite IX with rectangular ventral struts (Fig. 19E–F). Sternite VIII rectangular, with a projection (Fig. 19G). Sternite IX straight, constricted centrally and thicker apically (Fig. 19F). Aedeagus sclerotized, apex of median lobe short; openings in dorsal view forming an acute angle (Fig. 20A–C); internal sac with weak irregular sclerites, with drop-like sclerites (Fig. 20D–E); parameres short, enlarged apically in lateral view (Fig. 20A).

Females

Measurements (n = 1, paratype; in mm). Antennomeres (length(width)): 0.14(0.05), 0.11(0.05), 0.11(0.04), 0.06(0.04), 0.06(0.05), 0.05(0.06), 0.10(0.11), 0.09(0.13), 0.07(0.13), 0.08(0.14), 0.12(0.12); (n = 7, paratypes; in mm): TL 2.10–2.35 (mean = 2.26, standard deviation ± 0.09), PL 0.76–0.86 (0.81 ± 0.04), PA 0.66–0.74 (0.71 ± 0.02), PB 1.34–1.50 (1.43 ± 0.06), SL 0.09–0.13 (0.11 ± 0.01), SW 0.12–0.14 (0.13 ± 0.01), EI 1.30–1.40 (1.35 ± 0.04), EL 1.48–1.66 (1.58 ± 0.06), EW 0.76–0.84 (0.81 ± 0.03), EH 0.52–0.65 (0.60 ± 0.04), HW 0.61–0.66 (0.63 ± 0.02), IS 0.18–0.20 (0.18 ± 0.01), WA 0.13–0.15 (0.14 ± 0.00), MC 0.57–0.65 (0.62 ± 0.03), MB 0.25–0.32 (0.30 ± 0.02), VL 0.43–0.52 (0.50 ± 0.03).

Antennae larger than in males; antennal club more distinct (Fig. 15C). Tergite VIII hexagonal, with a posterior invagination; punctuation inconspicuous; subglabrous (Fig. 21A). Sternite VIII rectangular with a projection (Fig. 21B). Vagina membranous; bursa copulatrix with sclerites on wall (Fig. 21C, Supp. file 2A). Vaginal plate with an apical sclerite, more or less developed (Fig. 21C–D, Supp. file 2A). Two filiform spermatheca (Supp. file 2A). Distal gonocoxites straight, thin (Fig. 21C–E); gonostyli long, somewhat thick, and parallel (Fig. 21C–E).

Host fungi

Adults were collected from *Psathyrella candolleana* (Fr.) Maire (Agaricales, Psathyrellaceae) (1 record, 1 individual), *Psathyrella* sp. (1, 11), *Agaricus* sp. (1, 18; von Groll *et al.* 2021: figs 1–4), *A. dulcidulus* Schulzer (1, 4), *A. sylvaticus* Schaeff. (1, 20) and *Entoloma* (*Inocephalus*) sp. (Agaricales, Entolomataceae) (1, 2).

Remarks

Measurements similar to those of *C. newtoni*, except for the comparatively longer antennae. It was found co-occurring with *C. newtoni* in the same host fungi. However, they differ at first view by the coloration: *C. lescheni* sp. nov. is brown with few individuals of the same coloration as *C. newtoni* (pronotum reddish brown and elytra black); a few individuals of *C. newtoni* are brown, but darker than *C. lescheni*. They also differ by the microsculpture of the metaventrite: present in *C. lescheni* and absent

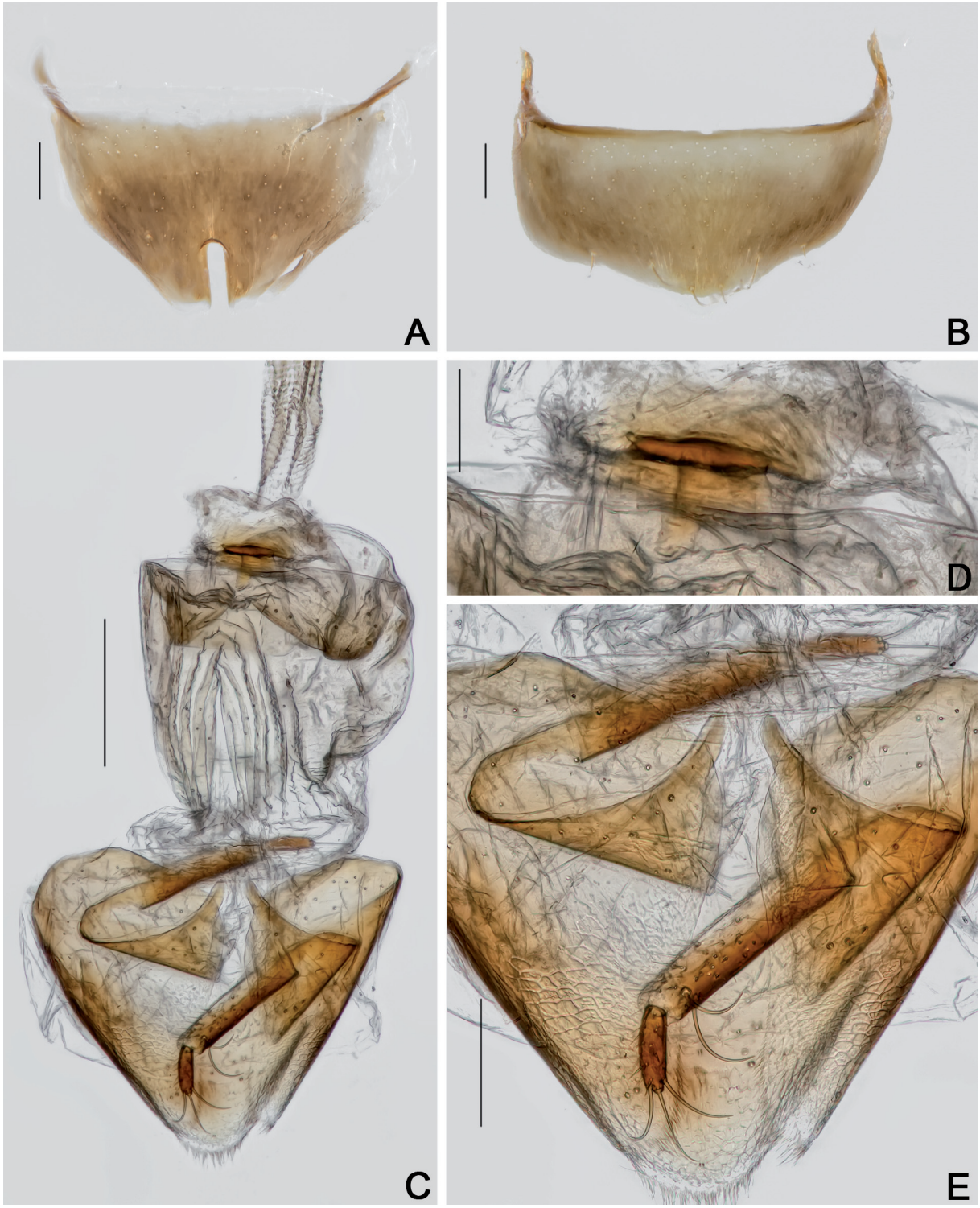

Fig. 21. *Cyparium lescheni* sp. nov., paratype, ♀ (CELC). **A**. Tergite VIII. **B**. Sternite VIII. **C**. Terminalia. **D**. Sclerite of vaginal plate. **E**. Ovipositor. Specimen collected at Mata da Biologia, Viçosa (MG, Brazil). Scale bars: A–B, E = 0.1 mm; C = 0.2 mm; D = 0.05 mm.

in *C. newtoni*. Tergite VIII in males is triangular in *C. lescheni* and straight apically in *C. newtoni*. Parameres in *C. newtoni* are longer and the sclerite of the internal sac is also different. Tergite VIII in females has an invagination in *C. lescheni*, while in *C. newtoni* it is entire.

Distribution

Known only from Mata da Biologia and Mata do Paraíso, campus of the Universidade Federal de Viçosa, Viçosa, state of Minas Gerais, Southeast Brazil (Fig. 46).

Cyparium loebli sp. nov.
urn:lsid:zoobank.org:act:88FF6EF0-5AED-4505-9E56-2200ED4ABEEF
Figs 4, 22–29, 46; Supp. file 1C

Diagnosis

TL: 2.53–2.78 mm in males and 2.34–2.68 mm in females. Pronotum, hypomeron and scutellum reddish brown (Fig. 22A). Elytra black, anterior region reddish brown (Fig. 22A). Hypomeron and mesanepisternum with strigulate microsculpture. Metaventrite smooth, coarsely punctate above intercoxal plates (Fig. 25D). Metanepisternum and metepimeron with imbricate microsculpture. Aedeagus apex long, parameres longish, weak sclerites in internal sac (Fig. 28A–E). Distal gonocoxites straight and slender (Fig. 29E).

Etymology

In homage to Dr Ivan Löbl (Muséum d'histoire naturelle, Genève, CH), for his remarkable contributions to the systematics of Scaphidiinae, which are the greatest source of information for our ongoing works on these beetles.

Material examined

Holotype

BRAZIL • ♂; Minas Gerais, Viçosa, EPTEA Mata do Paraíso; 12 Nov. 2019; LabCol leg.; "\\ Em *Xylodon flaviporus* \\ *Cyparium loebli* von Groll & Lopes-Andrade HOLOTYPUS" [red paper]; CELC (Supp. file 1C).

Paratypes

BRAZIL • 1 ♂, 1 ♀ (same pin); same collection data as for holotype; 8 Dec. 2014; I.S.C. Pecci-Maddalena leg.; CELC • 1 ♂, 2 ♀ (1 ♀, abdomen and head dissected, stored in glycerin); same collection data as for holotype, "Trilha dos Gigantes"; 15 Feb. 2015; S. Aloquio, A. Orsetti and M. Bento leg.; CELC • 2 specs; same collection data as for holotype; 19 Feb. 2015; FIT; A. Orsetti, S. Aloquio and M. Bento leg.; CELC • 1 ♂; same collection data as for holotype; S. Aloquio, A. Orsetti and M. Bento leg.; CELC • 6 ♂♂, 2 ♀♀ (1 ♂ entirely dissected, preserved in glycerin); same collection data as for holotype; "T. da Madeira"; 27 Feb. 2015; I.S.C. Pecci-Maddalena *et al*. leg.; CELC • 1 ♂, 1 ♀; same collection data as for holotype; CAMB • 1 ♀ (head dissected, preserved in glycerin); same collection data as for holotype; 13 Mar. 2015; S. Aloquio, A. Orsetti, C. Lopes-Andrade and M. Bento leg.; CELC • 1 ♂; same collection data as for holotype; 20 Mar. 2015; A. Orsetti and I. Gonçalves leg.; CELC • 6 ♂♂, 2 ♀♀ (2 ♂♂ dissected, preserved in glycerin); same collection data as for holotype; 9 Nov. 2016; I. Pecci-Maddalena and C. Lopes-Andrade leg.; "\\ ex *Psathyrella candolleana*"; CELC • 1 ♂, 1 ♀; same collection data as for holotype; CERPE • 2 ♂♂, 5 ♀♀ (1 ♀, abdomen dissected, preserved in glycerin); same collection data as for holotype; 19 Nov. 2019; LabCol leg.; "\\ em *Agaricus sylvaticus*"; CELC.

All paratypes additionally labelled "*Cyparium loebli* von Groll & Lopes-Andrade PARATYPUS [yellow paper]".

Description

Measurements (holotype, in mm). TL 2.59, PL 1.00, PA 0.80, PB 1.72, EW 1.06, EL 1.86, IS 0.22, HW 0.72.

Coloration. Black, iridescent (Fig. 22A–C). Frons dark brown; clypeus yellowish-brown; mouthparts yellow (Fig. 23A); antennomeres I–VI and apex of XI yellow; VII– basal part of XI darker (Fig. 23A–C). Pronotum, hypomeron and scutellum reddish brown (Fig. 22A). Elytra black, anterior region reddish brown (Fig. 22A). Meso- and metathorax in ventral view brown to dark brown. Procoxae dark ochre; meso- and metacoxae brownish red; femora dark brown, apex light brown; tibiae dark ochre, base and apex lighter; tarsi yellow (Fig. 22B–C). Ventrite 1 dark brown to brown; each next segment lighter; ventrites 5 and 6 yellowish. Variation: some paratypes with pronotum and base of elytra ochreous (Fig. 22D–F).

Head. Punctation dense, fine (Fig. 23A). Eyes wide and rounded (Fig. 23A). Labrum rectangular, lateral margins rounded, well delimited apically; central margins straight and wide; sclerotized portion inwardly curved; lateral setae well exceeding margins of labrum; densely porose centrally (Fig. 23D). Mandibles strongly curved and somewhat long apically; subapical serrations on left mandible conspicuous (Fig. 23E–F). Maxillae with palpomere III short; galea with a row of lateral setae; galea densely pubescent, lacinia moderately pubescent, wider than galea (Fig. 23G). Mentum forming a straight projection apically (Fig. 24A). Setae of labial palpomere II far exceeding palpomere III; palpomere III longish, with short apical setae (Fig. 24A–B). Post-gena microsculptured with close transversal lines; gula densely porose, but limited to central region; gula long and narrow (Fig. 24C). Antennal club well distinct; antennomere XI pentagonal, rounded apically (straight in some individuals); no notable difference between sexes (Fig. 23B–C).

Prothorax. Pronotum smooth, shining; punctuation dense, fine; pubescence short, fine (Fig. 24D–E); transverse, sub-straight laterally, forming an obtuse angle at lateral areas of posterior margin (Fig. 24E). Hypomeron with strigulate microsculpture. Notosternal suture straight, slightly inward directed (Fig. 24F). Profurca thin, only reaching half length of foramen (Fig. 24G). Prosternal process rounded (Fig. 25A).

Mesothorax. Mesonotum with prescutellar suture (= scutellar lines, Leschen & Löbl 2005) wavy (Fig. 25B). Scutellum tapering posteriorly (Fig. 25B). Anterior phragma large and obtuse (Fig. 25C). Mesanepisternum with strigulate microsculpture. Procoxal rests triangular, strongly curved posteriorly (Fig. 25D). Mesoventral and median lines wavy; area between median and mesocoxal lines not specially enlarged (Fig. 25D). Process of metaventrite curved at top and straight at base, forming a ridge (Fig. 25E).

Metathorax. Metanotum with alacrista enlarged anteriorly and turned to sides; scutoscutellar suture curved; median membranous area wide and short (Fig. 25F). Metaventrite smooth, punctuation sparse and fine; coarsely punctate above intercoxal plates (Figs 22B, 25D). Mesocoxal line forming an angle between coxal cavities, and finely punctate under coxal cavities (Fig. 25D). Metanepisternum and metepimeron with imbricate microsculpture. Intercoxal plates smooth. Metendosternite with arms almost straight; 'stalk ridge' exceeding half length of stalk (Fig. 26A); ventral longitudinal flange curved in lateral view (Fig. 26B).

Wings. Elytra slightly wider than longer; partially covering tergite VI (Fig. 26A); basal and lateral lines punctate (Fig. 24D); sutural line dashed; adsutural area with a row of setae; six rows of coarse punctures (not including sutural line), but rows 5 and 6 somewhat intermixed (Figs 22A, 26C); apical coarse punctation sparse; apical serrations small, sparse; pubescence short and fine (Fig. 26D). Epipleuron with diffuse, coarse, and close punctures. Hind wings fully developed (Fig. 26E).

Legs. Pro-, meso- and metacoxae, and femora with strigulate microsculpture. Femora somewhat fusiform (Fig. 26F–H). Pro- and mesofemora sparsely and coarsely punctate; metafemora with shallow and fine

punctation. Mesotibia densely spinose, spines fine (Fig. 26G). Metatibiae sparsely spinose, spine fine (Fig. 26H).

Abdomen. Tergites VI–VIII with imbricate microsculpture (Fig. 27A). Tergite VII triangular; punctation sparse, coarse; pubescence sparse, fine (Fig. 27A). Ventrites (Fig. 27B) sparsely pubescent; with strigulate microsculpture. Ventrite 1 sparsely and coarsely punctate (Fig. 27C). Ventrites 2–5 moderately sparse and finely punctate. Metacoxal lines finely punctate.

Males

Measurements (n = 1, paratype; in mm). Antennomeres (length(width)): 0.15(0.06), 0.11(0.05), 0.10(0.04), 0.08(0.04), 0.08(0.05), 0.06(0.06), 0.09(0.11), 0.08(0.12), 0.08(0.13), 0.08(0.14), 0.13(0.14);

Fig. 22. *Cyparium loebli* sp. nov. **A–C**. Holotype, ♂ (CELC). **A**. Dorsal view. **B**. Ventral view. **C**. Lateral view. **D–F**. Paratype, ♂ (CELC). **D**. Dorsal view. **E**. Ventral view. **F**. Lateral view. Specimens collected at Mata do Paraíso, Viçosa (MG, Brazil). Scale bars = 1.0 mm.

(n = 7, including the holotype; in mm): TL 2.53–2.78 (mean = 2.65, standard deviation ± 0.08), PL 1.00–1.08 (1.02 ± 0.03), PA 0.80–0.84 (0.82 ± 0.02), PB 1.60–1.80 (1.70 ± 0.06), SL 0.13–0.17 (0.15 ± 0.02), SW 0.13–0.16 (0.14 ± 0.01), EI 1.48–1.62 (1.52 ± 0.05), EL 1.74–1.90 (1.82 ± 0.05), EW 0.92–1.06 (0.98 ± 0.05), EH 0.43–0.71 (0.63 ± 0.10), HW 0.70–0.74 (0.72 ± 0.01), IS 0.20–0.23 (0.21 ± 0.01), WA 0.16–0.19 (0.17 ± 0.01), MC 0.68–0.74 (0.70 ± 0.02), MB 0.26–0.36 (0.32 ± 0.04), VL 0.52–0.56 (0.54 ± 0.02).

Pro- and mesotarsomeres I–III enlarged, with tenet setae (Fig. 26F–G). Tergite VIII heptagonal, acuminate posteriorly; punctuation fine, almost inconspicuous; subglabrous (Fig. 27D). Tergite IX with more or less bent ventral struts (Fig. 27E–F). Sternite VIII rectangular, with a small projection (Fig. 27G). Sternite IX triangular at ends and centrally constricted (Fig. 27F). Aedeagus sclerotized, enlarged at base, apex of median lobe long (Fig. 28A–C); openings in dorsal view long and somewhat enlarged, forming an acute angle (Fig. 28C); internal sac with weak irregular sclerites, with two hooks (Fig. 28D–E); parameres thin, longish (Fig. 28A–B).

Females

Measurements (n = 1, paratype). Antennomeres (length(width)): 0.16(0.06), 0.10(0.05), 0.09(0.04), 0.07(0.04), 0.07(0.05), 0.05(0.06), 0.08(0.11), 0.08(0.13), 0.08(0.15), 0.08(0.15), 0.14(0.14); (n = 7,

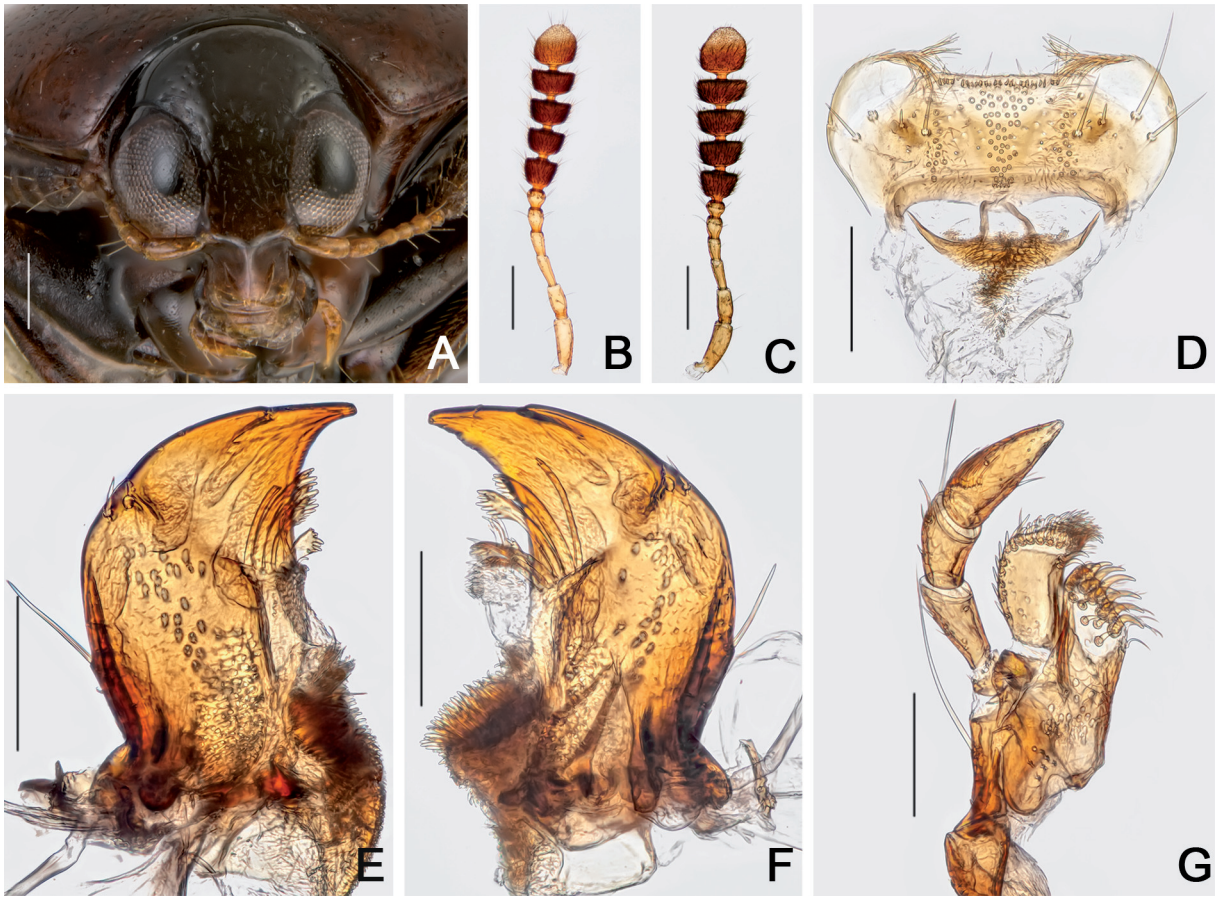

Fig. 23. *Cyparium loebli* sp. nov. **A**. Holotype, ♂ (CELC), frontal view. **B–C**. Antennae. **B**. Paratype, ♂ (CELC). **C**. Paratype, ♀ (CELC). **D–G**. Paratype, ♂ (CELC). **D**. Labrum. **E**. Left mandible. **F**. Right mandible. **G**. Maxilla. Specimens collected at Mata do Paraíso, Viçosa (MG, Brazil). Scale bars: A–C = 0.2 mm; D–G = 0.1 mm.

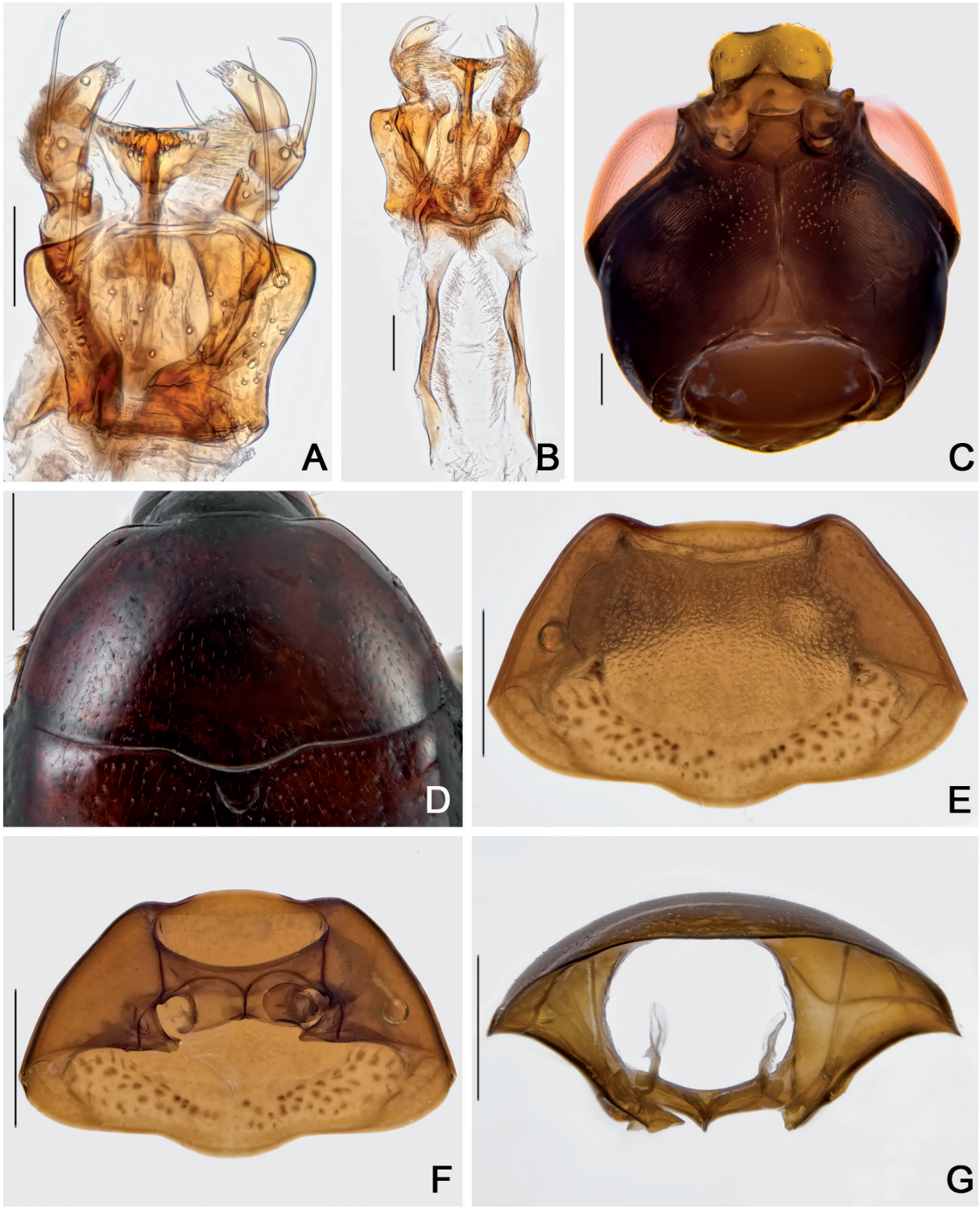

Fig. 24. *Cyparium loebli* sp. nov. **A–C, E–G**. Paratype, ♂ (CELC). **D**. holotype, ♂ (CELC). **A**. Labium. **B**. Hypopharynx. **C**. Head, ventral view. **D–E**. Pronotum, dorsal view. **F**. Prothorax, ventral view. **G**. Prothorax, inner view. Specimens collected at Mata do Paraíso, Viçosa (MG, Brazil). Scale bars: A–B = 0.05 mm; C = 0.1 mm; D–G = 0.5 mm.

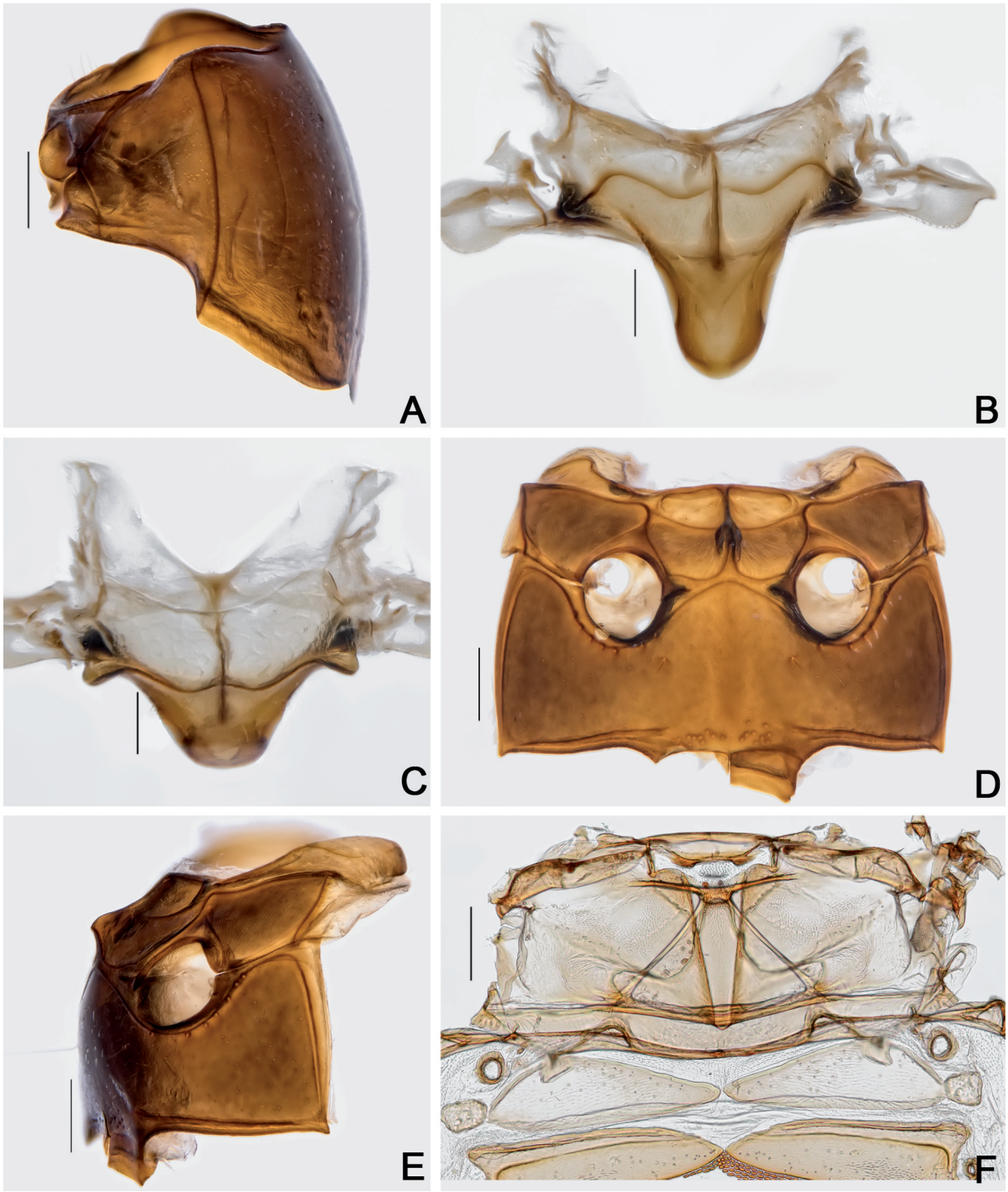

Fig. 25. *Cyparium loebli* sp. nov., paratype, ♂ (CELC). **A**. Prothorax, lateral view. **B–C**. Scutellar plate. **B**. Dorsal view. **C**. Apically slanted view. **D–E**. Meso- and metathorax. **D**. Ventral view. **E**. Lateral view. **F**. Metanotum. Specimen collected at Mata do Paraíso, Viçosa (MG, Brazil). Scale bars: A, D–F = 0.2 mm; B–C = 0.1 mm.

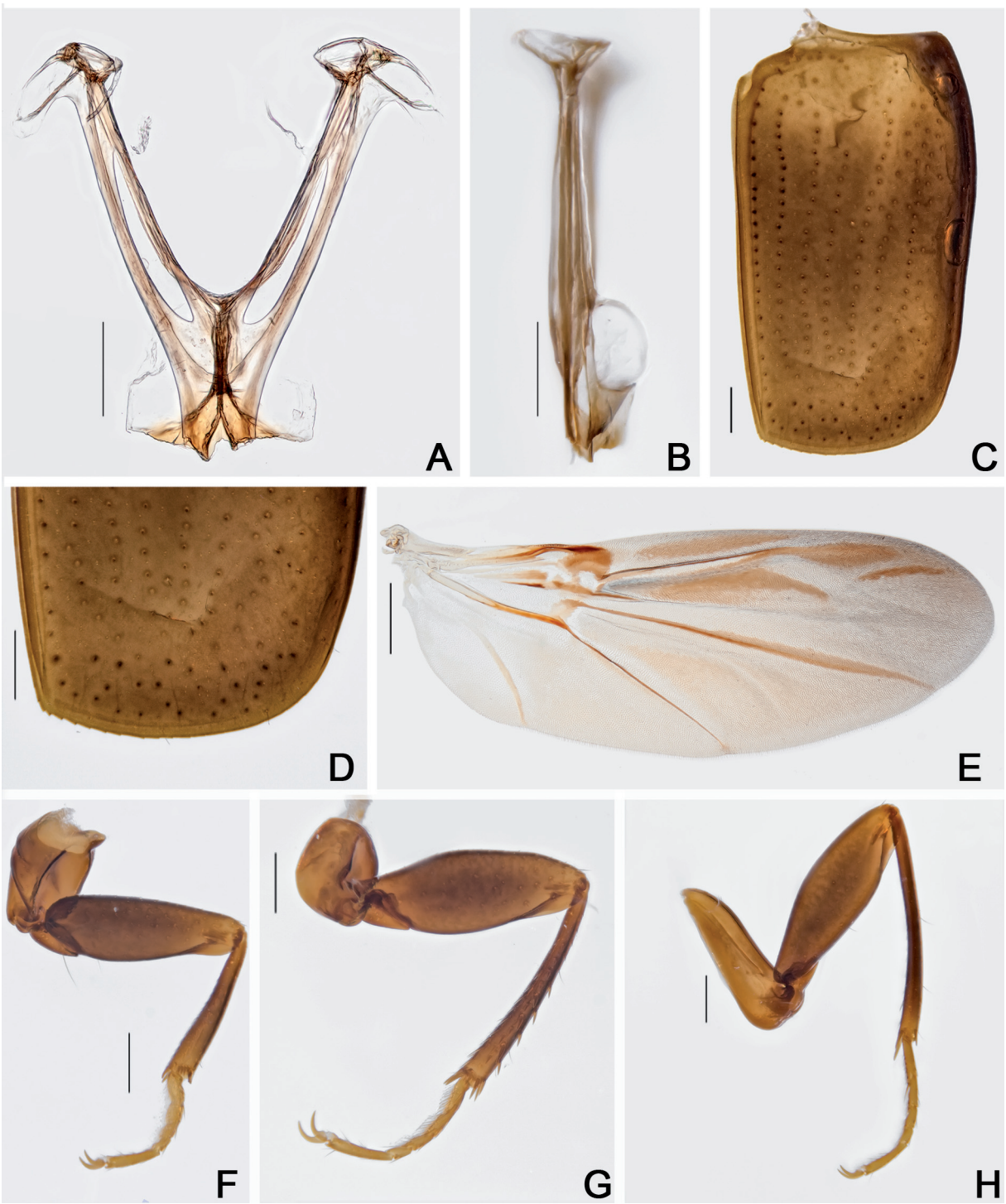

Fig. 26. *Cyparium loebli* sp. nov., paratype, ♂ (CELC). **A–B**. Metendosternite. **A**. Dorsal view. **B**. Lateral view. **C–D**. Elytron. **C**. Entire. **D**. Apex. **E**. Hind wing. **F–H**. Legs. **F**. Fore. **G**. Middle. **H**. Hind. Specimen collected at Mata do Paraíso, Viçosa (MG, Brazil). Scale bars: A–D, F–H = 0.2 mm; E = 0.5 mm.

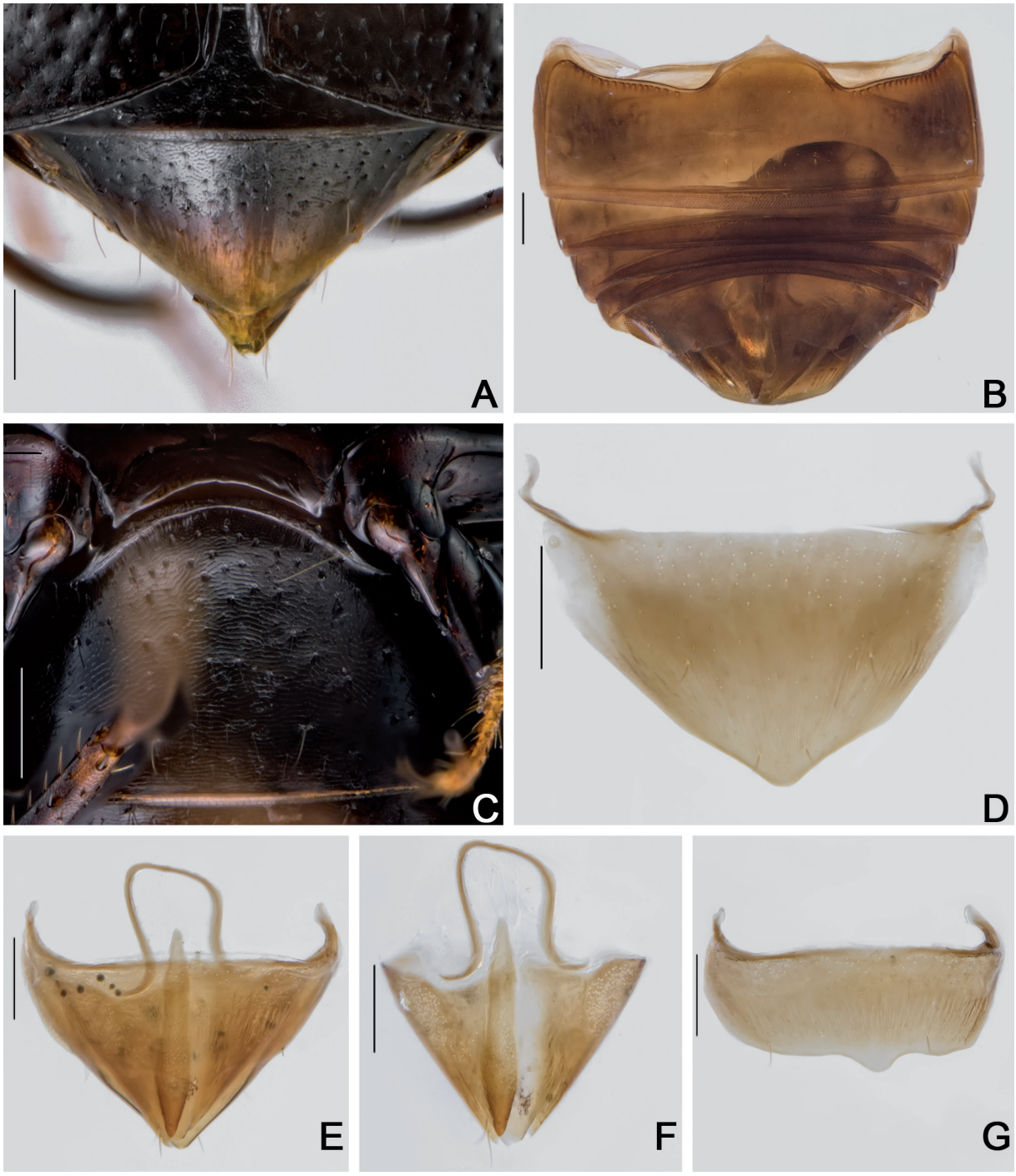

Fig. 27. *Cyparium loebli* sp. nov. **A–C**. Holotype, ♂ (CELC). **D–G**. Paratype, ♂ (CELC). **A**. Abdomen, dorsal view. **B**. Abdomen, ventral view. **C**. Ventrite 1. **D**. Tergite VIII. **E**. Terminalia. **F**. Tergite IX. **G**. Sternite VIII. Specimens collected at Mata do Paraíso, Viçosa (MG, Brazil). Scale bars = 0.2 mm.

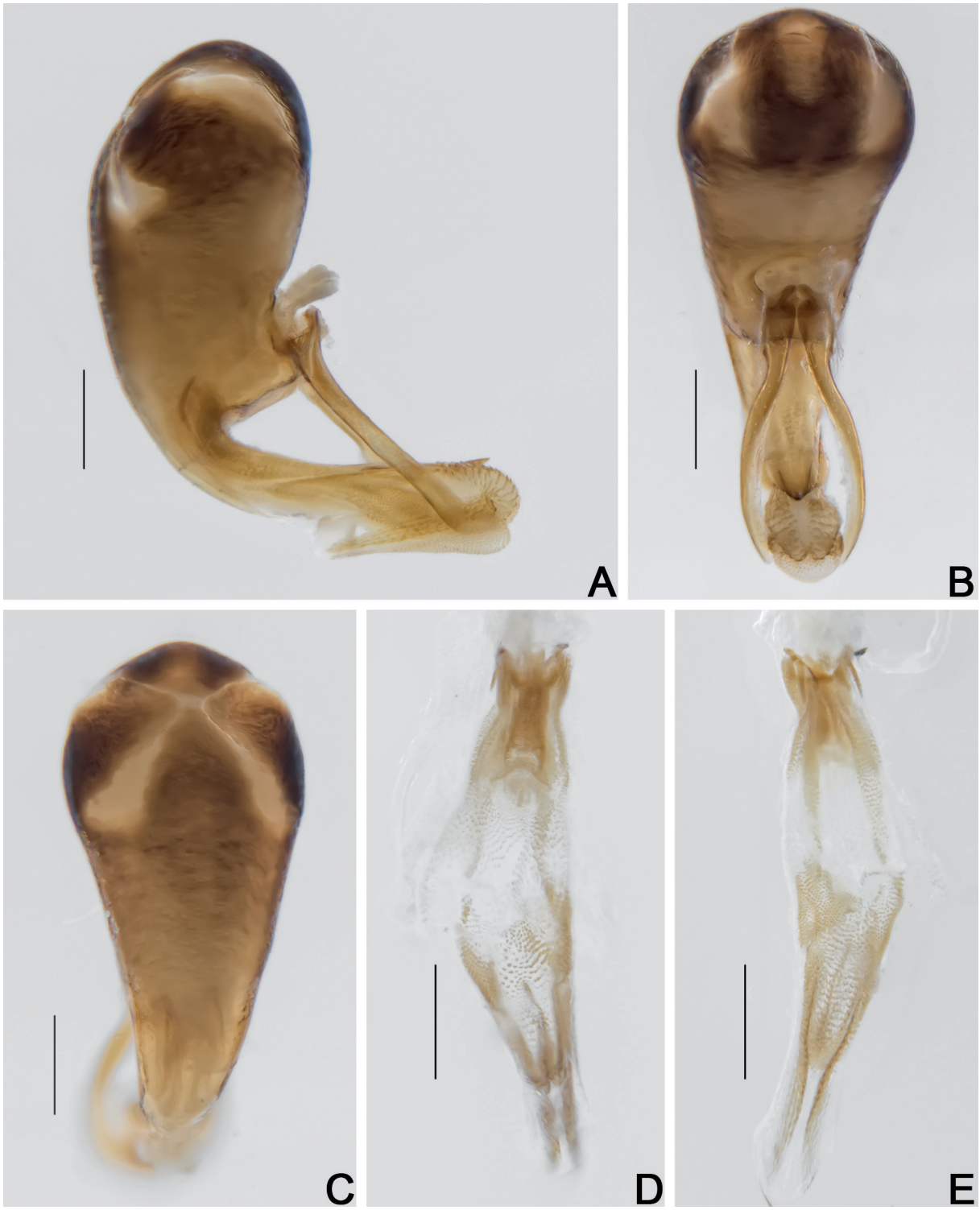

Fig. 28. *Cyparium loebli* sp. nov., paratype, ♂ (CELC). **A–C**. Aedeagus. **A**. Lateral view. **B**. Frontal view. **C**. Dorsal view. **D–E**. Internal sac. **D**. Frontal view. **E**. Dorsal view. Specimen collected at Mata do Paraíso, Viçosa (MG, Brazil). Scale bars = 0.2 mm.

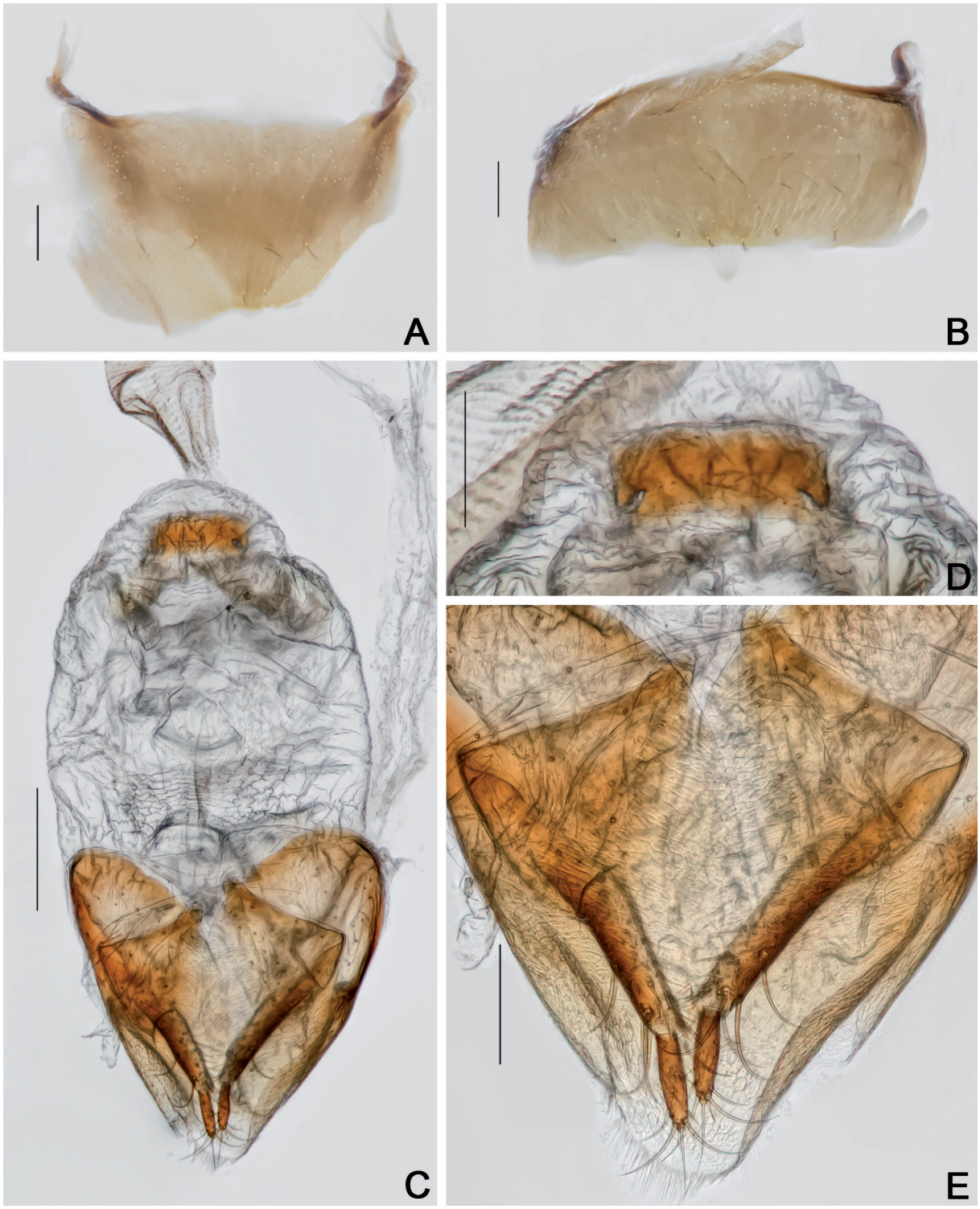

Fig. 29. *Cyparium loebli* sp. nov., paratype, ♀ (CELC). **A**. Tergite VIII. **B**. Sternite VIII. **C**. Terminalia. **D**. Sclerite of vaginal plate. **E**. Ovipositor. Specimen collected at Mata do Paraíso, Viçosa (MG, Brazil). Scale bars: A–B, D–E = 0.1 mm; C = 0.2 mm.

paratypes; in mm): TL 2.34–2.68 (mean = 2.57, standard deviation ± 0.12), PL 0.86–1.02 (0.96 ± 0.05), PA 0.76–0.86 (0.82 ± 0.04), PB 1.50–1.78 (1.68 ± 0.09), SL 0.13–0.17 (0.15 ± 0.01), SW 0.13–0.17 (0.14 ± 0.01), EI 1.40–1.64 (1.52 ± 0.08), EL 1.64–1.98 (1.83 ± 0.11), EW 0.86–1.06 (0.95 ± 0.07), EH 0.65–0.75 (0.69 ± 0.03), HW 0.66–0.74 (0.70 ± 0.02), IS 0.20–0.25 (0.23 ± 0.02), WA 0.17–0.19 (0.18 ± 0.01), MC 0.60–0.76 (0.71 ± 0.06), MB 0.29–0.36 (0.32 ± 0.03), VL 0.46–0.58 (0.54 ± 0.04).

Tergite VIII triangular; punctation inconspicuous; subglabrous (Fig. 29A). Sternite VIII rectangular with a distinct thin projection (Fig. 29B). Vagina and bursa copulatrix membranous without sclerites (Fig. 29C). Vaginal plate with an apical T-shaped sclerite (Fig. 29D). Spermatheca not detected. Distal gonocoxites straight, slender (Fig. 29C, E); gonostyli parallel, long, and slender (Fig. 29C, E).

Host fungi

Adults were collected from *Psathyrella candolleana* (1 record, 10 individuals), *Xylodon flaviporus* (Berk. & M.A. Curtis ex Cooke) Riebesehl & E.Langer (Hymenochaetales, Schizoporaceae) (1, 1) and *Agaricus sylvaticus* (1, 7).

Remarks

Similar to *C. lescheni* sp. nov., especially the teneral specimens, in the strigulate microsculpture of the hypomeron and metaventrite, reddish brown pronotum, and the size of the antennae, but differ in the comparatively larger body length and in the reddish brown anterior region of the elytra.

Distribution

Known only from Mata da Biologia and Mata do Paraíso, campus of the Universidade Federal de Viçosa, Viçosa, state of Minas Gerais, Southeast Brazil (Fig. 46).

Cyparium newtoni sp. nov.
urn:lsid:zoobank.org:act:8E4DB834-61A4-47B2-B9B3-2C0606708142
Figs 4, 30–37, 46; Supp. file 1D

Diagnosis

TL: 2.00–2.22 mm in males and 2.00–2.30 mm in females. Pronotum reddish brown (Fig. 32D). Elytra black (Fig. 30A). Hypomeron with strigulate microsculpture. Metaventrite smooth; coarsely punctate above intercoxal plates (Figs 30B, 33D). Intercoxal plates smooth. Apex of tergite VIII in males straight (Fig. 35D). Aedeagus openings in dorsal view narrow, forming an obtuse angle (Fig. 36C). Internal sac with a plate-like sclerite (Fig. 36D). Tergite VIII in females without apical invagination (Fig. 37A).

Etymology

In homage to Dr Alfred F. Newton (Field Museum, Chicago, USA) for his significant contribution to the systematics of Staphylinidae and more specifically of Scaphidiinae.

Material examined

Holotype

BRAZIL • ♂; Minas Gerais, Viçosa, EPTEA Mata do Paraíso; 19 Nov. 2019; LabCol leg.; "\\ em *Agaricus sylvaticus*\\ *Cyparium newtoni* von Groll & Lopes-Andrade HOLOTYPUS" [red paper]; CELC (Supp. file1D).

Paratypes

BRAZIL • 1 ♀; same collection data as for holotype; 19 Feb. 2015; S. Aloquio, A. Orsetti and M. Bento leg.; "\\ Trilha caminho das águas embaixo de casca de tronco caído"; CELC • 1 ♀; same collection

data as for holotype, "T. dos Gigantes"; 15 Feb. 2015; S. Aloquio, A. Orsetti and M. Bento leg.; CELC • 3 ♂♂, 1 ♀, 2 specs; same collection data as for holotype, "Trilha da Madeira"; 27 Feb. 2015; I.S.C. Pecci-Maddalena *et al*. leg.; CELC • 1 ♂, 1 ♀; same collection data as for holotype; CAMB • 2 ♂♂, 1 ♀; same collection data as for holotype; 13 Mar. 2015; S. Aloquio, A. Orsetti, C. Lopes-Andrade and M. Bento leg.; CELC • 5 ♂♂, 4 ♀♀ (2 ♂♂ dissected, preserved in glycerin); same collection data as for holotype; 9 Nov. 2016; I. Pecci-Maddalena and C. Lopes-Andrade leg.; "\\ ex. *Psathyrella candolleana*"; CELC • 2 ♂♂, 2 ♀♀ (1 ♂ dissected, preserved in glycerin); same collection data as for holotype; 21 Nov. 2019; LabCol leg.; "\\ Em *Agaricus dulcidulus* e *Leucocoprinus brebissoni*"; CELC • 1 ♂, 2 ♀♀, 1 spec. (1 ♂, abdomen dissected, preserved in glycerin); same collection data as for holotype; "\\ Em *Agaricus sylvaticus*"; CELC • 1 ♂, 1 ♀ (1 ♂, abdomen dissected, preserved in glycerin); Viçosa, Recanto das Cigarras, Mata da Biol.; 20 Nov. 2019; LabCol leg.; "Fungo 29 \\ Em *Entoloma* (*Inocephalus*) sp."; CELC • 2 ♂♂, 3 ♀♀, 1 spec. (1 ♂, entirely dissected, preserved in glycerin; 1 ♂, 1 ♀ (abdomen dissected, preserved in glycerin); same collection data as for preceding; "Fungo 08 \\ Em *Psathyrella* sp."; CELC • 1 ♂, 3 ♀♀; Viçosa, Mata da Biologia; 15 Oct. 2021; E. von Groll and A. Orsetti leg.; "Fungo 20 \\ Em *Agaricus* sp."; CELC.

All paratypes additionally labelled "*Cyparium newtoni* von Groll & Lopes-Andrade PARATYPUS [yellow paper]".

Description

Measurements (holotype, in mm). TL 2.00, PL 0.72, PA 0.60, PB 1.30, EW 0.74, EL 1.44, IS 0.17, HW 0.56.

Coloration. Frons dark brown; clypeus and mouthparts yellowish brown (Fig. 30D); antennomeres I–VI yellowish brown; VII–XI darker (Fig. 31A–C). Pronotum and hypomeron reddish brown (Fig. 30A–B). Scutellum ochre or black (Fig. 32D). Meso- and metathorax reddish-brown, each sclerite lighter laterally (Fig. 30B). Elytra black; epipleuron dark ochre (Fig. 30A). Coxae and trochanters dark ochre; femora dark ochre, apex lighter; tibiae dark ochre; lighter anteriorly and posteriorly; tarsi yellow (Fig. 30B–C). Tergite VIII yellow. Ventrite 1 dark ochre, 2–4 ochre, 5 and 6 yellow (Fig. 35C). Variation: few paratypes entirely dark brown, with lighter tarsi; others with reddish brown area less vibrant.

Head. Punctation dense, fine (Fig. 31A). Eyes globose in frontal view (Fig. 31A). Labrum rectangular, lateral margins rounded, well delimited apically; central margin straight; sclerotized portion inwardly curved; lateral setae extending well beyond margins of labrum; little porose centrally (Fig. 31D). Mandibles slightly curved; subapical serrations on left mandible conspicuous (Fig. 31E–F). Maxillary palps elongated; galea and lacinia moderately pubescent, lacinia elongated (Fig. 31G). Mentum slightly curved apically (Fig. 32A–B). Setae of labial palpomere II extending beyond palpomere III; palpomere III longish with short apical setae (Fig. 32A–B). Hypopharynx with wide and rounded sclerotized plate (Fig. 32A–B). Post gena microsculptured with transversal lines; few gular pores (Fig. 32C); gula narrow. Antennal club well distinct; antennomere XI longish, hexagonal (apex rounded in some specimens); antennal club different between sexes (Fig. 31B–C).

Prothorax. Pronotum smooth, shining; punctuation dense, fine; pubescence short, fine (Fig. 32D–E); transverse, sub-straight laterally, forming an obtuse angle at lateral areas of posterior margin (Fig. 32E). Hypomeron with strigulate microsculpture. Notosternal suture straight, inward directed (Fig. 32F). Profurca thin and elongated, slightly extending beyond half of foramen (Fig. 32G). Prosternal process acuminated (Fig. 33A).

Mesothorax. Mesonotum with prescutellar suture (= scutellar lines, Leschen & Löbl 2005) strongly wavy (Fig. 33B). Scutellum rounded posteriorly (Fig. 33B). Anterior phragma large and straight (Fig. 33C). Mesanepisternum with strigulate microsculpture. Procoxal rests wide; slightly curved posteriorly

(Fig. 33D). Mesoventral lines wavy and obtuse; median lines moderately wavy; area between median and mesoventral lines not specially enlarged (Fig. 33D). Process of metaventrite short, slightly curved at top and base, forming a small ridge (Fig. 33E).

Metathorax. Metanotum with alacrista enlarged anteriorly and turned to the sides; scutoscutellar suture strongly curved; median membranous area wide and short (Fig. 33F). Metaventrite smooth; punctuation sparse, fine; coarsely punctate above intercoxal plates (Fig. 33D). Mesocoxal line not forming an angle between coxal cavities, just a simple triangle, and finely punctate under coxal cavities (Fig. 33D). Metanepisternum smooth; metepimeron with imbricate microsculpture. Intercoxal plates smooth.

Fig. 30. *Cyparium newtoni* sp. nov. **A–C**. Holotype, ♂ (CELC). **A**. Dorsal view. **B**. Ventral view. **C**. Lateral view. **D–E**. Paratype, unknown sex (CELC). **D**. Dorsal view. **E**. Lateral view. **F**. Paratype, ♀ (CELC), dorsal view. Specimens collected at Mata do Paraíso (A–C) and Mata da Biologia (D–F), Viçosa (MG, Brazil). Scale bars = 1.0 mm.

Metendosternite with arms almost straight; 'stalk ridge' not exceeding half of stalk (Fig. 34A); ventral longitudinal flange small, curved in lateral view (Fig. 34B).

Wings. Elytra slightly wider than longer; partially covering tergite VI (Fig. 30A); basal and lateral lines punctate; sutural lines dashed (Fig. 32D); adsutural area with a row of setae; six rows of coarse punctures (not including sutural line) (Figs 30A, 34C); apical coarse punctation sparse; apical serrations almost inconspicuous (Fig. 34D); pubescence short and fine. Epipleuron with diffuse and coarse punctures. Hind wings fully developed (Fig. 34E).

Legs. Pro-, meso- and metacoxae, and femora with strigulate microsculpture. Femora longish, somewhat fusiform (Fig. 34F–H). Pro- and mesofemora sparsely and coarsely punctate; metafemora with shallow and sparse punctuation. Mesotibiae densely spinose, spines fine (Fig. 34G); metatibiae sparsely spinose, spines fine (Fig. 34H).

Abdomen. Tergite VI–VIII with imbricate microsculpture (Fig. 35A). Tergite VII trapezoidal (Fig 35A) – triangular in some paratypes with tergite VIII not exposed; punctation sparse, fine; pubescence sparse, fine. Ventrites 1–5 (Fig. 35B) sparsely and finely punctate; pubescence sparse, fine; with strigulate microsculpture (Fig. 35C). Metacoxal lines finely punctate.

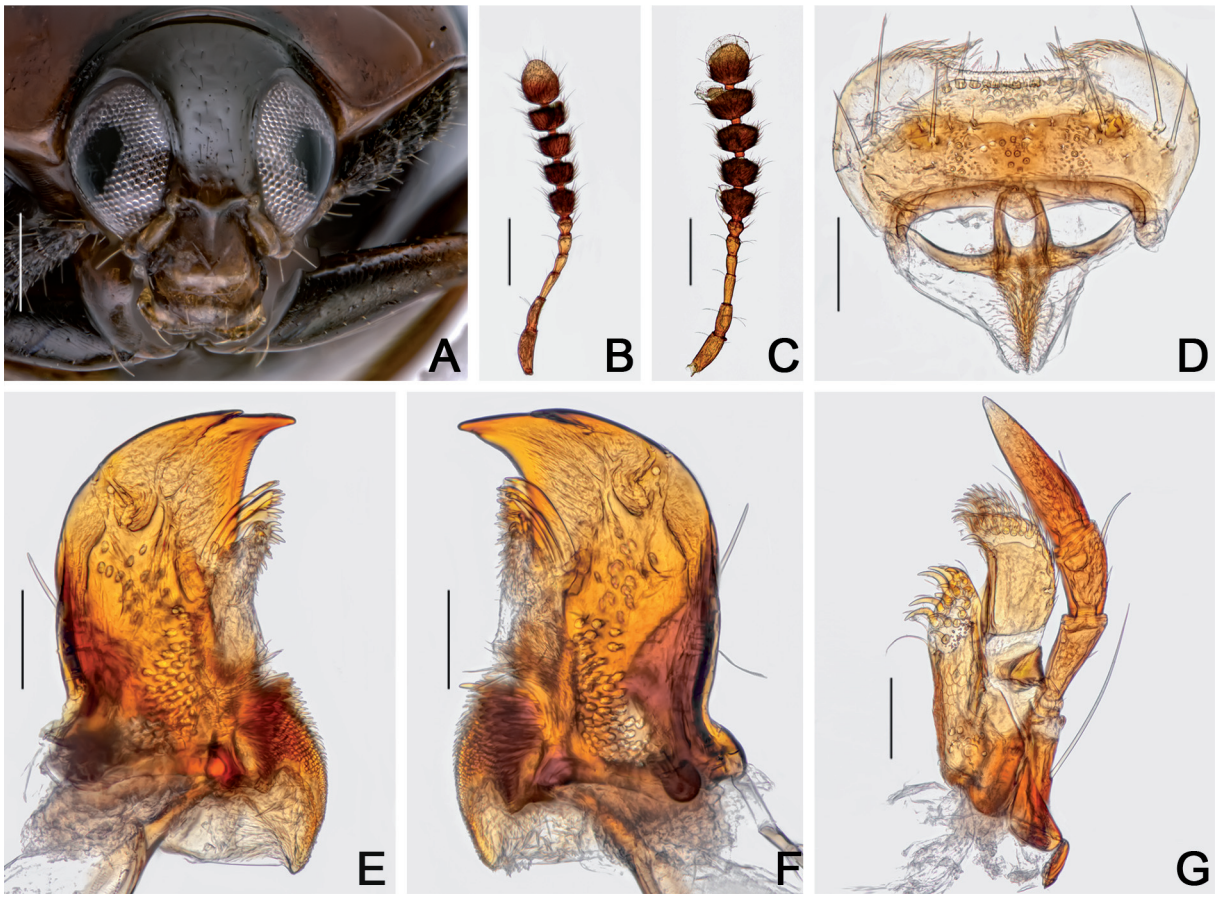

Fig. 31. *Cyparium newtoni* sp. nov. **A**. Holotype, ♂ (CELC), frontal view. **B–G**. Paratypes. **B**. Male antenna. **C**. Female antenna. **D**. Labrum. **E**. Left mandible. **F**. Right mandible. **G**. Maxilla. Specimens collected at Mata do Paraíso (A) and Mata da Biologia (B–G), Viçosa (MG, Brazil). Scale bars: A–C =1.0 mm; D–F = 0.2 mm; G–J = 0.05 mm.

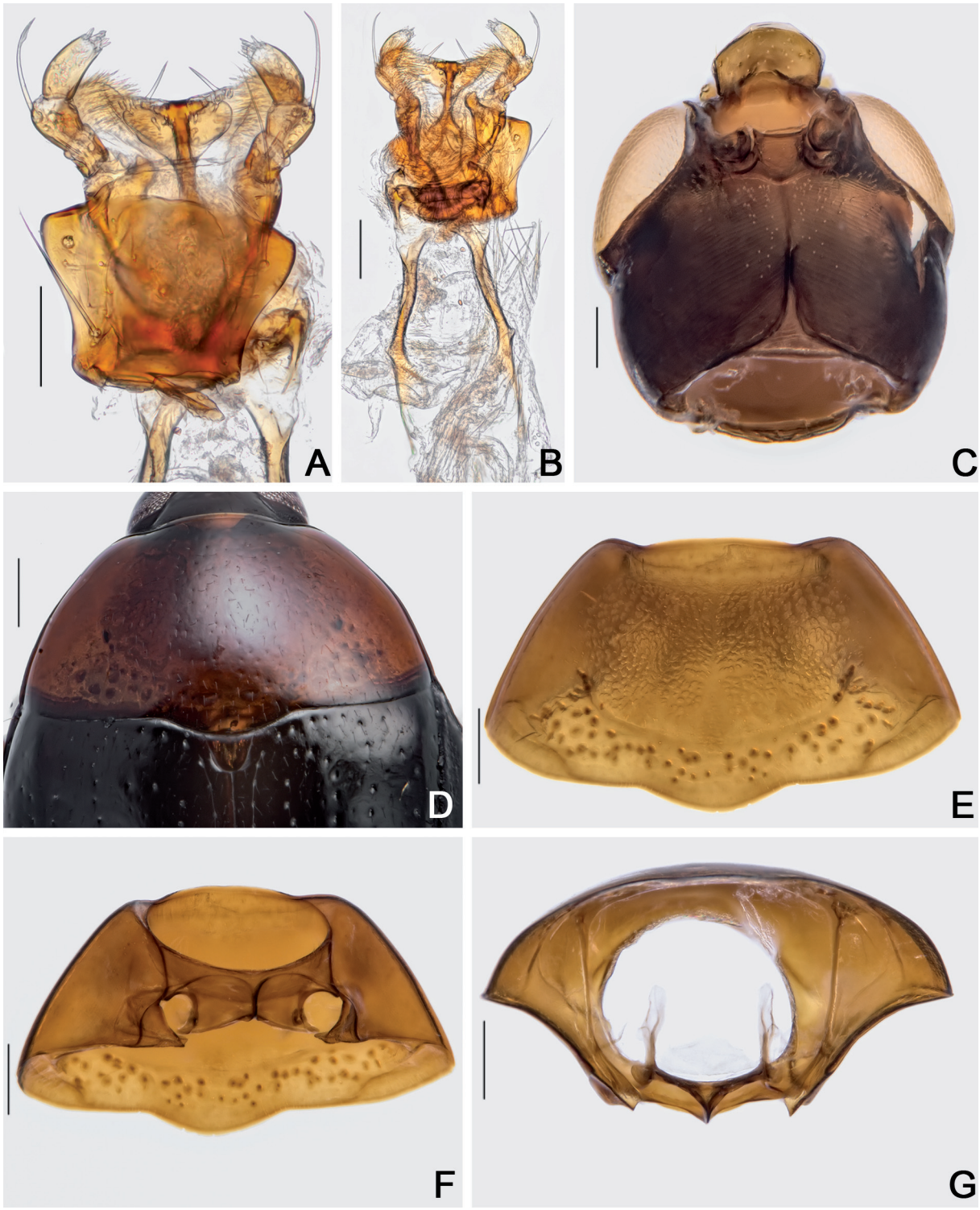

Fig. 32. *Cyparium newtoni* sp. nov. **A–C, E–G**. Paratype, ♂ (CELC). **A**. Labium. **B**. Hypopharynx. **C**. Head, ventral view. **D**. Holotype, ♂ (CELC), pronotum, dorsal view. **E–G**. Prothorax. **E**. Dorsal view. **F**. Ventral view. **G**. Inner view. Specimens collected at Mata da Biologia (A–C) and Mata do Paraíso (D–G), Viçosa (MG, Brazil). Scale bars: A–B = 0.05 mm; C = 0.1 mm; D–G = 0.2 mm.

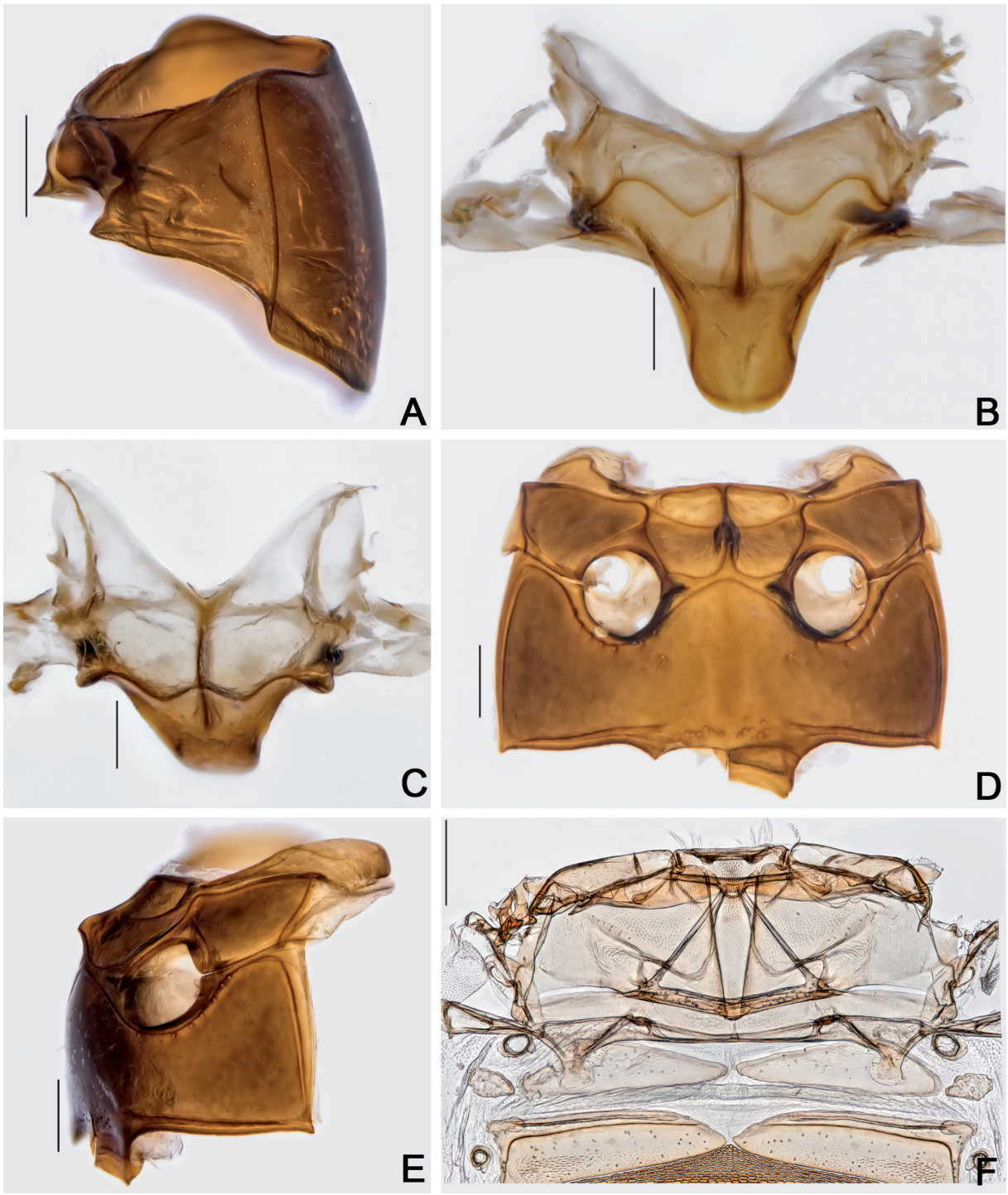

Fig. 33. *Cyparium newtoni* sp. nov., paratype, ♂ (CELC). **A**. Prothorax, lateral view. **B–C**. Scutellar plate. **B**. Dorsal view. **C**. Apically slanted view. **D–E**. Meso- and metathorax. **D**. Ventral view. **E**. Lateral view. **F**. Metanotum. Specimens collected at Mata do Paraíso (A. D–F) and Mata da Biologia (B–C), Viçosa (MG, Brazil). Scale bars: A, D–F = 0.2 mm; B–C = 0.1 mm.

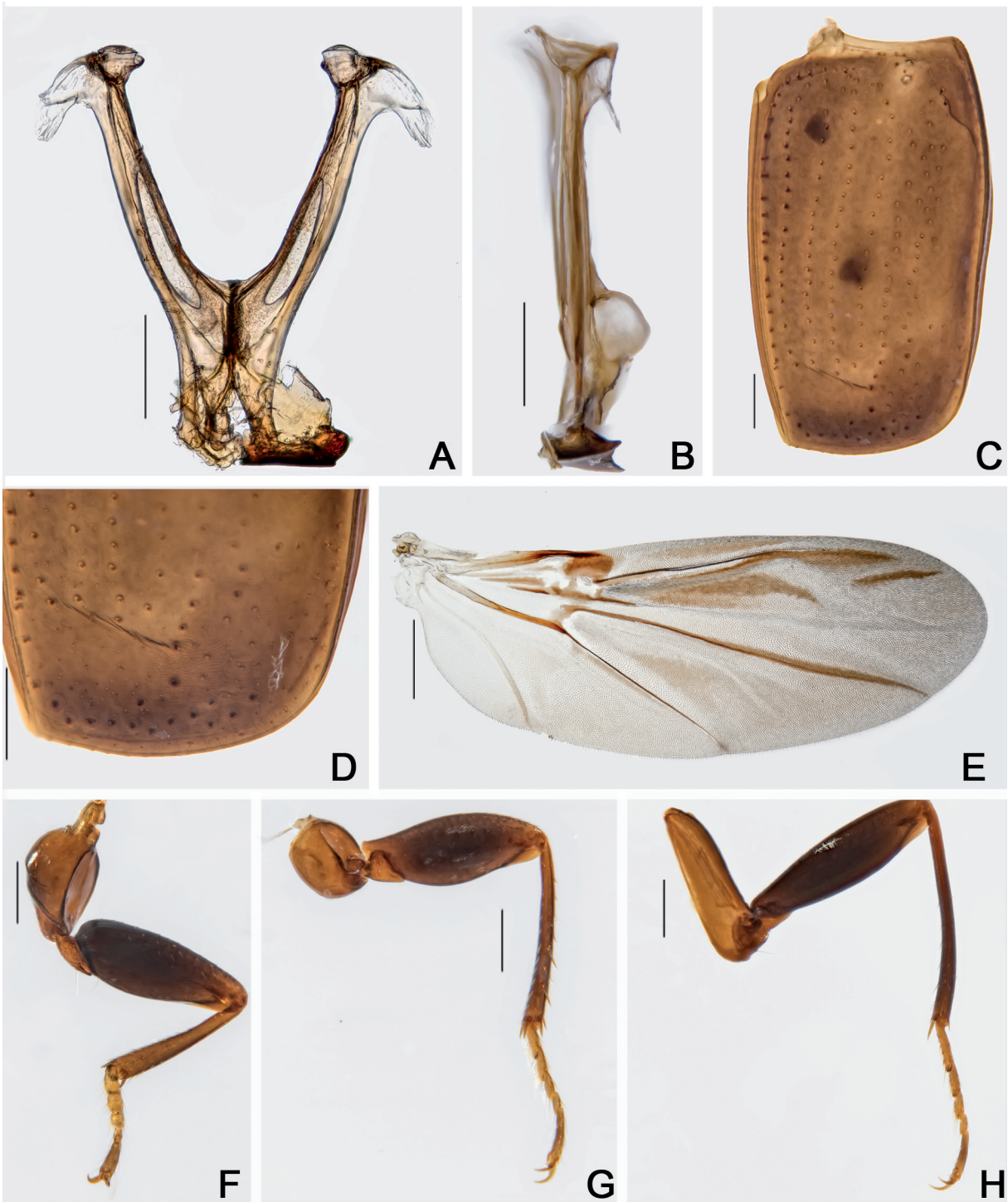

Fig. 34. *Cyparium newtoni* sp. nov., paratype, ♂ (CELC). **A–B**. Metendosternite. **A**. Dorsal view. **B**. Lateral view. **C–D**. Elytron. **C**. Entire. **D**. Apex. **E**. Hind wing. **F–H**. Legs. **F**. Fore. **G**. Middle. **H**. Hind. Specimens collected at Mata da Biologia, Viçosa (MG, Brazil). Scale bars: A–D, F–H = 0.2 mm; E = 0.5 mm.

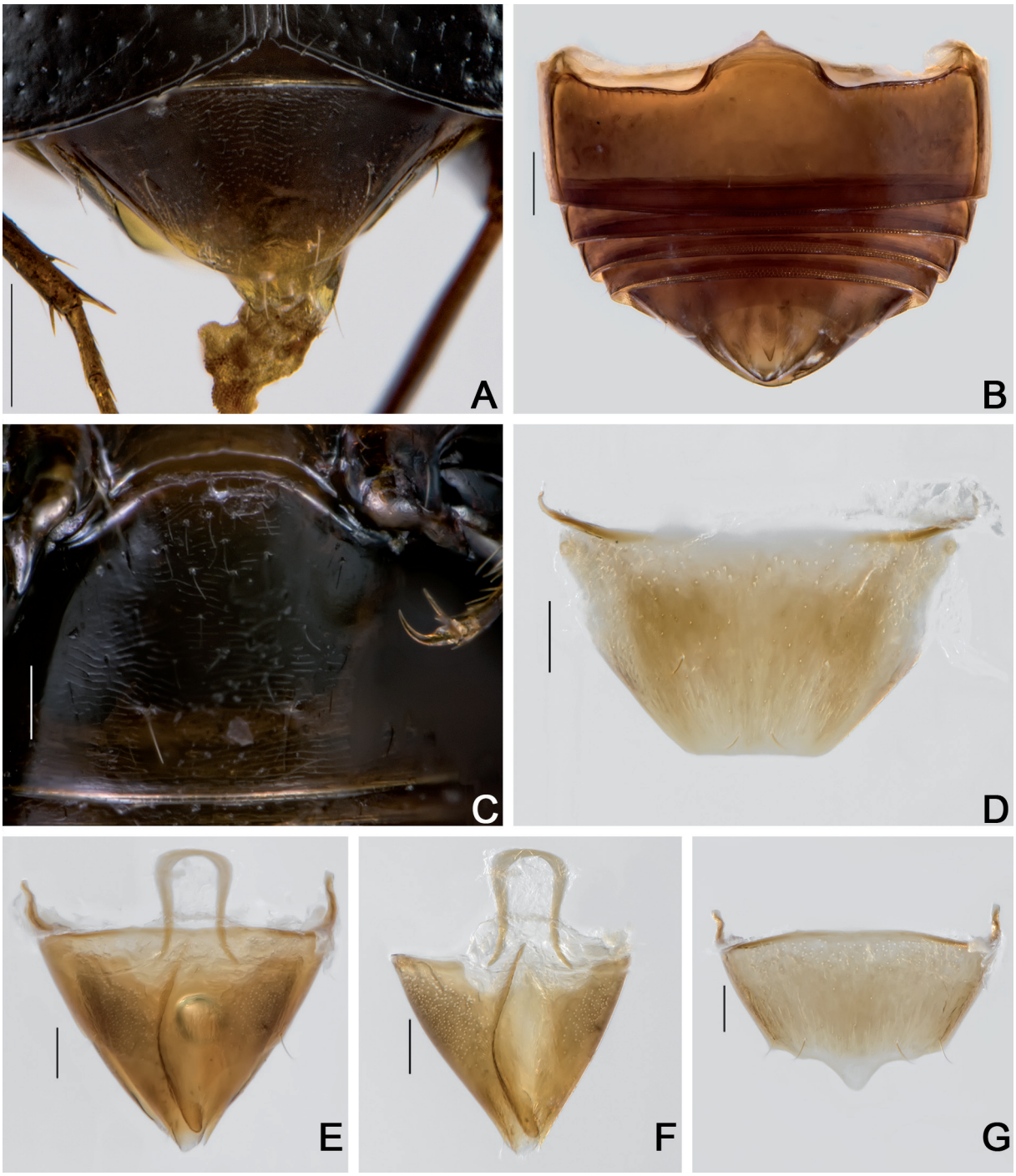

Fig. 35. *Cyparium newtoni* sp. nov. **A, C**. Holotype, ♂ (CELC). **B, D–G**. Paratype, ♂ (CELC). **A**. Abdomen, dorsal view. **B**. Abdomen, ventral view. **C**. Ventrite 1. **D**. Tergite VIII. **E**. Terminalia. **F**. Tergite IX. **G**. Sternite VIII. Specimens collected at Mata do Paraíso, Viçosa (MG, Brazil). Scale bars: A–B = 0.2 mm; C–G= 0.1 mm.

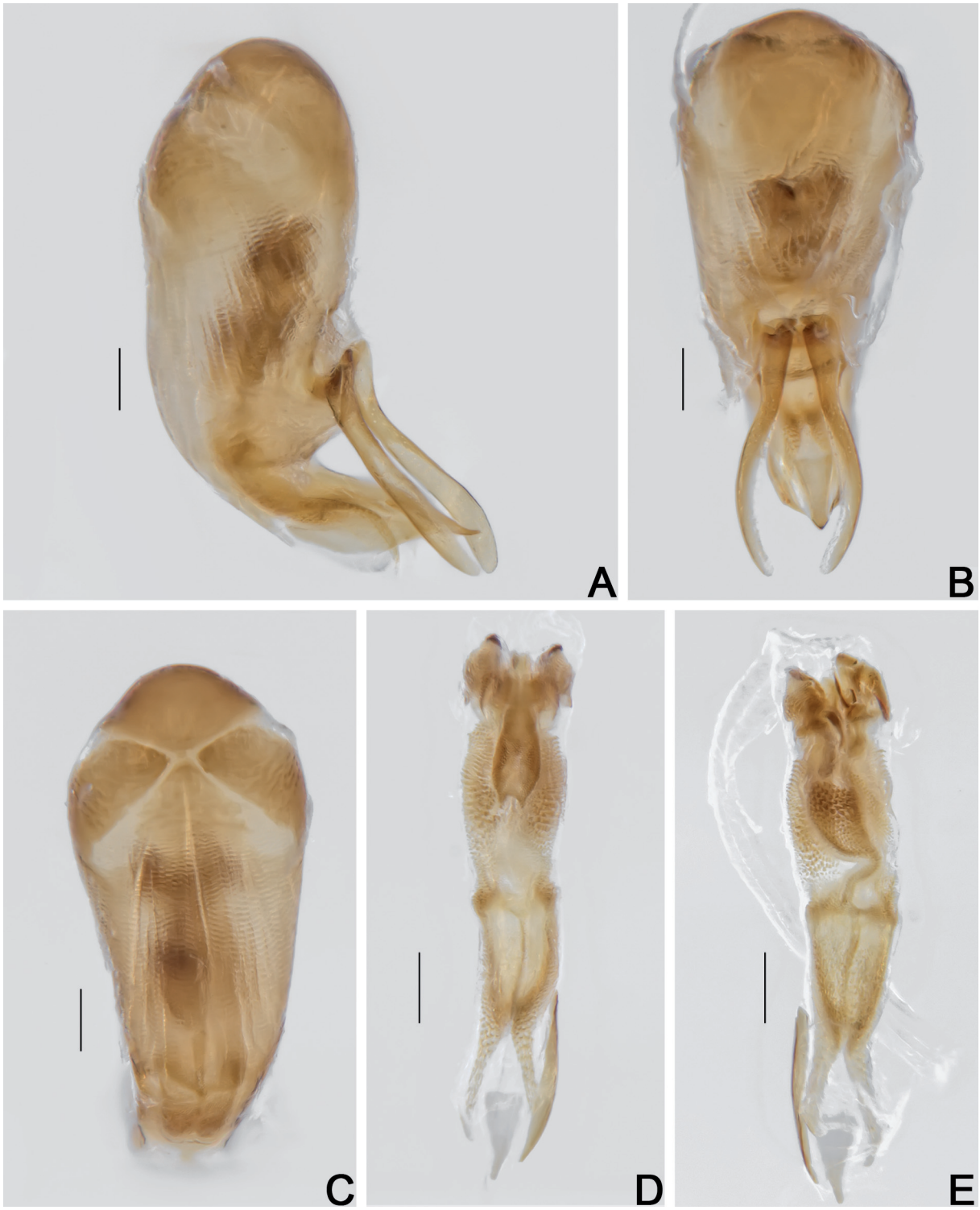

Fig. 36. *Cyparium newtoni* sp. nov., paratype, ♂ (CELC). **A–C**. Aedeagus. **A**. Lateral view. **B**. Frontal view. **C**. Dorsal view. **D–E**. Internal sac. **D**. Frontal view. **E**. Dorsal view. Specimen collected at Mata do Paraíso, Viçosa (MG, Brazil). Scale bars = 0.1 mm.

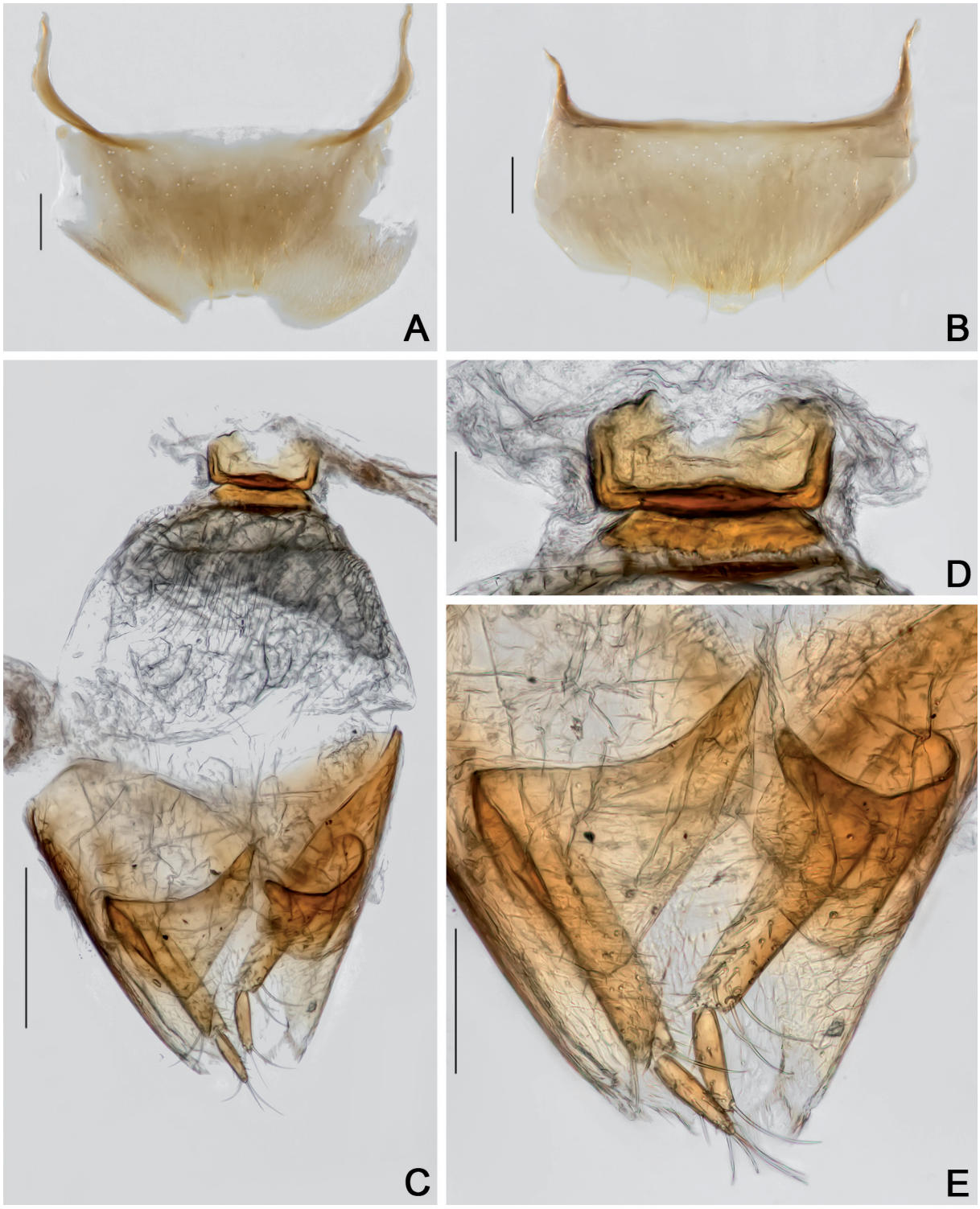

Fig. 37. *Cyparium newtoni* sp. nov., paratype, ♀ (CELC). **A**. Tergite VIII. **B**. Sternite VIII. **C**. Terminalia. **D**. Sclerite of vaginal plate. **E**. Ovipositor. Specimen collected at Mata da Biologia, Viçosa (MG, Brazil). Scale bars: A–B, E = 0.1 mm; C = 0.2 mm; D = 0.05 mm.

Males

Measurements (n = 1, paratype; in mm). Antennomeres (length(width)): 0.13(0.06), 0.10(0.04), 0.08(0.03), 0.05(0.03), 0.06(0.04), 0.05(0.05), 0.08(0.09), 0.06(0.09), 0.07(0.10), 0.06(0.11), 0.13(0.11); (n = 7, including holotype; in mm): TL 2.00–2.22 (mean = 2.07, standard deviation ± 0.08), PL 0.70–0.80 (0.74 ± 0.03), PA 0.60–0.68 (0.63 ± 0.02), PB 1.28–1.40 (1.33 ± 0.04), SL 0.09–0.12 (0.10 ± 0.01), SW 0.10–0.12 (0.10 ± 0.01), EI 1.20–1.32 (1.25 ± 0.05), EL 1.40–1.54 (1.46 ± 0.05), EW 0.66–0.86 (0.77 ± 0.06), EH 0.50–0.62 (0.58 ± 0.04), HW 0.52–0.62 (0.57 ± 0.03), IS 0.17–0.18 (0.17 ± 0.00), WA 0.10–0.14 (0.13 ± 0.01), MC 0.52–0.61 (0.57 ± 0.02), MB 0.25–0.28 (0.27 ± 0.01), VL 0.42–0.56 (0.48 ± 0.04).

Antennal club less distinct than in females (Fig. 31B). Pro- and mesotarsomeres I–III enlarged, with tenet setae (Fig. 34F–G). Tergite VIII hexagonal, straight posteriorly; punctuation inconspicuous; subglabrous (Fig. 35D). Tergite IX with constricted ventral struts (Fig. 35E–F). Sternite VIII sub-rectangular, with projection (Fig. 35G). Sternite IX curved (Fig. 35F). Aedeagus sclerotized, apex of median lobe short (Fig. 36A,B); openings in dorsal view narrow, forming an obtuse angle (Fig. 36C); internal sac with weak irregular sclerites with two hooks and a central plate (Fig. 36D–E); parameres long, thin (Fig. 36B).

Females

Measurements (n = 1, paratype; in mm). Antennomeres (length(width)): 0.13(0.05), 0.10(0.05), 0.09(0.03), 0.05(0.04), 0.06(0.04), 0.05(0.05), 0.08(0.10), 0.09(0.11), 0.09(0.13), 0.09(0.14), 0.13(0.12); (n = 7, paratypes; in mm): TL 2.00–2.30 (mean = 2.19, standard deviation ± 0.12), PL 0.76–0.84 (0.78 ± 0.03), PA 0.6–0.7 (0.64 ± 0.04), PB 1.30–1.48 (1.41 ± 0.07), SL 0.11–0.15 (0.12 ± 0.01), SW 0.11–0.14 (0.12 ± 0.01), EI 1.22–1.44 (1.34 ± 0.07), EL 1.44–1.64 (1.58 ± 0.06), EW 0.80–0.88 (0.83 ± 0.02), EH 0.57–1.07 (0.65 ± 0.18), HW 0.31–0.62 (0.55 ± 0.11), IS 0.16–0.18 (0.17 ± 0.01), WA 0.14–0.17 (0.15 ± 0.01), MC 0.56–0.65 (0.61 ± 0.03), MB 0.27–0.32 (0.30 ± 0.01), VL 0.45–0.52 (0.50 ± 0.03).

Antennal club more distinct than in males (Fig. 31B–C). Tergite VIII hexagonal; punctuation inconspicuous; subglabrous (Fig. 37A). Sternite VIII rectangular with a smooth projection (Fig. 37B). Vagina and bursa copulatrix membranous without sclerites (Fig. 37C). Vaginal plate with an apical sclerite (Fig. 37D). Spermatheca not detected. Distal gonocoxites straight and thin (Fig. 37C, E); gonostyli long, slender, larger at base (Fig. 37C, E).

Host fungi

Adults were collected from *Psathyrella candolleana* (1 record, 9 individuals), *Psathyrella* sp. (1, 6), *Agaricus* sp. (1, 4; von Groll *et al.* 2021: figs 1–4), *A. dulcidulus* (1, 4), *A. sylvaticus* (1, 5) and *Entoloma* (*Inocephalus*) sp. (1, 2).

Remarks

Extremely similar to *C. lescheni* sp. nov. (for comparison, see remarks under *C. lescheni* above and comparison of morphology below).

Distribution

Known only from Mata da Biologia and Mata do Paraíso, campus of the Universidade Federal de Viçosa, Viçosa, state of Minas Gerais, Southeast Brazil (Fig. 46).

Cyparium pici sp. nov.
urn:lsid:zoobank.org:act:7BE94FA9-A727-4779-B8FE-975D5C178ABC
Figs 5, 38–46; Supp. file 1E

Diagnosis

TL: 3.35–4.20 mm in males and 4.20–4.35 mm in females. Black. Antennae entirely yellow; club lighter (Fig. 38A). Anterior region of elytra reddish brown (Fig. 38A). Hypomeron and mesanepisternum with

close strigulate microsculpture. Metaventrite smooth; coarsely punctate above intercoxal plates (Fig. 38B, E). Ventrites 1–5 densely and coarsely punctate (Fig. 43C). Aedeagus strongly sclerotized, apex short; parameres short (Fig. 44A–B). Sclerites of internal sac strong (Fig. 44D–E). Distal gonocoxites short, straight and thick (Fig. 45E).

Etymology

In homage to Maurice Pic (1866–1957), who was responsible for gathering many specimens of scaphidiines deposited in museums, especially in the MNHN.

Material examined

Holotype

BRAZIL • ♂; Mato Grosso, Cotriguaçu, Faz. São Nicolau, matinha do Fernando [Fernando's woods]; 09°50′19″ S, 58°15′15″ W; FIT; 3 Nov. 2017; Vaz-de-Mello *et al*. leg.; "\\ *Cyparium pici* von Groll & Lopes-Andrade HOLOTYPUS" [red paper]; CEMT (Supp. file 1E).

Paratypes

BRAZIL • 8 ♂♂, 5 ♀♀ (1 ♂ entirely dissected, preserved in glycerin); same collection data as for holotype; CEMT • 3 ♂♂, 2 ♀♀ (2 ♂♂, 1 ♀, entirely dissected, preserved in glycerin; 1 ♀, abdomen dissected, preserved in glycerin); same collection data as for holotype; CELC.

All paratypes additionally labelled "*Cyparium pici* von Groll & Lopes-Andrade PARATYPUS [yellow paper]".

Description

Measurements (in mm). TL 3.45, PL 1.30, PA 1.12, PB 2.15, EW 1.42, EL 2.71, IS 0.28, HW 0.93.

Coloration. Black (Fig. 38A–C). Frons dark brown; clypeus light brown; mouth parts and antennae yellow, club lighter (Fig. 39A). Anterior region of elytra reddish brown (Fig. 38A); epipleuron dark ochre. Femora dark brown; tibiae lighter; tarsi yellow (Fig. 38B). Tergite VIII and ventrite 6 yellowish (Fig. 38B). Variation: (1) entirely light brown (Fig. 38D); (2) entirely dark brown with antennae, tarsi and tergite VIII yellow (Fig. 38E–F).

Head. Punctation dense, coarse (Fig. 39A). Eyes slightly wider than head, rounded (Fig. 39A). Labrum rectangular, lateral margins sub-straight, and well distinct from apical margin; central margin slightly curved centrally; sclerotized portion reaching apex; lateral setae slightly extending beyond margins; porose centrally (Fig. 39D). Left mandible slightly curved and right mandible more curved; subapical serrations on left mandible conspicuous (Fig. 39E–F). Maxillary palps elongated, palpomeres slender anteriorly; lacinia strongly robust, short and densely pubescent (Fig. 39G). Mentum with lateral areas strongly rounded and apex well delimited (Fig. 40A). Glossa heart-shaped (Fig. 40A). Setae of labial palpomere II slightly exceeding palpomere III; palpomere III longish, with short apical setae (Fig. 40A). Hypopharynx with wide and triangular sclerotized plate (Fig. 40B). Post gena microsculptured with very close transversal lines; densely porose, except at region of gula; gula triangular and narrow (Fig. 40C). Antennal club distinct; antennomere XI hexagonal, apex more or less acuminated, regardless of sex (Fig. 39B–C).

Prothorax. Pronotum smooth; punctuation dense, fine; pubescence short, fine (Fig. 40D); transverse, rounded laterally, forming a small obtuse angle at lateral areas of posterior margin (Fig. 40E). Hypomeron with close strigulate microsculpture. Notosternal suture straight (Fig. 40F). Profurca elongated, only reaching half length of foramen (Fig. 40G). Prosternal process short and round (Fig. 41A).

Mesothorax. Mesonotum with prescutellar suture (= scutellar lines, Leschen & Löbl 2005) wavy (Fig. 41B). Scutellum rounded posteriorly (Fig. 41B). Anterior phragma straight (Fig. 41C). Mesanepisternum with strigulate microsculpture. Procoxal rests triangular; slightly wavy posteriorly (Fig. 41D). Mesoventral and median lines strongly wavy; area between median and mesoventral lines enlarged (Fig. 41D). Process of metaventrite moderately long; apex more prominent, forming a ridge (Fig. 41E).

Metathorax. Metanotum with alacrista triangular, small anteriorly and turned to posterior end; scutoscutellar suture not strongly wavy; median membranous area narrow and long (Fig. 41F). Metaventrite smooth; punctuation sparse, fine; coarsely punctate above intercoxal plates (Figs 38B, E, 41D). Mesocoxal line forming a smooth angle between coxal cavities; finely punctate under coxal cavities (Fig. 41D). Metanepisternum and metepimeron with imbricate microsculpture. Intercoxal plates

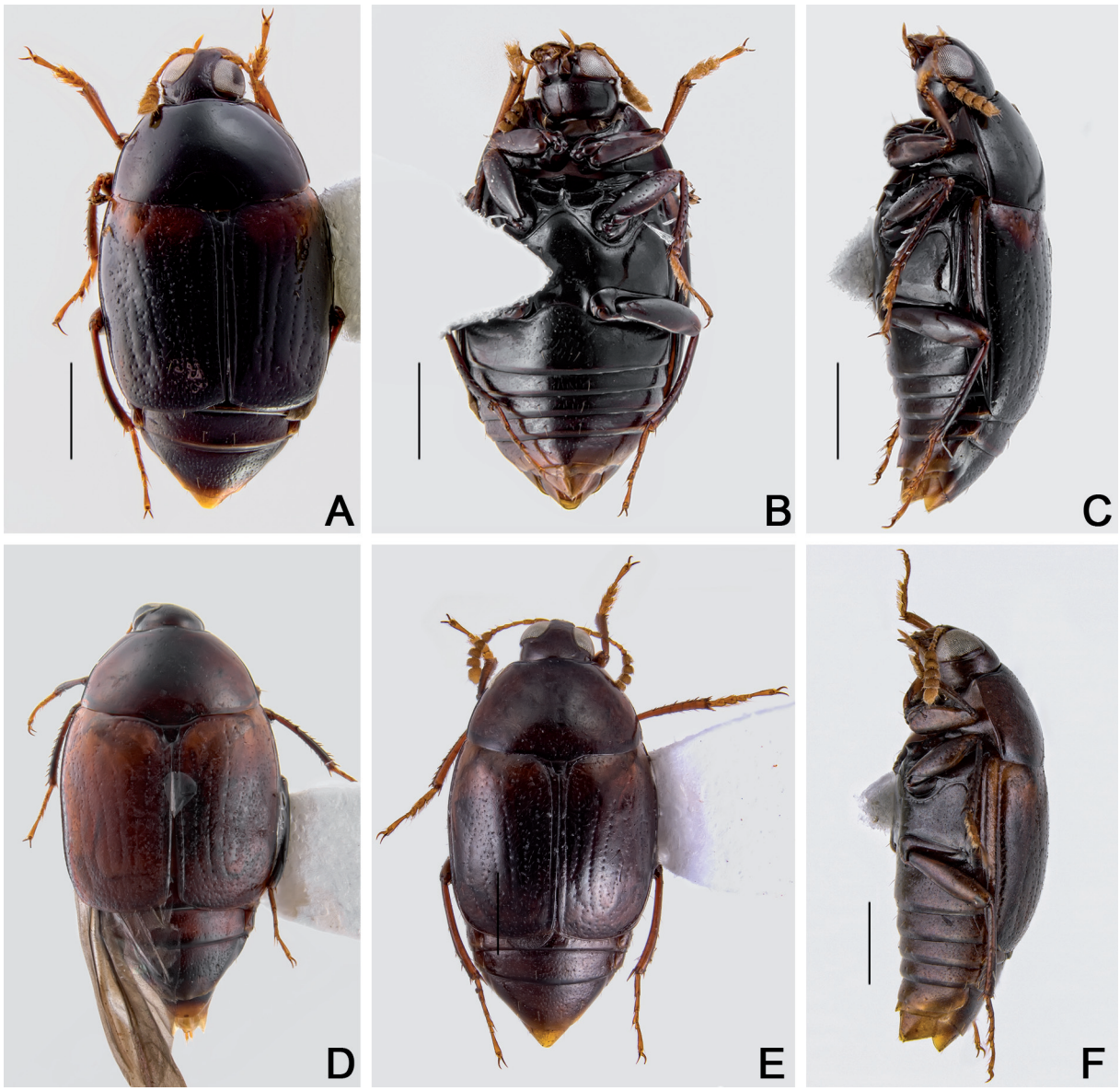

Fig. 38. *Cyparium pici* sp. nov. **A–C**. Holotype, ♂ (CEMT). **A**. Dorsal view. **B**. Ventral view. **C**. Lateral view. **D**. Paratype, ♀ (CEMT), dorsal view. **E–F**. Paratype, ♂ (CEMT). **E**. Dorsal view. **F**. Lateral view. Specimens collected at Cotriguaçu (MT, Brazil). Scale bars = 1.0 mm.

smooth. Metendosternite with arms slightly curved; 'stalk ridge' reaching half length of stalk (Fig. 42A); ventral longitudinal flange curved in lateral view (Fig. 42B).

Wings. Elytra slightly wider than longer; covering just until tergite V (Fig. 38A, D); each elytron subrectangular (Fig. 42C); basal (Fig. 40D) and sutural lines dashed; adsutural area with a row of setae; six rows of coarse punctures (not including sutural line) (Figs 38A, D, 42C); lateral line punctate; apical coarse punctation moderately sparse; apical serrations almost inconspicuous (Fig. 42D); pubescence short and fine. Epipleuron with a row of sparse and coarse punctures. Hind wings fully developed (Fig. 42E).

Legs. Pro-, meso- and metacoxae, and femora with strigulate microsculpture. Pro- and mesofemora fusiform (Fig. 42F–G); punctuation sparse, coarse; metafemora longish, punctuation sparse, shallow (Fig. 42H). Mesotibiae densely spinose, spines thick (Fig. 42G); metatibiae sparsely spinose, spines fine (Fig. 42H).

Abdomen. Tergites VI–VIII with narrow imbricate microsculpture; punctures dense, coarse; pubescence sparse, coarse (Fig. 43A). Ventrites 1–5 densely and coarsely punctate; pubescence moderately sparse, fine; close strigulate microsculpture (Fig. 43B–C). Metacoxal lines finely punctate.

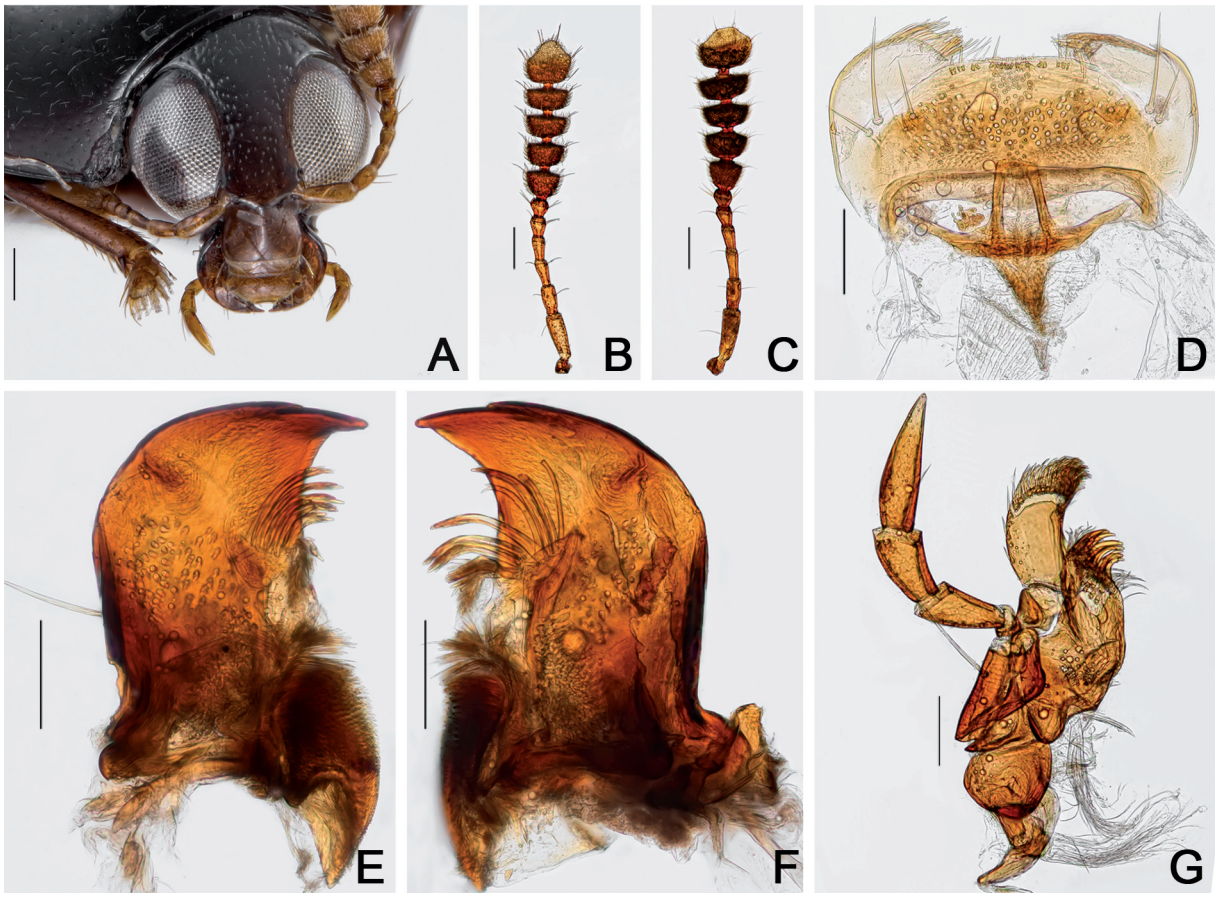

Fig. 39. *Cyparium pici* sp. nov. **A**. Holotype, ♂ (CEMT), frontal view. **B–G**. Paratypes (CELC). **B**. Male, antenna. **C**. Female antenna. **D**. Labrum. **E**. Left mandible. **F**. Right mandible. **G**. Maxilla. Specimens collected at Cotriguaçu (MT, Brazil). Scale bars: A–C = 0.2 mm; D–G = 0.1 mm.

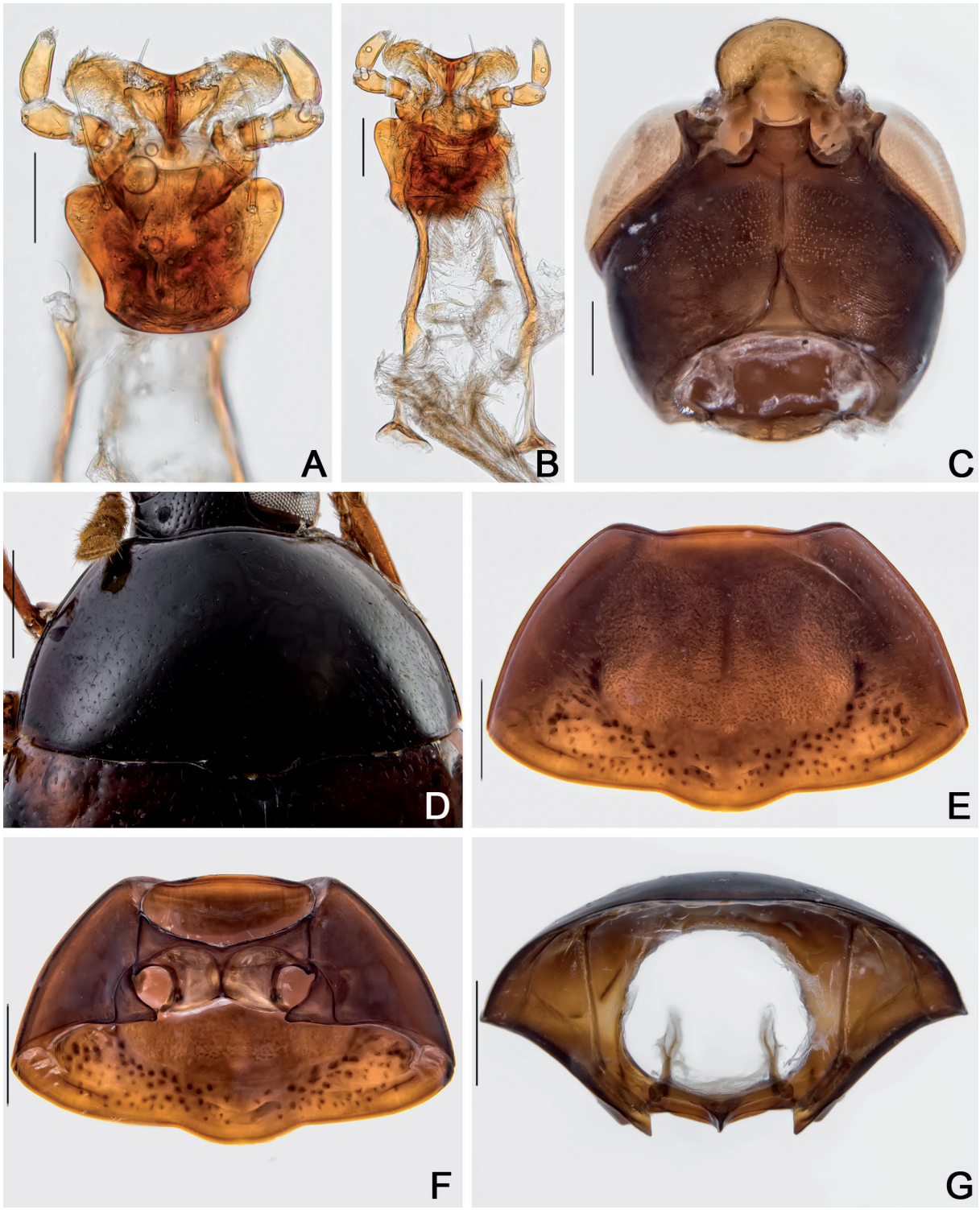

Fig. 40. *Cyparium pici* sp. nov. **A–C**. Paratype, ♂ (CELC). **A**. Labium. **B**. Hypopharynx. **C**. Head, ventral view. **D**. Holotype, ♂ (CEMT), pronotum, dorsal view. **E**. Paratype, ♂ (CEMT), pronotum, dorsal view. **F–G**. Paratype, ♂ (CELC), prothorax. **F**. Ventral view. **G**. Inner view. Specimens collected at Cotriguaçu (MT, Brazil). Scale bars: A–B = 0.1 mm; C = 0.2 mm; D–G = 0.5 mm.

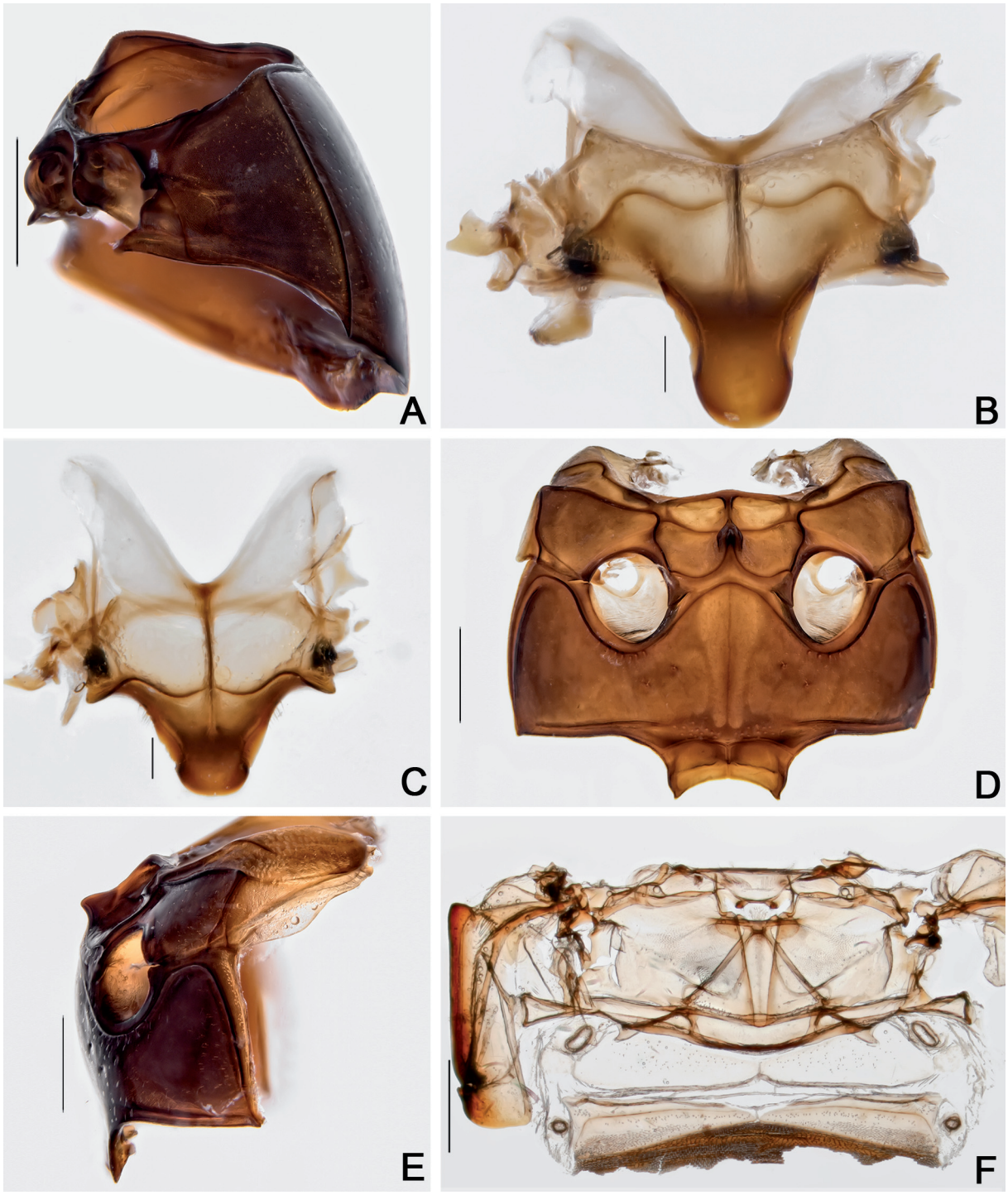

Fig. 41. *Cyparium pici* sp. nov., paratype, ♂ (CELC). **A**. Prothorax, lateral view. **B–C**. Scutellar plate. **B**. Dorsal view. **C**. Apically slanted view. **D–E**. Meso- and metathorax. **D**. Ventral view. **E**. Lateral view. **F**. Metanotum. Specimen collected at Cotriguaçu (MT, Brazil). Scale bars: A, D–F = 0.5 mm; B–C = 0.1 mm.

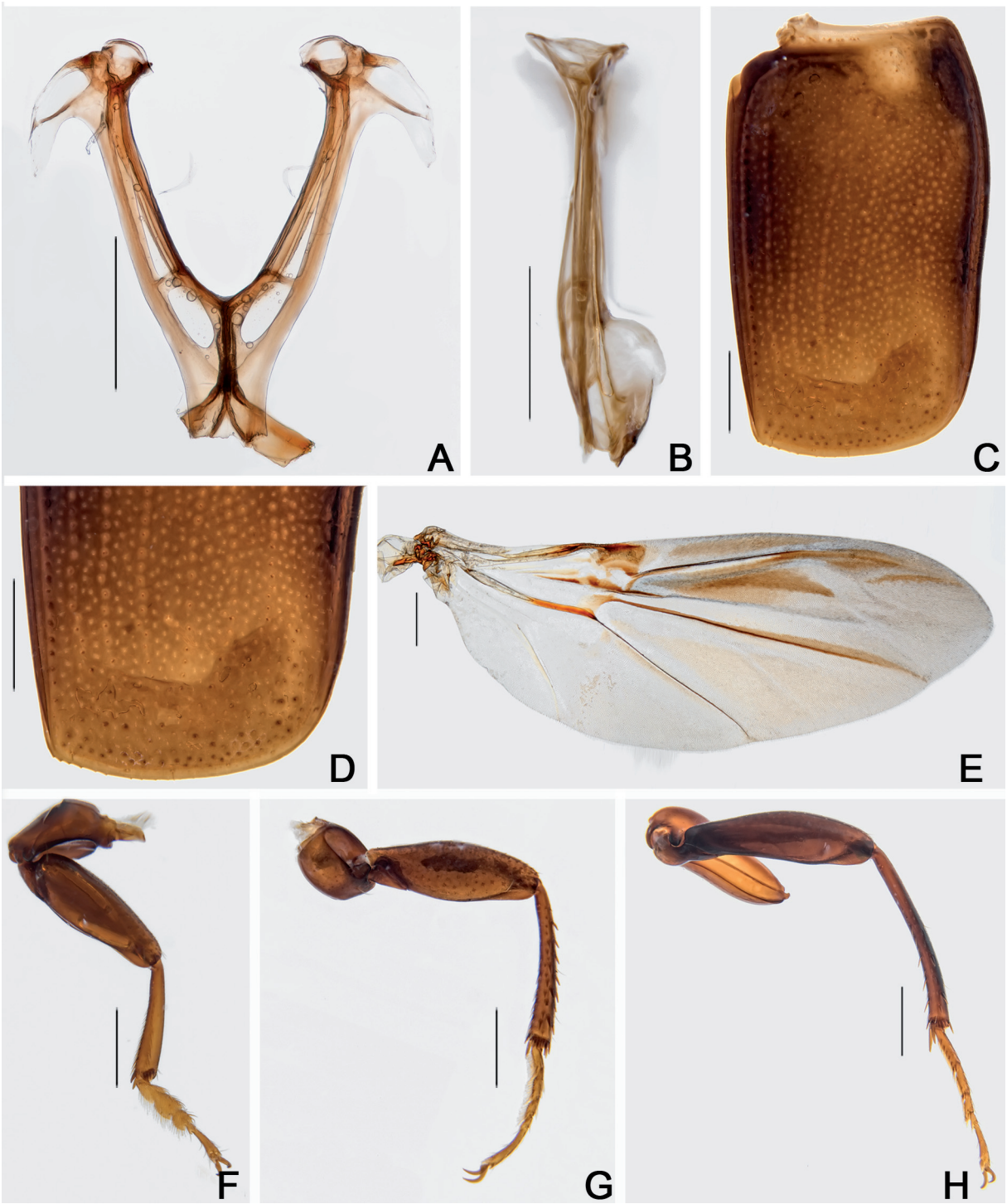

Fig. 42. *Cyparium pici* sp. nov., paratype, ♂ (CELC). **A–B**. Metendosternite. **A**. Dorsal view. **B**. Lateral view. **C–D**. Elytron. **C**. Entire. **D**. Apex. **E**. Hind wing. **F–H**. Legs. **F**. Fore. **G**. Middle. **H**. Hind. Specimen collected at Cotriguaçu (MT, Brazil). Scale bars = 0.5 mm.

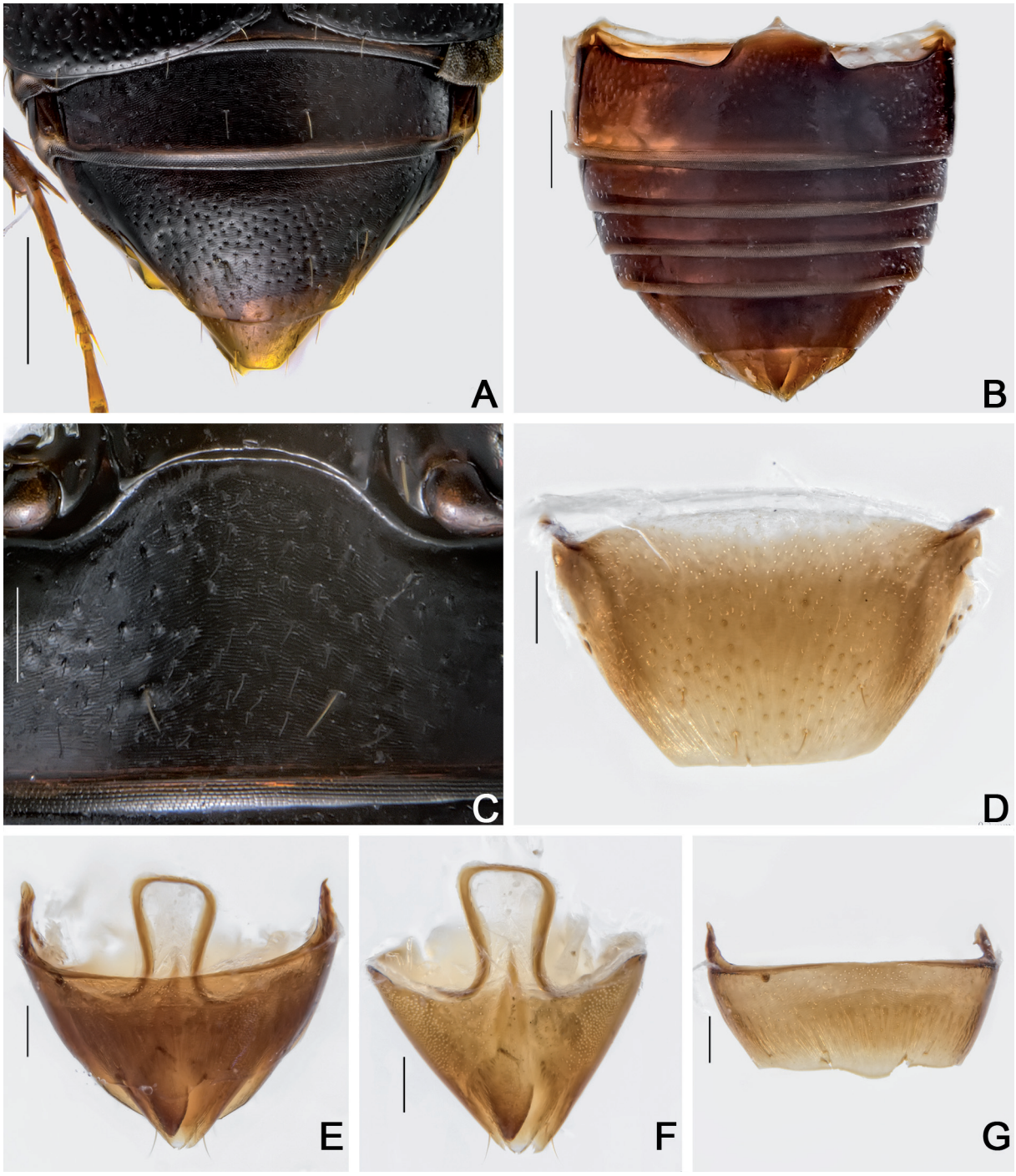

Fig. 43. *Cyparium pici* sp. nov. **A, C**. Holotype, ♂ (CEMT). **A**. Abdomen, dorsal view. **B**. Paratype, ♂ (CEMT), abdomen, ventral view. **C**. Ventrite 1. **D–G**. Paratype, ♂ (CELC). **D**. Tergite VIII. **E**. Terminalia. **F**. Tergite IX. **G**. Sternite VIII. Specimens collected at Cotriguaçu (MT, Brazil). Scale bars: A–B = 0.5 mm; C–G = 0.1.

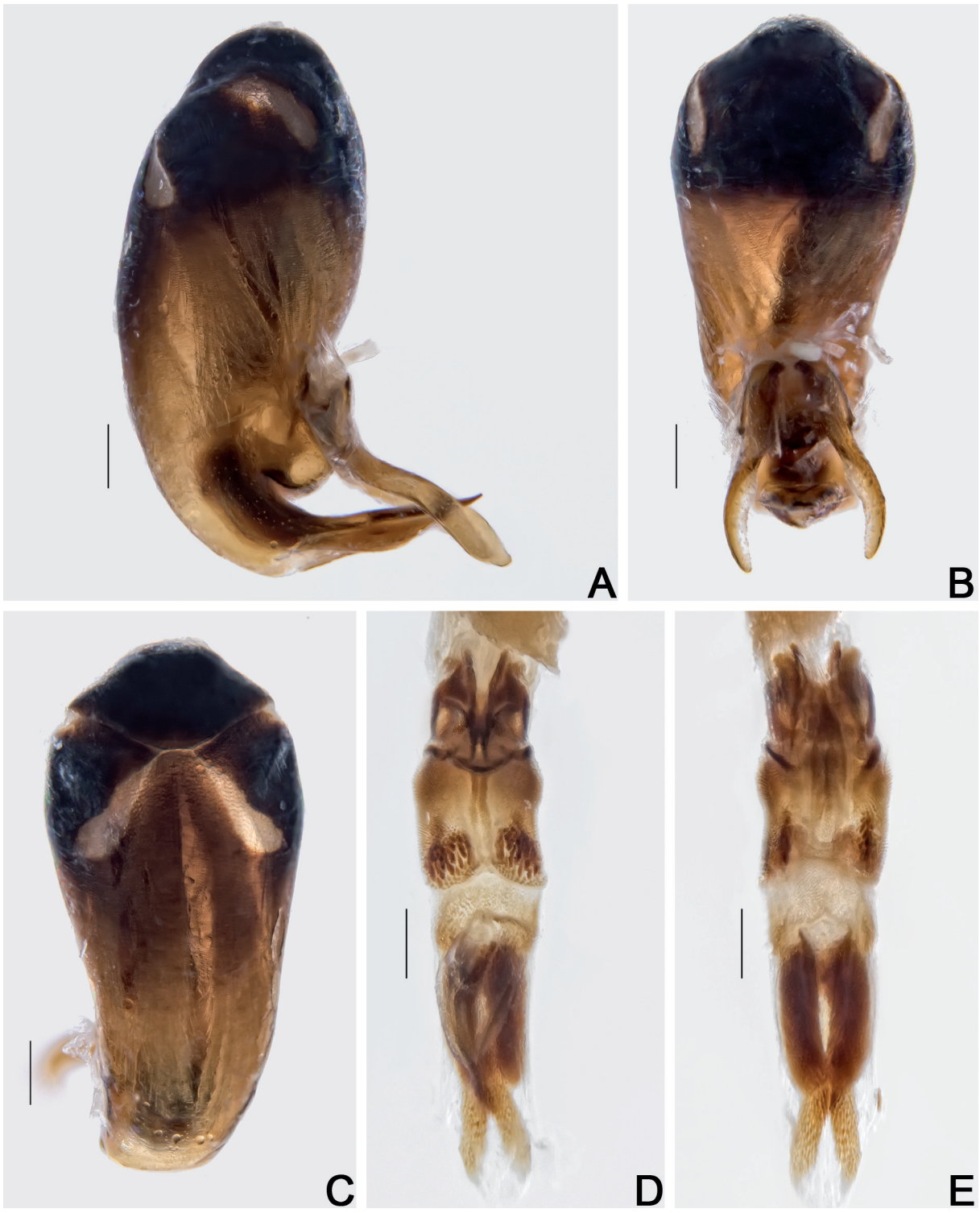

Fig. 44. *Cyparium pici* sp. nov., paratype, ♂ (CELC). **A–C**. Aedeagus. **A**. Lateral view. **B**. Frontal view. **C**. Dorsal view. **D–E**. Internal sac. **D**. Frontal view. **E**. Dorsal view. Specimen collected at Cotriguaçu (MT, Brazil). Scale bars = 0.2 mm.

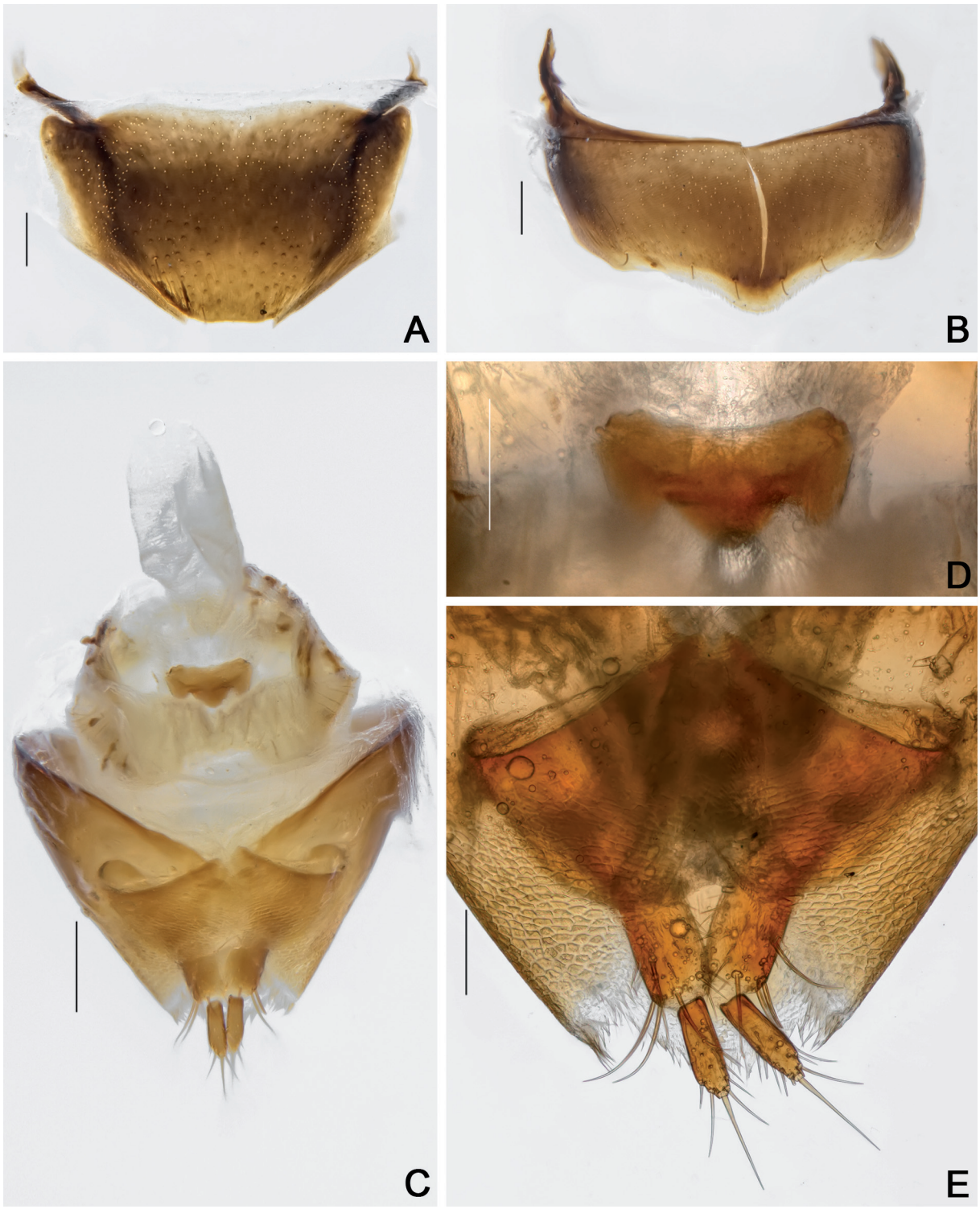

Fig. 45. *Cyparium pici* sp. nov., paratype, ♀ (CELC). **A**. Tergite VIII. **B**. Sternite VIII. **C**. Terminalia. **D**. Sclerite of vaginal plate. **E**. Ovipositor. Specimen collected at Cotriguaçu (MT, Brazil). Scale bars = 0.1 mm.

Males

Measurements (n = 1, paratype; in mm). Antennomeres (length(width)): 0.24(0.08), 0.14(0.07), 0.14(0.06), 0.11(0.06), 0.11(0.07), 0.08(0.09), 0.13(0.16), 0.12(0.18), 0.11(0.19), 0.11(0.20), 0.20(0.22); (n = 10, including the holotype, unless otherwise specified; in mm): TL 3.35–4.20 (mean = 3.75, standard deviation ± 0.32), PL 1.30–1.64 (1.45 ± 0.13), PA 1.07–1.32 (1.16 ± 0.07), PB 2.15–2.62 (2.36 ± 0.17), SL (n = 8) 0.13–0.23 (0.17 ± 0.03), SW (n = 8) 0.13–0.23 (0.18 ± 0.03), EI 1.85–2.28 (2.06 ± 0.15), EL (n = 9) 2.37–2.75 (2.60 ± 0.13), EW 1.37–1.65 (1.49 ± 0.08), EH 0.75–1.15 (0.96 ± 0.11), HW (n = 9) 0.91–1.08 (0.99 ± 0.06), IS (n = 9) 0.26–0.31 (0.28 ± 0.02), WA (n = 9) 0.21–0.30 (0.24 ± 0.03), MC 0.93–1.10 (1.03 ± 0.05), MB 0.37–0.50 (0.45 ± 0.04), VL 0.62–0.78 (0.70 ± 0.04).

Pro- and mesotarsomeres I–III enlarged, with tenet setae (Fig. 42F–G). Tergite VIII trapezoidal, straight posteriorly; triangular in some dry paratypes (Fig. 43D). Tergite IX with laterally curved ventral struts (Fig. 43E–F). Sternite VIII sub-rectangular, with a smooth projection (Fig. 43G). Sternite IX thick (Fig. 43F). Aedeagus strongly sclerotized, apex of median lobe short; openings in dorsal view moderately narrow, forming an acute angle, almost right (Fig. 44A–C); internal sac with strong and robust irregular sclerites (Fig. 44D–E), parameres short (Fig. 44A).

Females

Measurements (n = 1, paratype; in mm). Antennomeres (length(width)): 0.25(0.09), 0.15(0.07), 0.15(0.06), 0.11(0.07), 0.10(0.08), 0.08(0.09), 0.13(0.15), 0.13(0.20), 0.11(0.22), 0.11(0.24), 0.19(0.26); (n = 6, paratypes; in mm): TL 4.20–4.35 (mean = 4.26 , standard deviation ± 0.06), PL 1.38–1.70 (1.62 ± 0.12),

Fig. 46. A. Distribution map of species of *Cyparium* Erichson, 1845, South America. **B**. Mata da Biologia. **C**. Mata do Paraíso.

PA 1.22–1.35 (1.28 ± 0.05), PB 2.56–2.68 (2.62 ± 0.05), SL 0.15–0.25 (0.21 ± 0.03), SW 0.19–0.25 (0.22 ± 0.02), EI 2.25–2.47 (2.34 ± 0.10), EL 2.71–2.96 (2.79 ± 0.09), EW 1.62–1.80 (1.72 ± 0.06), EH 1.00–1.20 (1.10 ± 0.07), HW 1.05–1.15 (1.08 ± 0.03), IS 0.28–0.33 (0.31 ± 0.02), WA 0.22–0.28 (0.25 ± 0.02), MC 1.18–1.34 (1.26 ± 0.05), MB 0.56–0.62 (0.59 ± 0.03), VL 0.75–0.93 (0.85 ± 0.06).

Tergite VIII hexagonal (Fig. 45A), trapezoidal in dry specimens. Sternite VIII rectangular with a projection (Fig. 45B). Vagina and bursa copulatrix membranous; vagina without sclerites; bursa copulatrix with irregular sclerites (Fig. 45C). Vaginal plate with an apical M-shaped sclerite (Fig. 45D). Spermatheca not detected. Distal gonocoxites short, straight and thick; gonostyli somewhat thick, parallel (Fig. 45C–E).

Remarks

Similar in body length to *Cyparium rufohumerale*, but differs in the yellowish antennae (bicolored in *C. rufohumerale*) and in the comparatively larger reddish brown mark on the elytra (only at the humeral region in *C. rufohumerale*). Also similar to *C. humerale* in body length and the entirely yellow antennae, but differs in the non-triangular mark on the elytra and in the shorter elytra.

Distribution

Known only from Cotriguaçu, Faz. São Nicolau (09°50′19″ S, 58°15′15″ W), state of Mato Grosso, Midwest, Brazil (Fig. 46).

Redescriptions and new records

Cyparium collare Pic, 1920
Figs 4, 47–55; Supp. file 2B, Supp. file 3 (Figs 1A–4H)

Cyparium collare Pic, 1920a: 4. Syntypes: Muséum national d'histoire naturelle (MNHN), Paris, France.

Material examined

BRAZIL – **Sergipe** • 3 ♂♂; Sta Luzia do Itanhi, Faz. Crasto; 9–12 Sep. 1999; A. Bonaldo leg.; MCN 166400 (abdomen dissected), 166404, 166405 • 3 ♀♀; same collection data as for preceding; MCN 166398, 166401, 167484 • 2 ♂♂; Areia Branca, Est. Ecol. Serra de Itabaiana; 14–20 Sep. 1999; A. Bonaldo leg.; MCN 166402, 166403 (abdomen dissected, preserved in glycerin) • 1 ♀; same collection data as for preceding; MCN 166406. – **Minas Gerais** • 1 ♂; Viçosa, EPTEA Mata do Paraíso; 8 Dec. 2014; I. Pecci-Maddalena leg.; CELC • 3 ♂♂, 5 ♀♀ (1 ♀, abdomen dissected, preserved in glycerin); same collection data as for preceding; 6 Dec. 2018; LabCol leg; CELC • 7 ♂♂, 3 ♀♀ (1 ♀ entirely dissected, preserved in glycerin; 1 ♂, 1 ♀, abdomen dissected, preserved in glycerin); same collection data as for preceding; 5 Nov. 2019; LabCol leg.; "Fungo 02 \\ Em *Pleurotus pulmonarius*"; CELC • 1 ♀; same collection data as for preceding; "Fungo 03 \\ Em *Mycena* sp."; CELC • 14 ♂♂, 4 ♀♀ (1 ♂, 1 ♀ entirely dissected, preserved in glycerin; 1 ♂, 1 ♀, abdomen dissected, preserved in glycerin); same collection data as for preceding; "Fungo 01 \\ Em *Xerocomus* aff. *brasiliensis*"; CELC • 9 ♂♂, 3 ♀♀ (3 ♂♂ entirely dissected, preserved in glycerin); same collection data as for preceding; 7 Nov. 2019; LabCol leg.; "Fungo 17"; CELC • 1 ♂; same collection data as for preceding; "Fungo 14 \\ Em *Leucoagaricus rubrotinctus*"; CELC • 1 ♂, 1 ♀; same collection data as for preceding; "Fungo sem id"; CELC • 1 ♀; same collection data as for preceding; "Fungo A21 \\ Fotos: 712-713; 728-729, Em *Heimiomyces neovelutipes*"; CELC • 1 ♀; same collection data as for preceding; "Fungo Que"; CELC • 1 ♂, 2 ♀♀; same collection data as for preceding; 12 Nov. 2019; LabCol leg.; "Fungo 09"; CELC • 2 ♀♀ (1 ♀, abdomen dissected, preserved in glycerin); same collection data as for preceding; 13 Nov. 2019; LabCol leg.; "Fungo 18 \\ Em *Macrolepiota colombiana*"; CELC • 1 ♂; same collection data as for preceding; 14 Nov. 2019; "Fungo 22 \\ Em *Marasmiellus* sp."; CELC • 1 ♂; same collection data as for preceding; 19 Nov. 2019; "Fungo 18; Em *Marasmiellus cubensis*"; CELC • 1 ♀; same collection data as for preceding; "Fungo 16 \\ Em *Marasmiellus* sp."; CELC • 1 ♀; same collection data as for preceding; "Fungo 22 \\

Em *Leucoprinus ianthinus*"; CELC • 1 ♂, 2 ♀♀; same collection data as for preceding; "Fungo 13 \\ Em *Marasmiellus cubensis*"; CELC • 2 ♀♀; same collection data as for preceding; "Fungo 05 \\ Em *Marasmius* sp."; CELC • 2 ♀♀; same collection data as for preceding; "Fungo 24 \\ Em *Marasmiellus cubensis*"; CELC • 1 ♀; same collection data as for preceding; 21 Nov. 2019; LabCol leg.; "Fungo 38 \\ Em *Marasmiellus* sp."; CELC • 1 ♀; same collection data as for preceding; "Fungo 06 \\ Em *Agaricus dulcidulus* e *Leucocoprinus brebissoni*"; CELC • 5 ♂♂, 2 ♀♀ (1 ♂, abdomen dissected, preserved in glycerin); same collection data as for preceding; "Fungo 26 \\ Em *Lulesia lignicola*"; CELC • 2 ♀♀; same collection data as for preceding; "Fungo 16 \\ Em *Marasmius araucariae*"; CELC • 2 ♂♂, 3 ♀♀ (1 ♀, abdomen dissected, preserved in glycerin); same collection data as for preceding; "Fungo 12 \\ Em *Marasmiellus* aff. *ramealis*"; CELC • 1 ♀; same collection data as for preceding; "Fungo 52 \\ Em *Marasmiellus* sp."; CELC • 2 ♂♂, 1 ♀; same collection data as for preceding; "Fungo 41 \\ Em *Lepiota* sp."; CELC • 2 ♂♂; same collection data as for preceding; 26 Nov. 2019; LabCol leg.; "Fungo 23 \\ Em *Marasmiellus cubensis*"; CELC • 1 ♂; same collection data as for preceding; "Fungo 18 \\ Em *Entoloma* (*Inocephalus*) sp."; CELC • 2 ♀♀ (1 ♀, abdomen dissected, preserved in glycerin); same collection data as for preceding; "Fungo 46 \\ Em *Volvariella* sp."; CELC • 1 ♂, 1 ♀; same collection data as for preceding; "Fungo 24 \\ Em *Marasmius* sp."; CELC • 1 ♀; same collection data as for preceding; "Fungo 19 \\ *Pleteus* sp."; CELC • 1 ♂; same collection data as for preceding; "Fungo 37 \\ *Conocybe* sp."; CELC • 1 ♂; same collection data as for preceding; "Fungo 26 \\ Em *Leucocoprinus* sp."; CELC • 3 ♂♂; same collection data as for preceding; "Fungo 17"; CELC • 1 ♀; same collection data as for preceding; "Fungo 39 \\ Em *Marasmius hematocephalus*"; CELC • 2 ♂, 1 ♀ (1 ♂ entirely dissected, preserved in glycerin); same collection data as for preceding; 28 Nov. 2019; LabCol leg.; "fotos 1103-05 \\ Em *Marasmius* sp."; CELC • 1 ♂; same collection data as for preceding, "Trilha dos Gigantes"; 3 Feb. 2019; LabCol leg.; CELC • 1 ♀; Viçosa, Mata da Biologia; 3 May 2014; S. Aloquio leg.; "\\ ex. *Lepiota* sp."; CELC • 2 ♂♂, 2 ♀♀; Viçosa, Recanto das Cigarras, Mata da Biol.; 13 Nov. 2019; LabCol leg; "Fungo 11 \\ Em *Coprinellus disseminatus*"; CELC • 1 ♂; Viçosa, Mata da Biologia; 15 Oct. 2021; E. von Groll and A. Orsetti leg.; "Fungo 06"; CELC • 1 ♂, 1 ♀; same collection data as for preceding; "Fungo 26 \\ Em *Leucocoprinus cepistipes*"; CELC • 1 ♂, 1 ♀; same collection data as for preceding; 23 Nov. 2021; E. von Groll and G.L.N. Martins leg.; "\\ Em *Favolus tenuiculus*"; CELC • 8 ♂♂, 1 ♀; same collection data as for preceding; 26 Nov. 2021; "\\ Em *Favolus tenuiculus*"; CELC.

Diagnosis

TL: 2.60–3.40 mm in males and 2.56–3.52 mm in females. Pronotum reddish brown, elytra black (Fig. 47A). Eyes remarkably wider than head, rounded (Fig. 48A). Antennomere XI hexagonal, longish (Fig. 48B–C). Hypomeron only laterally with imbricate microsculpture. Metaventrite smooth, but laterally with imbricate microsculpture. Tergite VIII of males coarsely punctate (Fig. 52D). Rounded ventral struts (Fig. 52F). Aedeagus with short apex; openings in dorsal view thin, forming a wide acute angle; parameres short (Fig. 53A–C). Distal gonocoxites curved and thick (Fig. 54E).

Redescription

Coloration. Iridescent**.** Frons ochre, reddish brown; clypeus yellowish to ochre; mouthparts yellow-brown (Fig. 48A, Supp. file 3 (Figs 1D, 3D)); antennomeres I–VI and apex of XI yellow-brown; VII–X and basal part of XI darker (Fig. 48B). Pronotum and hypomeron reddish brown (Fig. 47A–B, Supp. file 3 (Figs 1E, 3E)). Scutellum reddish brown or black (Fig. 49D). Elytra black (Fig. 47A); epipleuron dark ochre. Mesanepisternum, metanepisternum and metepimeron dark ochre. Metaventrite dark brown, lighter laterally (Fig. 47B). Coxae and trochanters dark ochre; femora yellowish brown, apex yellow; tibiae and tarsi ochre (Fig. 47B–C). Tergite VI and VII black; tergite VIII yellow. Ventrites 1–4 dark brown; 5 and 6 yellow. Teneral specimens entirely light brown (Fig. 47D–E) or with pronotum lighter (Fig. 47F).

Head. Punctation dense, fine (Fig. 48A). Eyes remarkably wider than head, rounded (Fig. 48A). Labrum transverse, lateral areas rounded, not well marked at apex; central margin slightly curved; sclerotized portion rounded; lateral setae slightly exceeding margins of labrum; almost without pores centrally (Fig. 48D). Mandibles smoothly curved, subapical serrations on left mandible conspicuous (Fig. 48E–F). Maxillae with palpomere II long and thin; palpomere III somewhat globose; galea densely pubescent and lacinia moderately pubescent (Fig. 48G). Mentum laterally rounded, curved apically (Fig. 49A). Setae of labial palpomere II not exceeding palpomere III; palpomere III longish, with short apical setae (Fig. 49A–B). Post gena microsculptured with close transversal lines; gular pores limited to region next to eyes and submentum; gula triangular, small (Fig. 49C). Antennae not reaching or surpassing mesanepisternum, regardless of sex; antennal club smoothly delimited; antennomere XI hexagonal, longish (Fig. 48B–C).

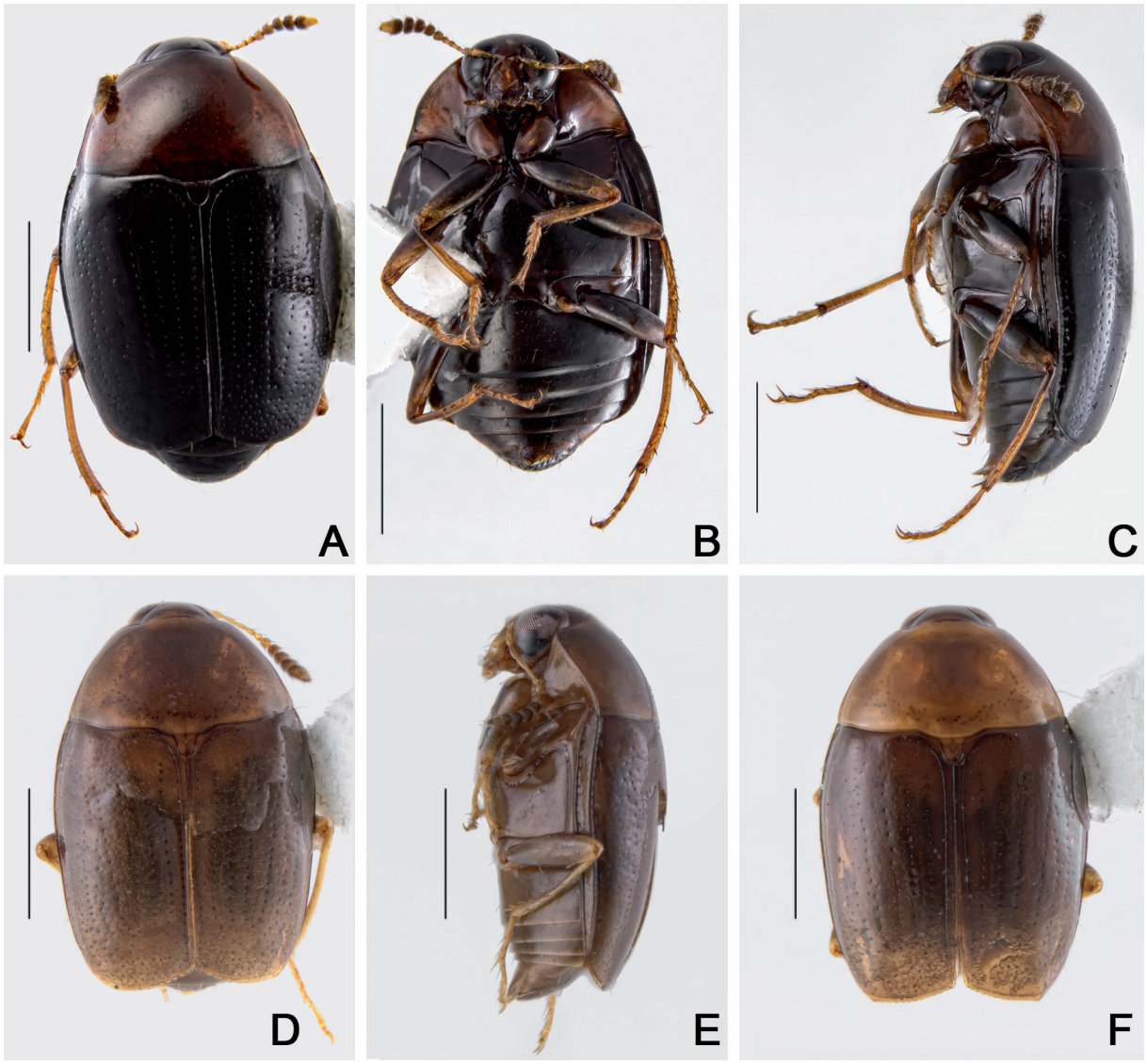

Fig. 47. *Cyparium collare* Pic, 1920. **A–C**. ♂ (CELC). **A**. Dorsal view. **B**. Ventral view. **C**. Lateral view. **D–F**. ♀ (CELC). **D**. Dorsal view. **E**. Lateral view. **F**. Dorsal view. Specimens collected at Mata do Paraíso (A–C) and Mata da Biologia (D–F), Viçosa (MG, Brazil). Scale bars = 1.0 mm.

Prothorax. Pronotum smooth, shining; punctation dense, fine; pubescence short, fine (Fig. 49D); transverse, sub-straight laterally, almost forming a right angle at posterior margin (Fig. 49E). Hypomeron laterally with imbricate microsculpture. Notosternal suture with an angle, outward directed (Fig. 49F). Profurca thin, short, not exceeding half of foramen (Fig. 49G). Prosternal process apically wavy (Fig. 50A).

Mesothorax. Mesonotum with prescutellar suture (= scutellar lines, Leschen & Löbl 2005) wavy (Fig. 50B). Scutellum rounded posteriorly (Fig. 50B). Anterior phragma thin and somewhat straight (Fig. 50C). Mesanepistenum with shallow imbricate microsculpture, inconspicuous in some. Procoxal rests triangular, straight posteriorly (Fig. 50D). Mesoventral and median lines strongly wavy; area between median and mesocoxal lines large (Fig. 50D). Mesoventral process curved, forming a well-marked ridge (Fig. 50E).

Metathorax. Metanotum with triangular alacrista, turned to the sides; scutoscutellar suture inconspicuous; median membranous area narrow and long (Fig. 50F). Metaventrite smooth, but with imbricate microsculpture laterally; punctation sparse, fine. Mesocoxal line forming an angle between coxal cavities; finely punctate under coxal cavities (Fig. 50D). Metanepisternum and metepimeron with imbricate microsculpture. Intercoxal plates smooth. Metendosternite with curved arms; 'stalk ridge'

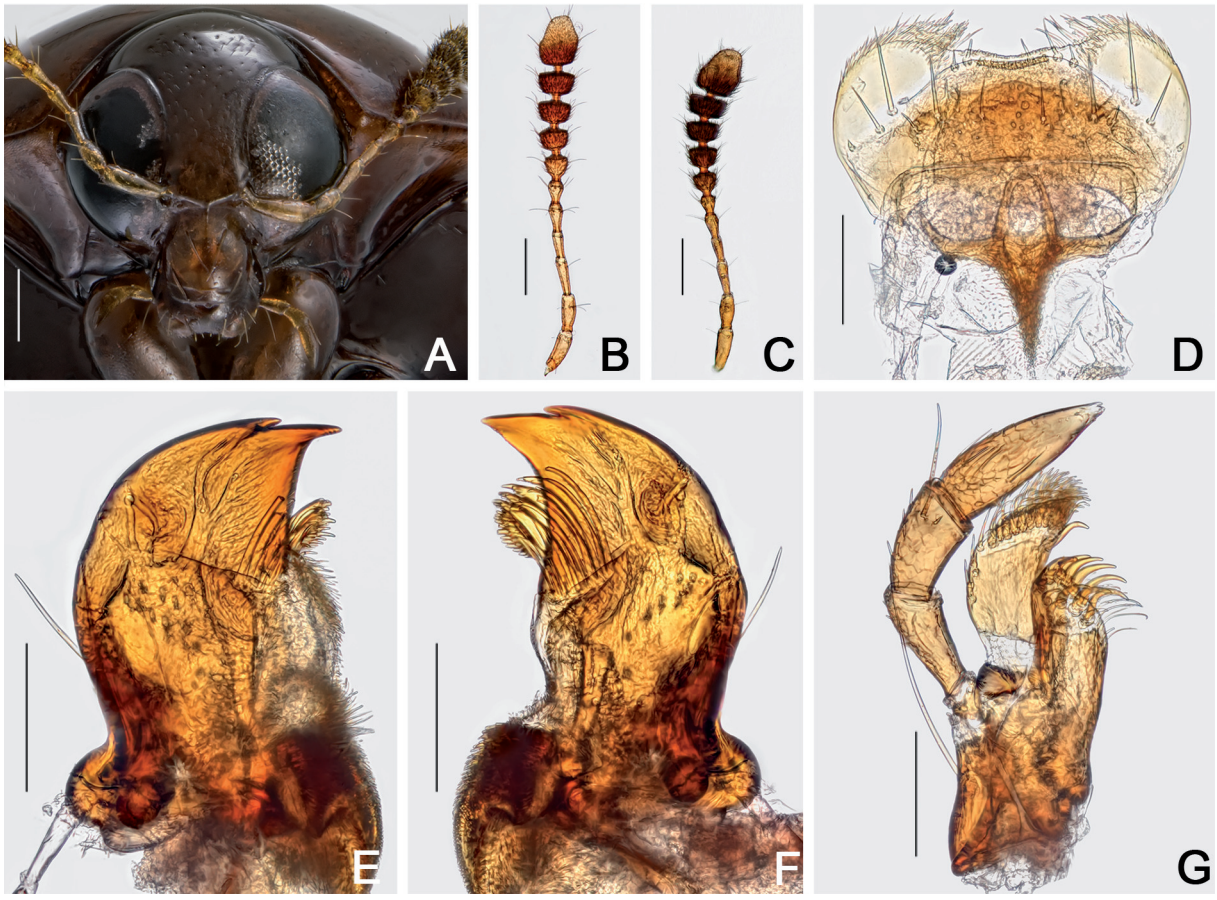

Fig. 48. *Cyparium collare* Pic, 1920. **A–B, D–G**. ♂ (CELC). **A**. Frontal view. **B**. Male antenna. **C**. Female antenna (CELC). **D**. Labrum. **E**. Left mandible. **F**. Rigth mandible. **G**. Maxilla. Specimens collected at Mata do Paraíso, Viçosa (MG, Brazil). Scale bars: A–C = 0.2 mm; D–G = 0.1 mm.

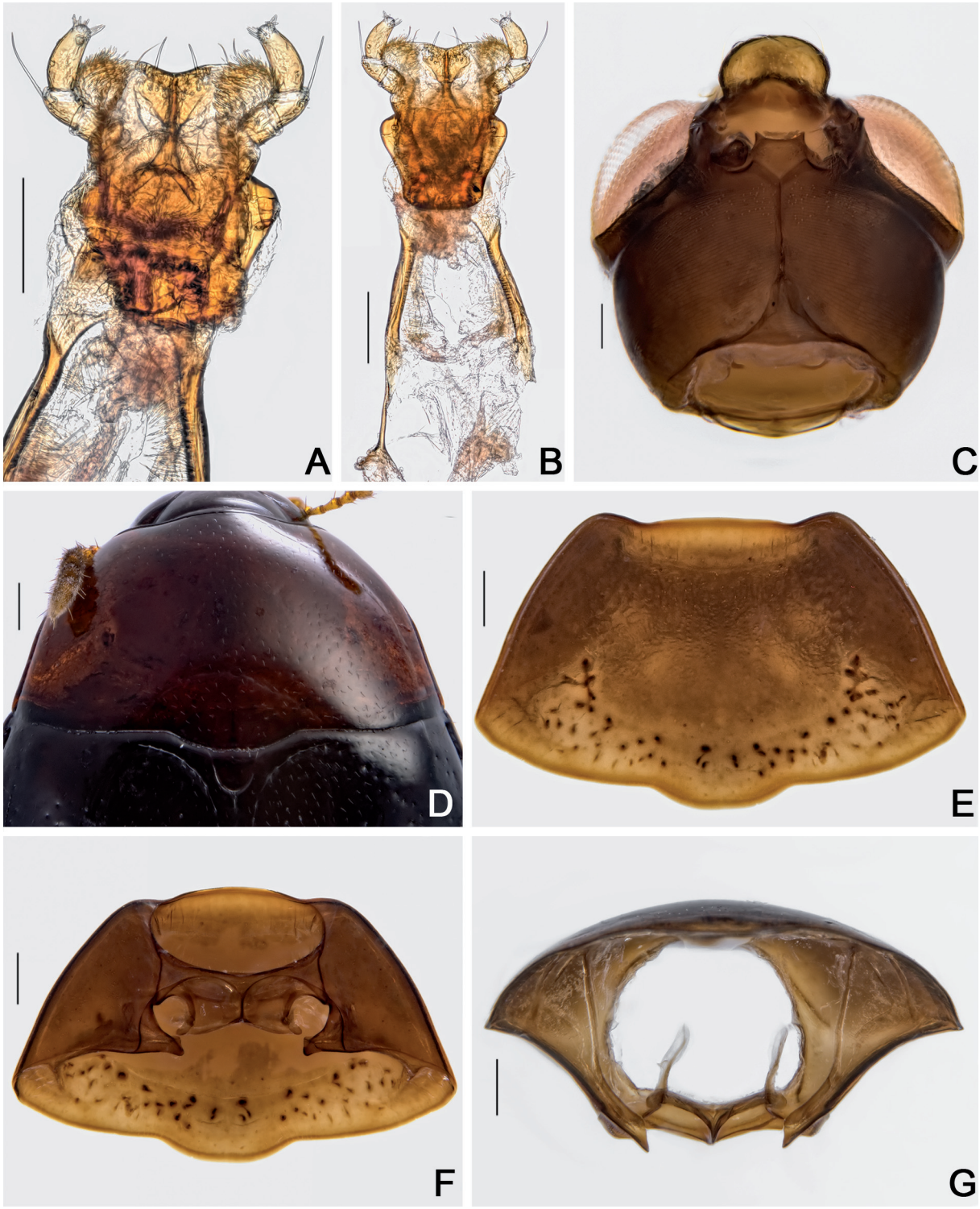

Fig. 49. *Cyparium collare* Pic, 1920, ♂♂ (CELC). **A**. Labium. **B**. Hypopharynx. **C**. Head, ventral view. **D–E**. Pronotum, dorsal view. **F–G**. Prothorax. **F**. Ventral view. **G**. Inner view. Specimens collected at Mata do Paraíso, Viçosa (MG, Brazil). Scale bars: A–C = 0.1 mm; D–G = 0.2 mm.

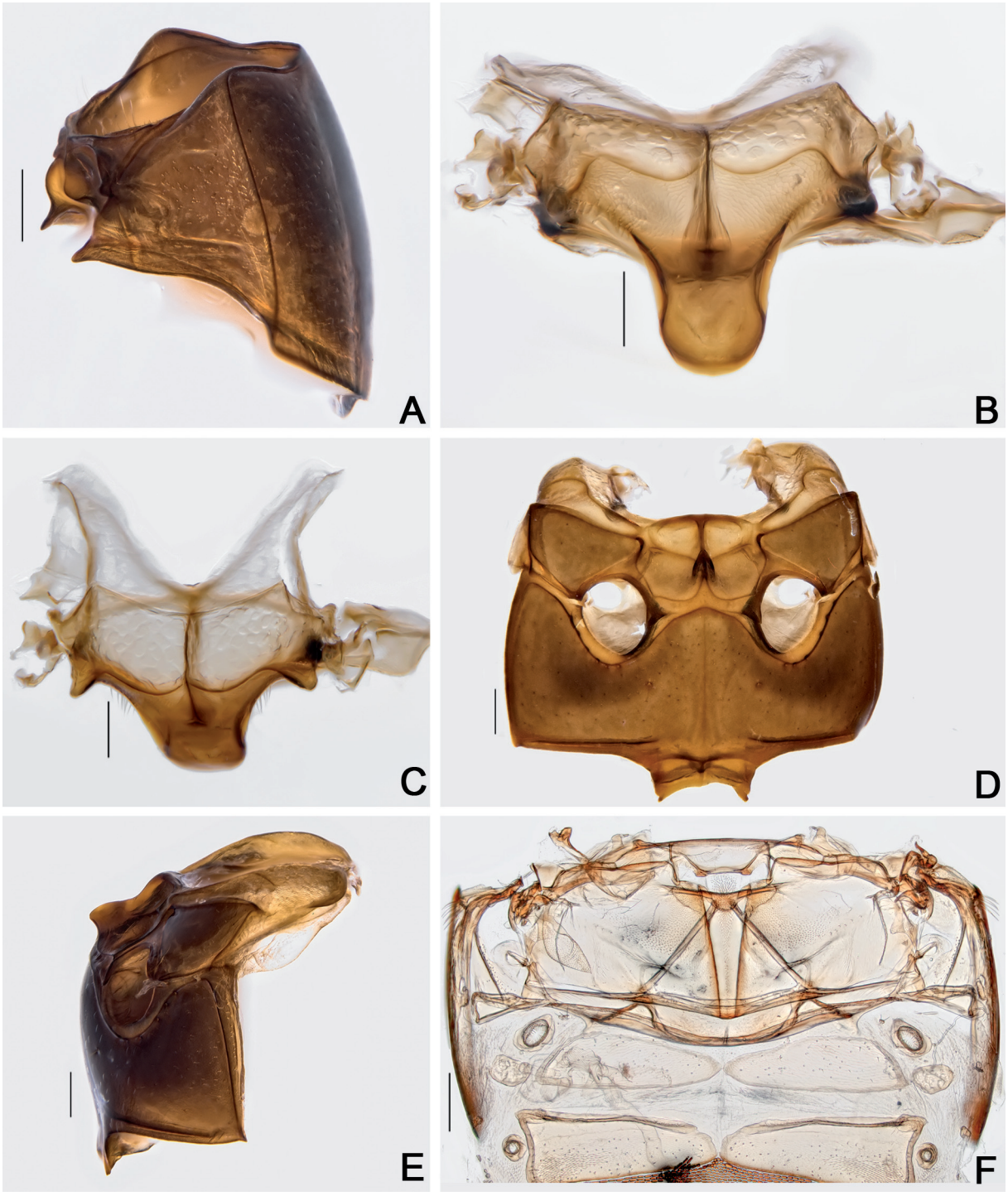

Fig. 50. *Cyparium collare* Pic, 1920, ♂ (CELC). **A**. Prothorax, lateral view. **B–C**. Scutellar plate. **B**. Dorsal view. **C**. Apically slanted view. **D–E**. Meso- and metathorax. **D**. Ventral view. **E**. Lateral view. **F**. Metanotum. Specimen collected at Mata do Paraíso, Viçosa (MG, Brazil). Scale bars: A, D–F = 0.2 mm; B–C = 0.1 mm.

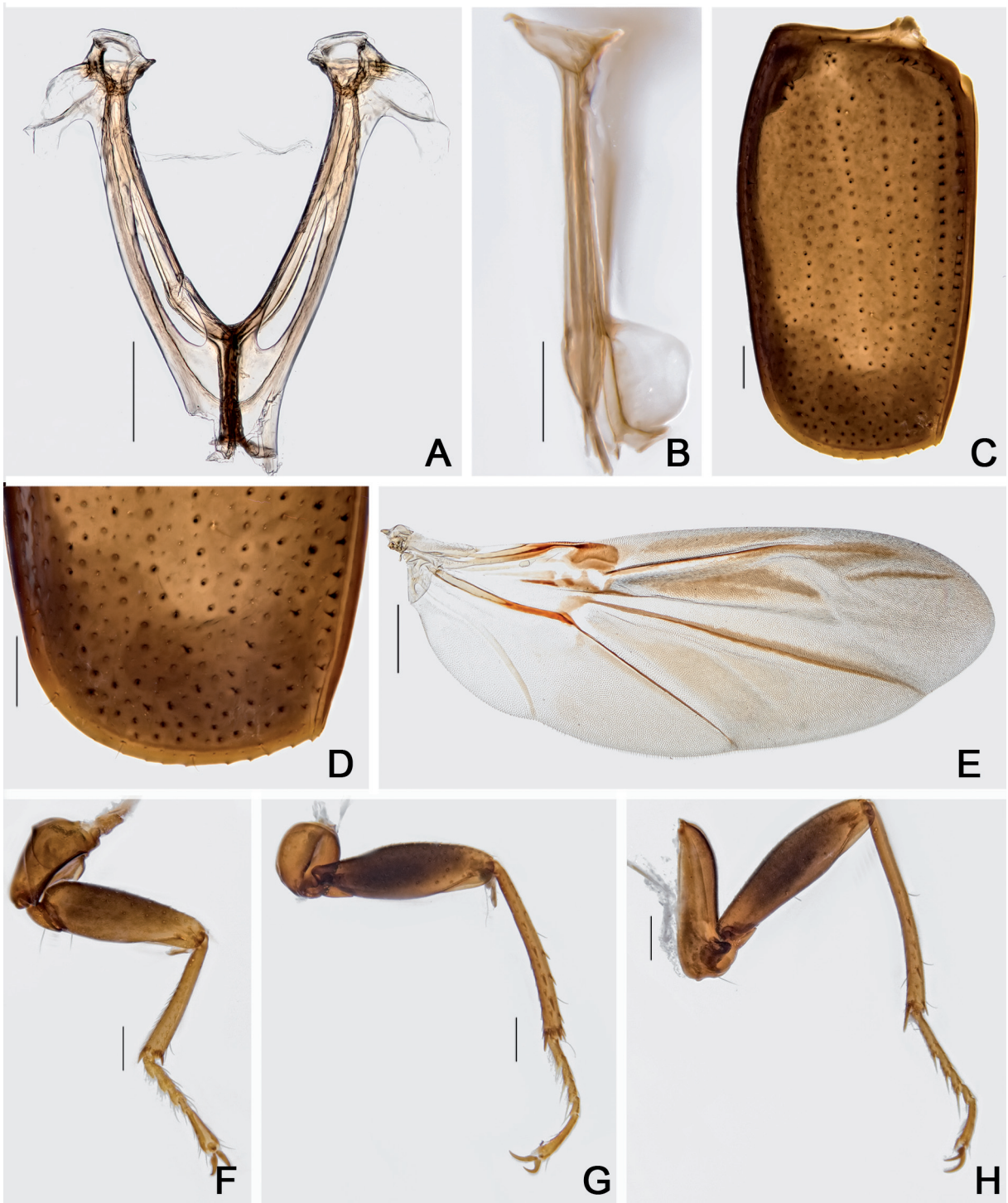

Fig. 51. *Cyparium collare* Pic, 1920, ♂ (CELC). **A–B**. Metendosternite. **A**. Dorsal view. **B**. Lateral view. **C–D**. Elytron. **C**. Entire. **D**. Apex. **E**. Hind wing. **F–H**. Legs. **F**. Fore. **G**. Middle. **H**. Hind. Specimen collected at Mata do Paraíso, Viçosa (MG, Brazil). Scale bars: A–D, F–H = 0.2 mm; E = 0.5 mm.

exceeding half length of stalk (Fig. 51A); ventral longitudinal flange wide and short in lateral view (Fig. 51B).

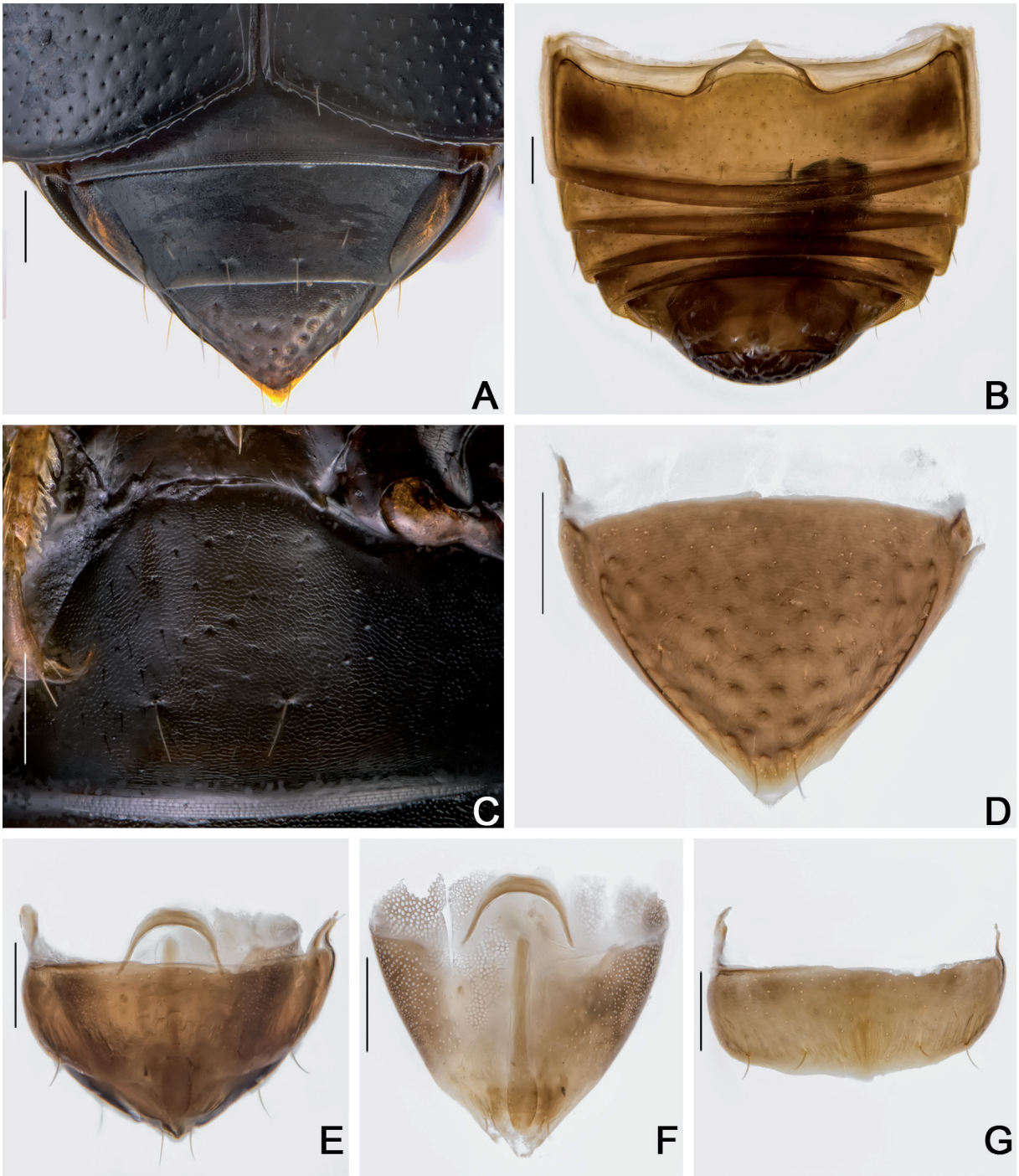

Fig. 52. *Cyparium collare* Pic, 1920, ♂♂ (CELC). **A–B**. Abdomen. **A**. Dorsal view. **B**. Ventral view. **C**. Ventrite 1. **D**. Tergite VIII. **E**. Terminalia. **F**. Tergite IX. **G**. Sternite VIII. Specimens collected at Mata do Paraíso, Viçosa (MG, Brazil). Scale bars = 0.2 mm.

Fig. 53. *Cyparium collare* Pic, 1920, ♂ (CELC). **A–C**. Aedeagus. **A**. Lateral view. **B**. Frontal view. **C**. Dorsal view. **D–E**. Internal sac. **D**. Frontal view. **E**. Dorsal view. Specimen collected at Mata do Paraíso, Viçosa (MG, Brazil). Scale bars = 0.1 mm.

Wings. Elytra slightly wider than long, partially covering tergite VI (Fig. 47A); basal (Fig. 49D) and sutural lines dashed and punctate; adsutural area with a row of setae, six rows of coarse punctures (not including sutural line) (Figs 47A, 51C); lateral lines punctate; apical coarse punctation dense; apical serrations moderately large, well visible (Fig. 51D); pubescence short, fine. Epipleuron with diffuse coarse punctures. Hind wings fully developed (Fig. 51E).

Legs. Pro-, meso- and metacoxae, and femora with strigulate microsculpture. Femora somewhat straight (Fig. 51F–H). Pro- and mesofemora sparsely and coarsely punctate; metafemora sparsely and finely punctate. Mesotibiae densely spinose, spines fine (Fig. 51G). Metatibiae sparsely spinose, spines fine (Fig. 51H).

Abdomen. Tergites VI–VIII with imbricate microsculpture; tergite VII trapezoidal; punctation sparse, fine; pubescence dense, fine (Fig. 52A). Ventrites 1–5 (Figs 52B, S5F) sparsely and coarsely punctate; pubescence sparse, fine; imbricate microsculpture anteriorly, and with strigulate microsculpture posteriorly (Fig. 52C). Metacoxal lines finely punctate.

Males

Measurements (n = 1; in mm). Antennomeres (length(width): 0.15(0.06), 0.13(0.05), 0.14(0.04), 0.09(0.04), 0.11(0.05), 0.08(0.06), 0.07(0.08), 0.07(0.11), 0.08(0.12), 0.08(0.13), 0.18(0.14); (n = 15, unless otherwise specified; in mm): TL 2.60–3.72 (mean = 3.16, standard deviation ± 0.34), PL 0.90–1.35 (1.12 ± 0.12), PA 0.75–1.00 (0.88 ± 0.07), PB 1.50–2.25 (1.90 ± 0.23), SL (n =14) 0.13–0.21 (0.16 ± 0.02), SW (n =14) 0.12–0.20 (0.16 ±0.02), EI 1.50–2.15 (1.84 ± 0.19), EL 1.77–2.55 (2.18 ± 0.23), EW 0.85–1.42 (1.12 ± 0.15), EH 0.30–0.95 (0.74 ± 0.20), HW 0.68–0.89 (0.79 ± 0.06), IS 0.15–0.25 (0.21 ± 0.02), WA 0.15–0.20 (0.18 ± 0.01), MC 0.70–1.15 (0.91 ± 0.12), MB 0.33–0.56 (0.44 ± 0.07), VL 0.46–0.75 (0.62 ± 0.08).

Pro- and mesotarsomeres I–III enlarged, with tenet setae (Fig. 51F–G). Tergite VIII triangular, acuminate posteriorly; punctation dense, coarse; subglabrous (Fig. 52A, D, Supp. file 3 (Figs 1F, 3G)). Tergite IX with rounded ventral struts (Fig. 52E–F, Supp. file 3 (Figs 1G, 4A–B)). Sternite VIII rectangular, short (Fig. 52G, Supp. file 3 (Figs 1H, 4C)). Sternite IX more or less spoon-like (Fig. 52F, Supp. file 3 (Figs 1G, 4B)). Aedeagus sclerotized enlarged at base, apex of median lobe short; openings in dorsal view thin, forming a very acute angle (Fig. 53A–C, Supp. file 3 (Figs 2A–C, 4D–F)); internal sac with irregular sclerites, crown-like (Fig. 53D–E, Supp. file 3 (Fig. 4G–H)); parameres short, curved and with denticular structures at base (Fig. 53A–B, Supp. file 3 (Figs 2A–B, 4D–E)).

Females

Measurements (n = 1; in mm). Antennomeres (length(width): 0.16(0.06), 0.12(0.06), 0.13(0.04), 0.08(0.04), 0.10(0.05), 0.06(0.06), 0.06(0.08), 0.08(0.10), 0.07(0.12), 0.08(0.14), 018(0.15); (n = 14, unless otherwise specified; in mm): TL 2.56–3.64 (mean = 3.15, standard deviation ± 0.30), PL 0.92–1.37 (1.14 ± 0.11), PA 0.77–1.02 (0.90 ± 0.06), PB 1.50–2.20 (1.92 ± 0.18), SL (n =12) 0.12–0.20 (0.16 ± 0.02), SW (n =12) 0.14–0.19 (0.16 ±0.01), EI (n =12) 1.52–2.12 (1.87 ± 0.16), EL (n =12) 1.85–2.52 (2.12 ± 0.19), EW 0.90–1.30 (1.14 ± 0.10), EH (n =12) 0.35–0.97 (0.75 ± 0.23), HW 0.65–0.88 (0.79 ± 0.02), IS 0.20–0.26 (0.22 ± 0.02), WA 0.15–0.22 (0.18 ± 0.02), MC (n =13) 0.72–1.06 (0.93 ± 0.09), MB 0.35–0.95 (0.49 ± 0.14), VL 0.52–0.77 (0.65 ± 0.07).

Tergite VIII triangular, rounded posteriorly; punctation dense, coarse; subglabrous (Fig. 54A). Sternite VIII rectangular with a sooth projection; with strigulate microsculpture (Fig. 54B). Vagina and bursa copulatrix membranous without sclerites; vaginal plate with an apical sclerite, more or less short; oviduct bilobed, each lobe bearing a filiform spermatheca (Fig. 54C–D, Supp. file 2B). Distal gonocoxites curved and thick; gonostyli long, slender (Fig. 54C, E).

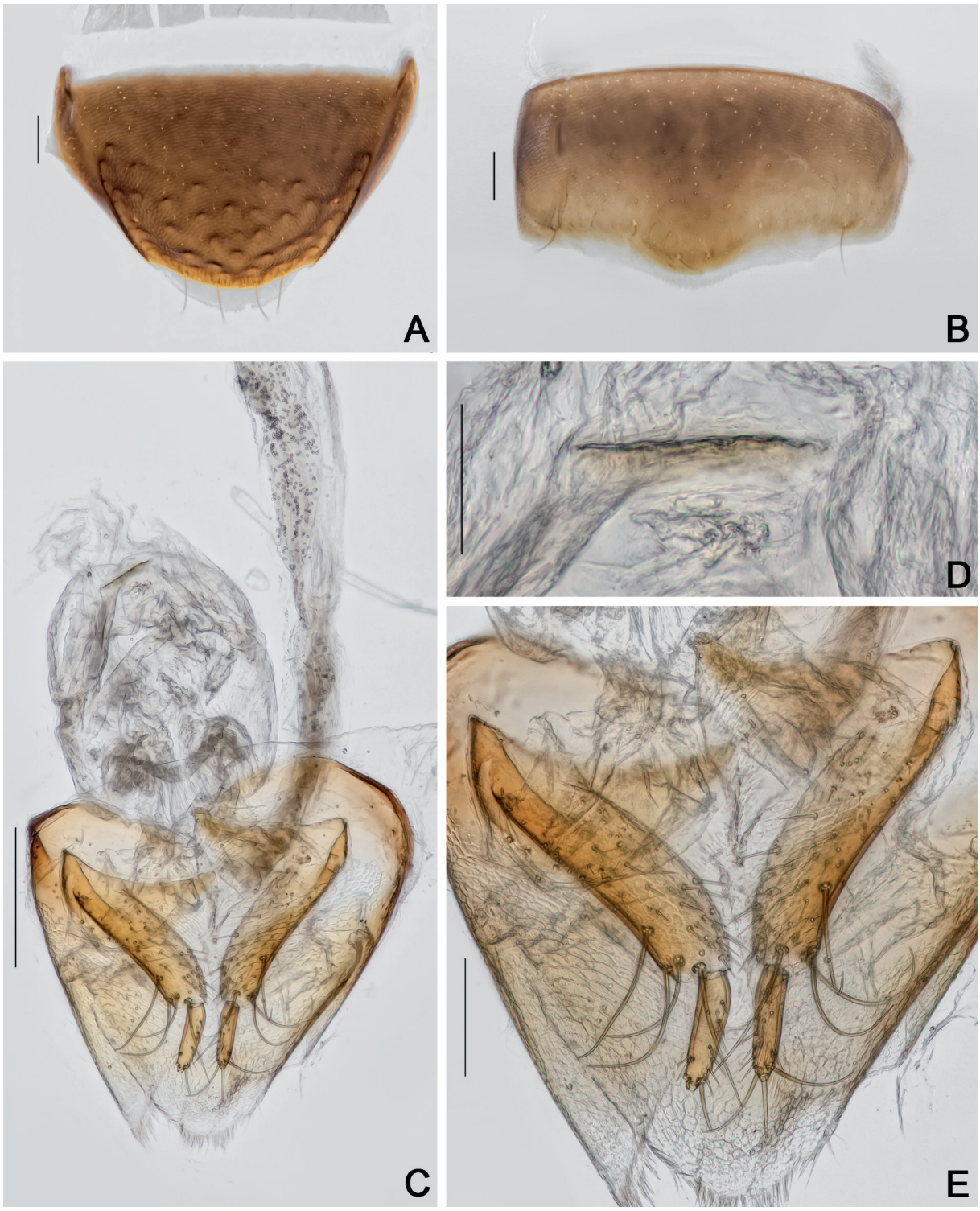

Fig. 54. *Cyparium collare* Pic, 1920, ♀ (CELC). **A**. Tergite VIII. **B**. Sternite VIII. **C**. Terminalia. **D**. Sclerite of vaginal plate. **E**. Ovipositor. Specimen collected at Mata do Paraíso, Viçosa (MG, Brazil). Scale bars: A–B, D–E = 0.1 mm; C = 0.2 mm.

Host fungi

Adults were collected from *Marasmiellus cubensis* (Berk. & M.A. Curtis) Singer (4 records, 8 individuals), *Marasmiellus* spp. (5, 6), *Marasmiellus* aff. *ramealis* (1, 5), cf. *Marasmiellus* sp. (yellow) (2, 5), cf. *Pleteus* sp. (1, 1), *Marasmius araucariae* Singer (1, 2), *Marasmius haematocephalus* (1, 1), *Leucocoprinus cepistipes* (1, 2), *Leucocoprinus ianthinus* (1, 1), *Leucoprinus* sp. (1, 1), *Inocybe* sp. (Agaricales, Inocybaceae) (1, 3), cf. *Valvariela* sp. (1, 2), *Leucoagaricus rubrotinctus* (Peck) Singer (1, 1), *Lepiota* sp. (Agaricales, Agaricaceae) (1, 3), *Macrolepiota colombiana* Franco-Mol. (Agaricales, Agaricaceae) (1, 2), *Heimiomyces neovelutipes* (Hongo) E.Horak (Agaricales, Mycenaceae) (1, 1), *Lulesia lignicola* B.E.Lechner & J.E.Wright (Agaricales) (1, 7), *Pleurotus pulmonarius* (Fr.) Quél. (Agaricales, Pleurotaceae) (2, 28), *Volvariella* sp. (Agaricales, Pleurotaceae) (1, 2), *Pluteus* sp. (Agaricales, Pleurotaceae) (1, 1), *Mycena* sp. (Agaricales, Mycenaceae) (1, 1), *Entoloma* (*Inocephalus*) sp. (1, 1), *Conocybe* sp. (Agaricales, Bolbitiaceae) (1, 1), *Coprinellus disseminatus* (Pers.) J.E.Lange (Agaricales, Psathyrellaceae) (1, 4), unidentified mushrooms (1, 18) and *Favolus tenuiculus* P.Beauv. (Polyporaceae, Polyporales).

Remarks

Images of the type series were requested from the MNHN, where these specimens were supposedly deposited (Löbl 2018a), but we were informed that they could not find any specimens. Nonetheless, we decided to treat the specimens that we examined as *C. collare* because their morphology and localities fit the original description and the known distribution of the species. Fourteen individuals of different body length and collected from different fungi at Viçosa, one from Areia Branca (SE) (Supp. file 3 (Figs 1–2)), and another one from Sta Luzia do Itanhi (SE) (Supp. file 3 (Figs 3–4)) were dissected. No differences were found in the terminalia, including the flagellum. Furthermore, no external differences were observed. The total body length is quite variable (2.60–3.72 mm). The three individuals from Areia Branca (SE) are the largest (3.64, 3.68 and 3.72 mm), while individuals collected at Viçosa (MG) and Sta Luzia do Itanhi (SE) are in the same size range (2.56–3.52 mm).

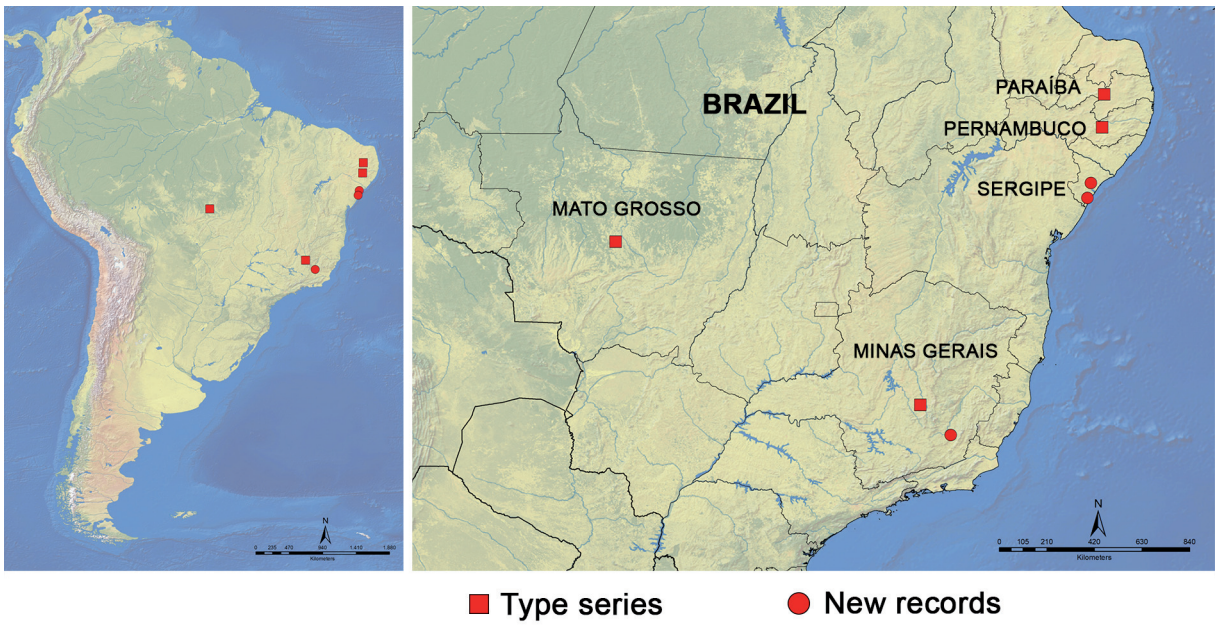

Fig. 55. *Cyparium collare* Pic, 1920, distribution. Squares = literature; circles = new records.

Distribution

Known from Brazil [“Matu Sinhos, Minas”; “Matto Grosso”; “Pery-Pery, Pernambuco”; “right bank of Parahyba”]. New records from Areia Branca and Santa Luzia do Itanhi, state of Sergipe, Northeast, Brazil, and from “Mata da Biologia” and “EPTEA Mata do Paraíso”, campus of the Universidade Federal de Viçosa, Viçosa, Minas Gerais, Southeast Brazil (Fig. 55).

Cyparium oberthueri Pic, 1956
Figs 5, 56–64

Cyparium oberthüri Pic, 1956: 175. Syntypes: Muséum national d’histoire naturelle (MNHN), Paris, France.

Material examined

BRAZIL – **Minas Gerais** • 1 ♀; Viçosa, Mata da Biologia; 26 Oct. 2016; A. Orsetti and I. Pecci-Maddalena leg.; CELC • 7 ♂♂, 3 ♀♀ (2 ♂♂, entirely dissected, preserved in glycerin; 2 ♂♂, 1 ♀, abdomen dissected, preserved in glycerin); same collection data as for preceding; 26 Jun. 2019; von Groll and A. Orsetti leg.; CELC • 1 ♂, 2 ♀♀; Viçosa, EPTEA Mata do Paraíso; 9 Nov. 2016; I. Pecci-Maddalena and C. Lopes-Andrade leg.; “\\ ex *Psathyrella candolleana*”; CELC • 1 ♂; same collection data as for preceding; 12 Nov. 2019; LabCol leg; CELC.

Diagnosis

TL: 4.43–5.12 mm in males and 4.68–5.25 mm in females. Black (Figs 56A–C, 64A). Hypomeron with close strigulate microsculpture. Scutellum tapered posteriorly (Fig. 59B). Mesanepisternum long with imbricate microsculpture. Metaventrite smooth (Fig. 56B). Intercoxal plates with long imbricate microsculpture. Aedeagus poorly sclerotized, almost membranous, apex very long; parameres L-shaped, very long (Fig. 62A–D). Distal gonocoxites curved and tapered (Fig. 63C, E).

Redescription

Coloration. Black, iridescent (Figs 56A–C, 64A). Frons dark brown; clypeus light brown (Fig. 57A); mouth parts and antennomeres I–VI and apex of XI testaceous; antennomeres VII–X and base of XI dark (Fig. 57B). Coxae and femora dark-brown reddish; tibiae lighter; tarsi and tergite VIII yellow; ventrites 5 and 6 brown. Variation: specimens entirely light brown to brown (Fig. 56D–F).

Head. Punctation dense, fine (Fig. 57A); vertex with strigulate microsculpture. Eyes slightly wider than head, rounded apically (Fig. 57A). Labrum rectangular, lateral margins rounded, and well distinct from apical margin; posterior margin slightly curved centrally; sclerotized portion curved; lateral setae slightly exceeding margins; porose centrally (Fig. 57D). Mandibles curved, subapical serrations on left mandible conspicuous (Fig. 57E–F). Maxillary palps elongated, palpomere III tapering smoothly; galea and lacinia densely pubescent, lacinia robust (Fig. 57G). Mentum with lateral areas rounded and apex not well delimited; glossa concave (Fig. 58A). Setae of labial palpomere II exceeding palpomere III; palpomere III longish, with long apical setae (Fig. 58A). Hypopharynx with wide and rounded sclerotized plate (Fig. 58A–B). Post gena microsculptured with very close transversal lines; densely porose all over; gula triangular with concave lateral areas (Fig. 58C). Base of antennae long, antennal club distinct; antennomere XI hexagonal (Fig. 57B–C), no difference between males and females.

Prothorax. Pronotum smooth, densely and coarsely punctate; pubescence short, fine (Fig. 58D–E); transverse and slightly curved laterally, forming an obtuse angle at lateral areas of posterior margin (Fig. 58E). Hypomeron with close strigulate microsculpture. Notosternal suture straight and slightly

turned to lateral areas (Fig. 58F). Profurca elongated, extending half length of foramen (Fig. 58G). Prosternal process short and curved (Fig. 59A).

Mesothorax. Mesonotum with prescutellar suture (= scutellar lines, Leschen & Löbl 2005) wavy (Fig. 59B). Scutellum tapered posteriorly (Fig. 59B). Anterior phragma large and straight (Fig. 59C). Mesanepisternum with long imbricate microsculpture. Procoxal rests sub-squared, somewhat rounded posteriorly (Fig. 59D). Mesoventral and median lines somewhat wavy; area between median and mesoventral lines somewhat enlarged (Fig. 59D). Mesoventral process moderately short, with apex more prominent, forming a ridge (Fig. 59E).

Metathorax. Metanotum with alacrista triangular, posterior portion longish; turned just slightly to posterior end; scutoscutellar suture long and wavy (Fig. 59F). Metaventrite smooth; punctuation sparse, fine (Figs 56B, E, 59D). Mesocoxal line not forming an angle between coxal cavities, just a simple curve and finely punctate under coxal cavities (Fig. 59D). Metanepisternum and metepimeron with imbricate microsculpture. Intercoxal plates with long imbricate microsculpture. Metendosternite with arms close and somewhat straight; 'stalk ridge' not exceeding half length of stalk (Fig. 60A); ventral longitudinal flange longish and rounded in lateral view (Fig. 60B).

Wings. Elytra large, slightly wider than longer; covering tergite VI (Fig. 56A); basal (Fig. 58D) and sutural lines dashed; adsutural area with a row of setae; six rows of coarse punctures (not including sutural line) (Figs 56A, 60C); lateral line coarse punctate; apical coarse punctation dense; apical serrations small (Fig. 60D); pubescence short and fine. Epipleuron with a row of sparse and coarse punctures. Hind wings fully developed (Fig. 60E).

Legs. Pro-, meso- and metacoxae, and femora with strigulate microsculpture. Profemora fusiform; punctuation sparse, fine (Fig. 60F). Mesofemora longish; punctures sparse, coarse (Fig. 60G). Metafemora longish; punctuation sparse, fine (Fig. 60H). Mesotibiae densely spinose; spines thick (Fig. 60G); metatibia sparsely spinose, spines fine (Fig. 60H).

Abdomen. Tergites VI–VIII with narrow imbricate microsculpture (Fig. 61A). Tergite VII trapezoidal when tergite VIII not exposed and triangular when exposed; punctation inconspicuous; pubescence sparse, fine. Ventrites 1–5 with strigulate microsculpture (Fig. 61B). Ventrite 1 densely and coarsely punctate; pubescence sparse, fine (Fig. 61C). Ventrites 2–5 densely and finely punctate; pubescence moderately sparse, fine. Metacoxal lines finely punctate.

Males

Measurements (n = 1, in mm). Antennomeres (length(width)): 0.33(0.10), 0.16(0.08), 0.21(0.08), 0.18(0.08), 0.19(0.09), 0.13(0.11), 0.15(0.17), 0.11(0.18), 0.12(0.21), 0.12(0.23), 0.23(0.25); (n = 8, unless otherwise specified; in mm): TL 4.43–5.12 (mean = 4.91, standard deviation ± 0.21), PL 1.68–2.00 (1.88 ± 0.09), PA 1.2–1.4 (1.34 ± 0.06), PB 2.72–3.16 (3.04 ± 0.14), SL 0.20–0.27 (0.24 ± 0.02), SW 0.21–0.28 (0.23 ± 0.02), EI 2.56–3.00 (2.85 ± 0.14), EL 2.96–3.56 (3.39 ± 0.19), EW 1.72–2.00 (1.90 ± 0.09), EH 1.00–1.25 (1.16 ± 0.08), HW 1.01–1.17 (1.13 ± 0.05), IS 0.30–0.37 (0.32 ± 0.02), WA 0.22–0.30 (0.26 ± 0.03), MC (n = 5) 1.36–1.44 (1.41 ± 0.03), MB (n = 6) 0.64–0.72 (0.68 ± 0.03), VL (n = 6) 0.80–0.96 (0.84 ± 0.06).

Pro- and mesotarsomeres I–III enlarged, with tenet setae (Fig. 60F–G). Tergite VIII pentagonal, slightly acuminate posteriorly; punctation sparse, fine; subglabrous (Fig. 61D). Tergite IX with rectangular ventral struts (Fig. 61E–F). Sternite VIII sub-rectangular, with a smooth projection (Fig. 61G). Sternite IX thick, centrally constricted (Fig. 61F). Aedeagus poorly sclerotized, almost membranous, apex of median lobe very long (Fig. 62A–C); internal sac with irregular sclerites, with a large hook (Fig. 62D–E); parameres L-shaped, very long (Fig. 62A).

Females

Measurements (n = 1, in mm). Antennomeres (length(width)): 0.28(0.10), 0.15(0.08), 0.20(0.07), 0.17(0.07), 0.17(0.08), 0.12(0.10), 0.14(0.16), 0.13(0.18), 0.11(0.20), 0.11(0.23), 0.22(0.23); (n = 6, unless otherwise specified; in mm): TL 4.68–5.25 (mean = 4.91, standard deviation ± 0.19), PL 1.76–2.04 (1.86 ± 0.09), PA 1.28–1.40 (1.34 ± 0.04), PB 2.84–3.28 (3.04 ± 0.15), SL 0.24–0.27 (0.25 ± 0.01), SW 0.21–0.30 (0.25 ± 0.03), EI 2.64–3.04 (2.82 ± 0.13), EL 3.16–3.60 (3.34 ± 0.15), EW 1.72–2.00 (1.90 ± 0.10), EH 1.15–1.40 (1.23 ± 0.08), HW 1.06–1.15 (1.11 ± 0.03), IS 0.30–0.35 (0.32 ± 0.01), WA 0.25–0.30 (0.26 ± 0.02), MC (n = 5) 1.32–1.52 (1.40 ± 0.07), MB (n = 5) 0.64–0.80 (0.74 ± 0.06), VL (n = 5) 0.88–1.04 (0.94 ± 0.06).

Fig. 56. *Cyparium oberthueri* Pic, 1956. **A–C**. Male specimen (CELC). **A**. Dorsal view. **B**. Ventral view. **C**. Lateral view. **D–F**. Different male specimen (CELC). **D**. Dorsal view. **E**. Ventral view. **F**. Lateral view. Specimens collected at Mata da Biologia (A–C) and Mata do Paraíso (D–F). Scale bars = 1.0 mm.

Tergite VIII triangular; punctation dense, fine; pubescence dense (Fig. 63A). Sternite VIII sub-rectangular with a triangular projection (Fig. 63B). Vagina and bursa copulatrix membranous, without sclerites (Fig. 63C). Vaginal plate with an apical rectangular sclerite (Fig. 63D) Spermatheca not detected. Distal gonocoxites curved and enlarged at base; gonostyli short, enlarged at base (Fig. 63C, E).

Host fungi

Adults were collected from *Psathyrella candolleana* (1 record, 3 individuals), unidentified mushroom ("*Lactarius*?") (1, 10).

Remarks

The dorsal photo of one specimen belonging to the type series (Fig. 64A) and the original description of *C. oberthueri* are consistent with the data of the specimens studied here. Furthermore, the itinerary of Philibert Germain (P. Germain) (Fig. 64C) was evaluated: in 1885 he was in Minas Gerais and in 1886 at "Province Matto Grosso" where the type series was collected (Fig. 64C) (Papavero 1971). The "Province Matto Grosso" at that time was a broad province that comprised what nowadays are the states of Mato Grosso, Mato Grosso do Sul and Rondônia. In 1887 he arrived in Cárceres (currently in the state of Mato Grosso) departing from Corumbá (currently Mato Grosso do Sul), and in 1889 he was in Cochabamba (Bolivia) (Fig. 64C) (Papavero 1971). It is likely that "Province Matto Grosso" refers to

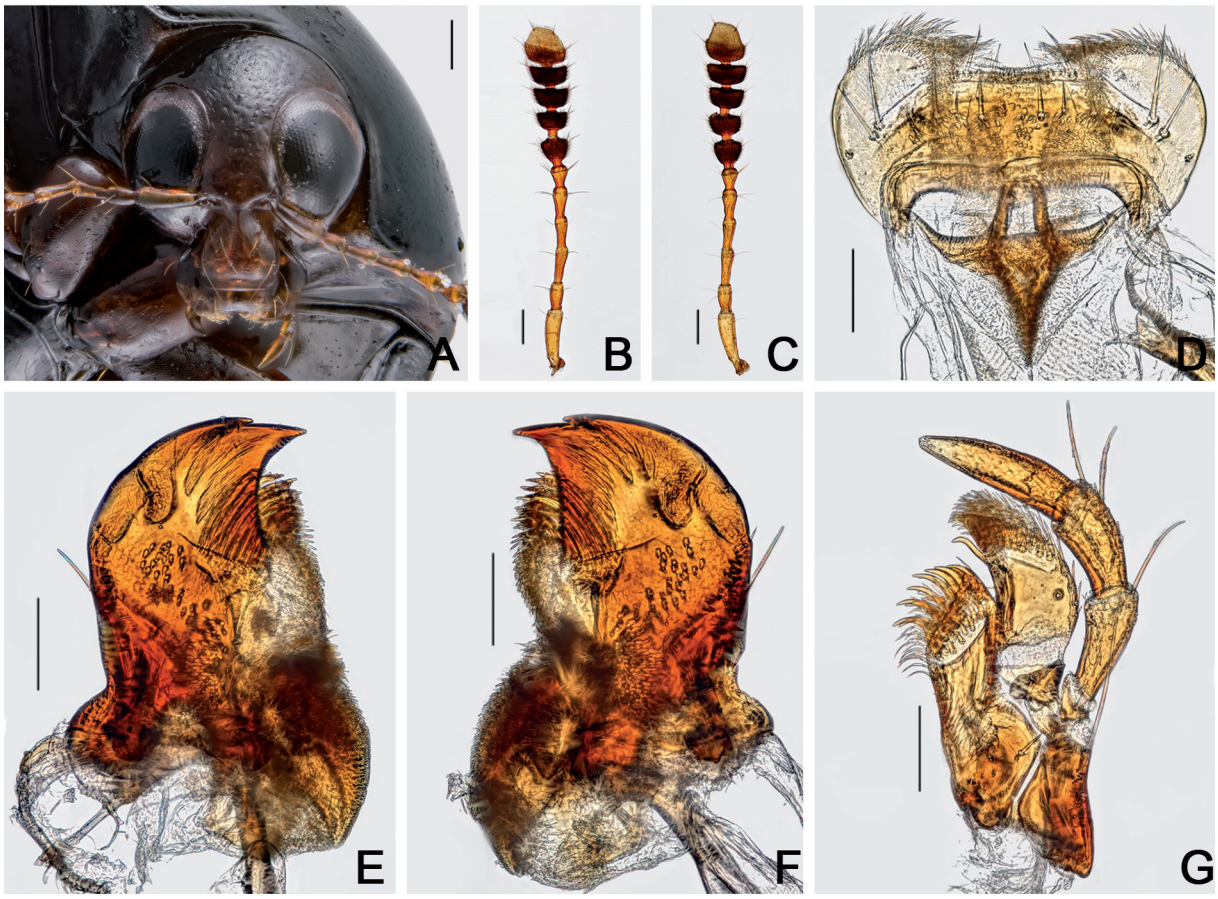

Fig. 57. *Cyparium oberthueri* Pic, 1956 (CELC). **A**. Frontal view. **B**. Male antenna. **C**. Female antenna. **D**. Labrum. **E**. Left mandible. **F**. Right mandible. **G**. Maxilla. Specimens collected at Mata da Biologia, Viçosa (MG, Brazil) (CELC). Scale bars: A–C = 0.2 mm; D–G = 0.1 mm.

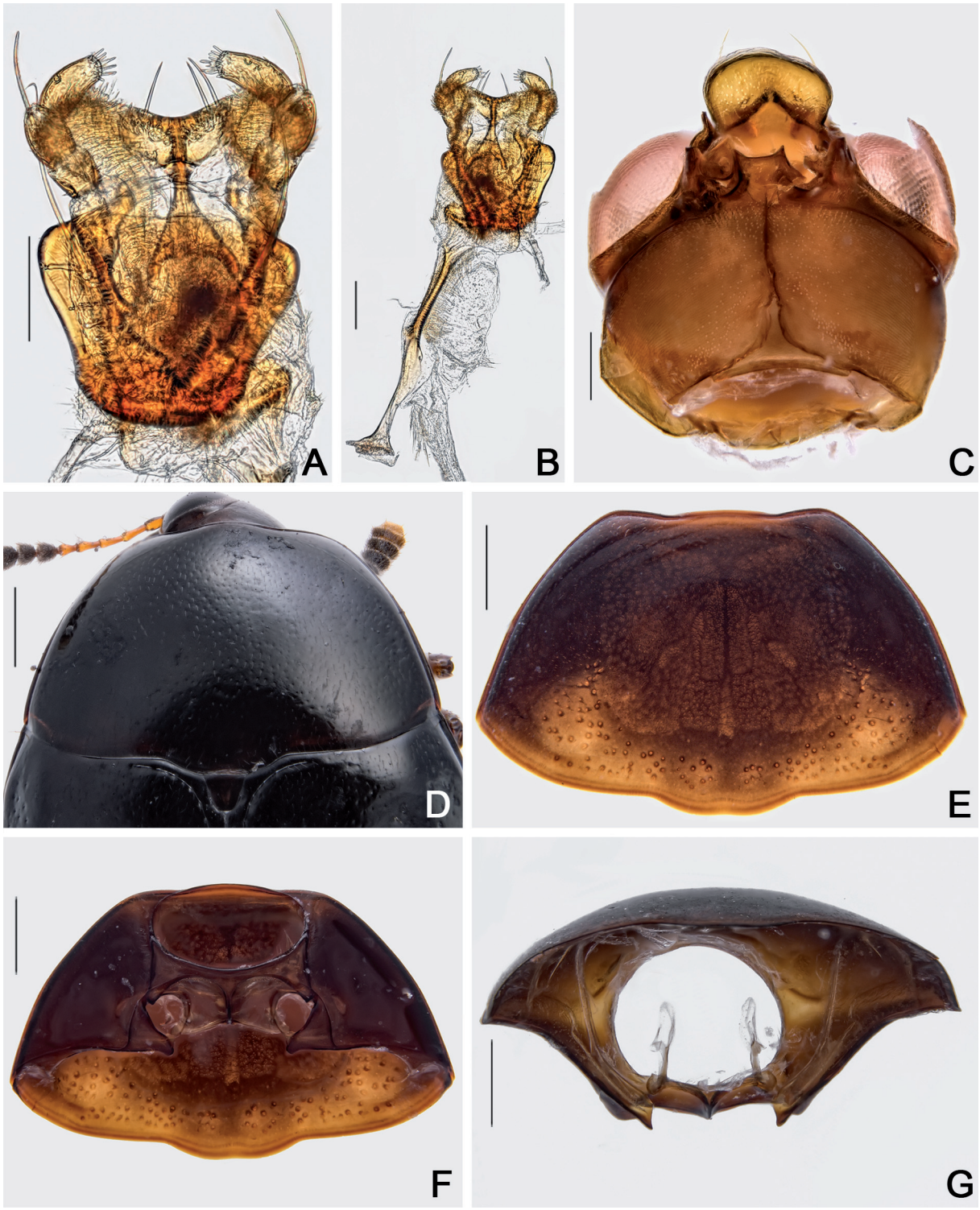

Fig. 58. *Cyparium oberthueri* Pic, 1956, ♂♂ (CELC). **A**. Labium. **B**. Hypopharynx. **C**. Head, ventral view. **D–E**. Pronotum, dorsal view. **F–G**. Prothorax. **F**. Ventral view. **G**. Inner view. Specimens collected at Mata da Biologia, Viçosa (MG, Brazil). Scale bars: A–B = 0.1 mm; C = 0.2 mm; D–G = 0.5 mm.

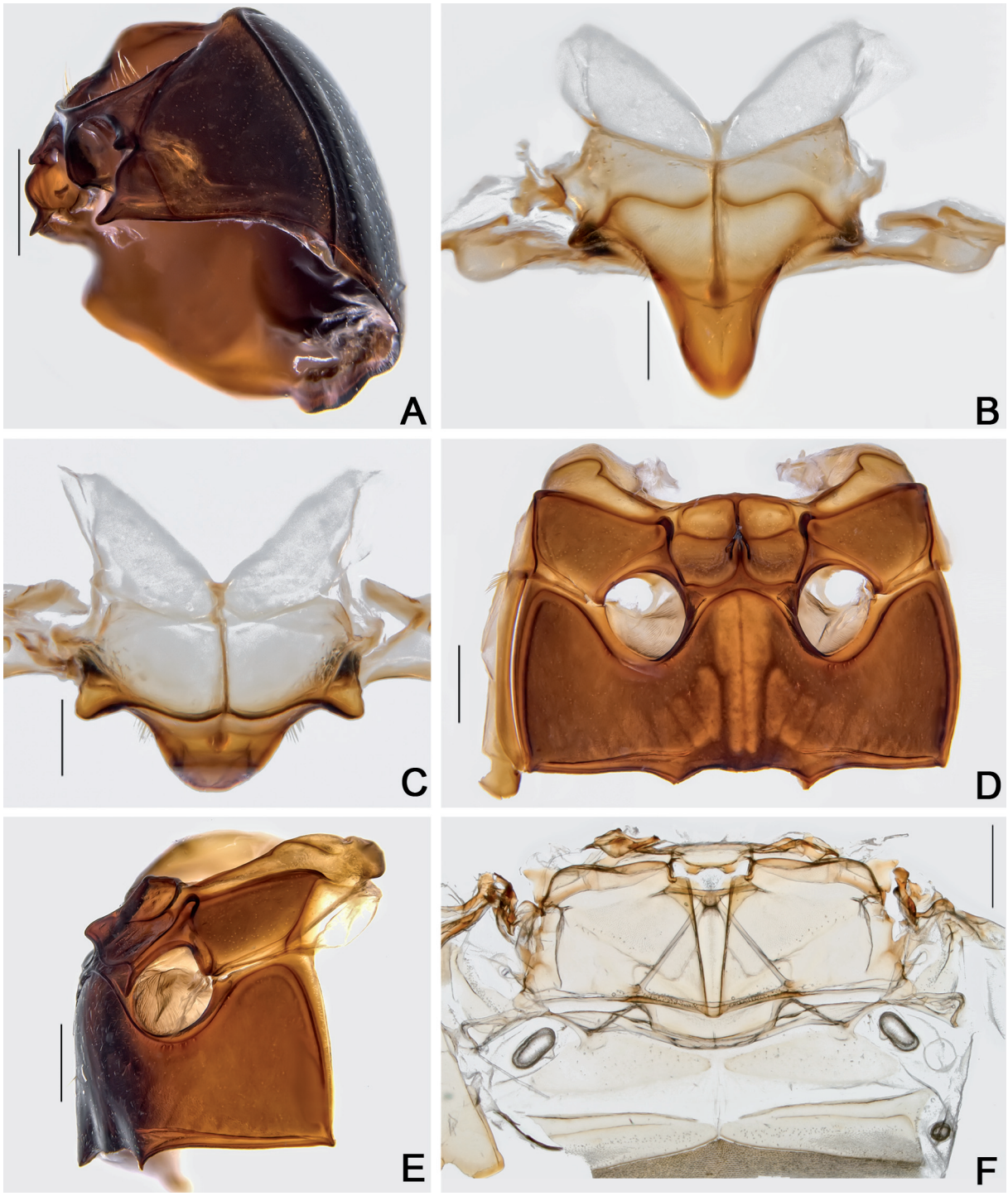

Fig. 59. *Cyparium oberthueri* Pic, 1956, ♂♂ (CELC). **A**. Prothorax, lateral view. **B–C**. Scutellar plate. **B**. Dorsal view. **C**. Apically slanted view. **D–E**. Meso- and metathorax. **D**. Ventral view. **E**. Lateral view. **F**. Metanotum. Specimens collected at Mata da Biologia, Viçosa (MG, Brazil) (CELC). Scale bars: A, D–F = 0.5 mm; B–C = 0.2 mm.

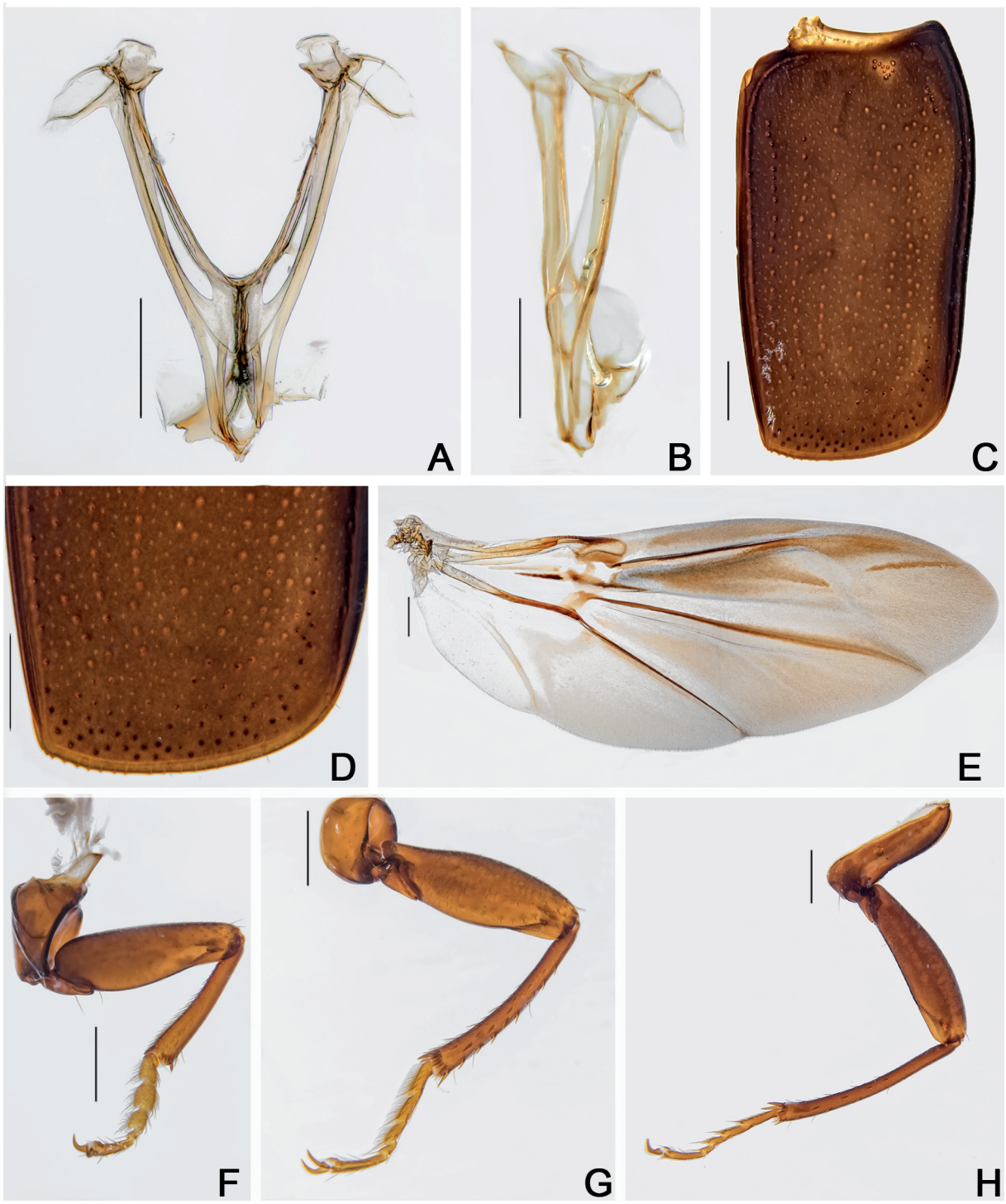

Fig. 60. *Cyparium oberthueri* Pic, 1956, ♂♂ (CELC). **A–B**. Metendosternite. **A**. Dorsal view. **B**. Lateral view. **C–D**. Elytron. **C**. Entire. **D**. Apex. **E**. Hind wing. **F–H**. Legs. **F**. Fore. **G**. Middle. **H**. Hind. Specimens collected at Mata da Biologia, Viçosa (MG, Brazil). Scale bars = 0.5 mm.

somewhere between what nowadays is the northern part of Mato Grosso do Sul, and the southern part of Mato Grosso. We do not know whether the type series was collected in the Cerrado biome or in riparian forest similar, or even linked, to areas of the Atlantic Forest biome. The specimens we examined are all from two Atlantic Forest remnants of Southeast Brazil, far away from the type locality, but they fit the

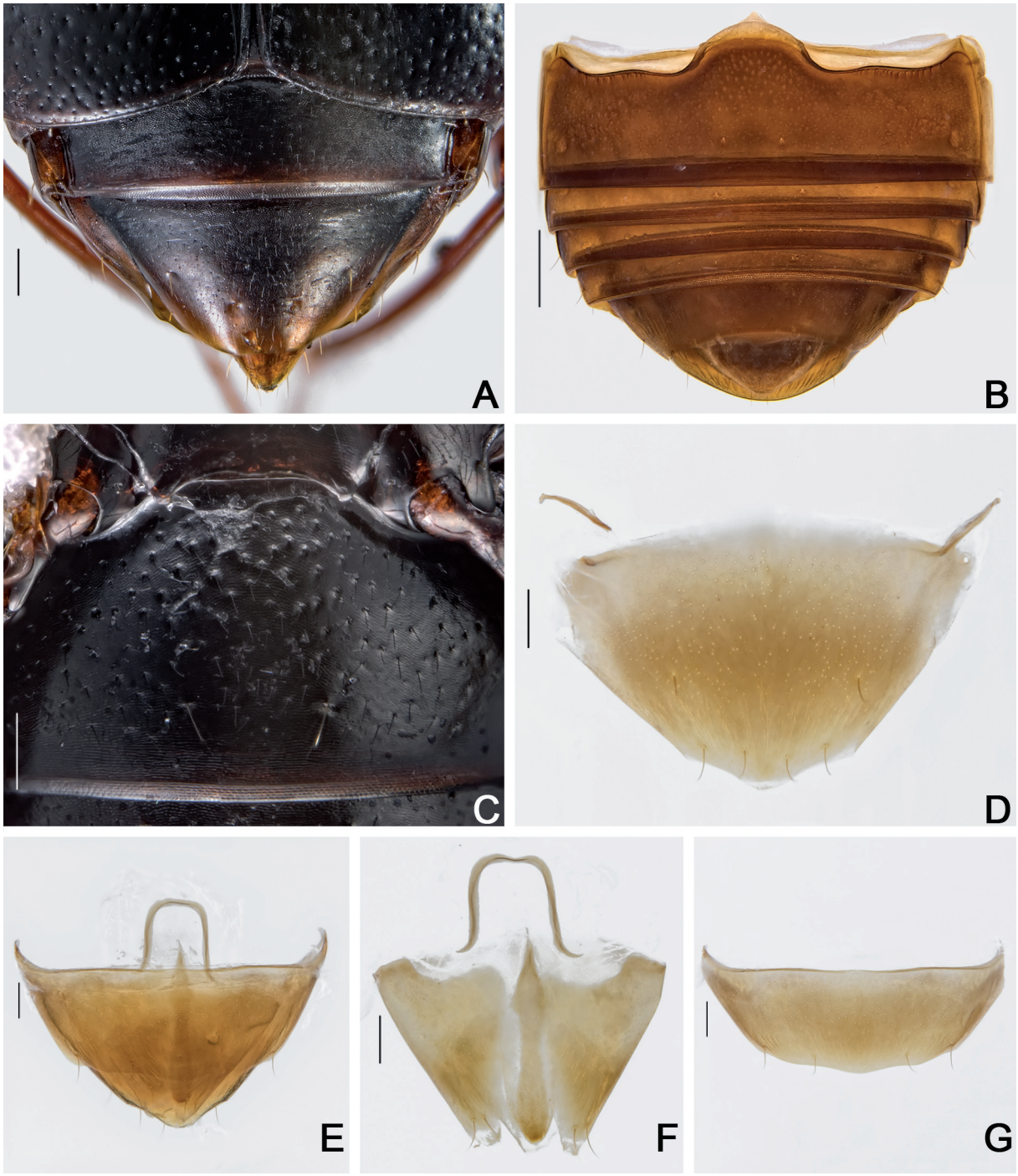

Fig. 61. *Cyparium oberthueri* Pic, 1956, ♂♂ (CELC). **A–B**. Abdomen. **A**. Dorsal view. **B**. Ventral view. **C**. Ventrite 1. **D**. Tergite VIII. **E**. Terminalia. **F**. Tergite IX. **G**. Sternite VIII. Specimens collected at Mata da Biologia, Viçosa (MG, Brazil). Scale bars: A, C–G = 0.2 mm; B = 0.5 mm.

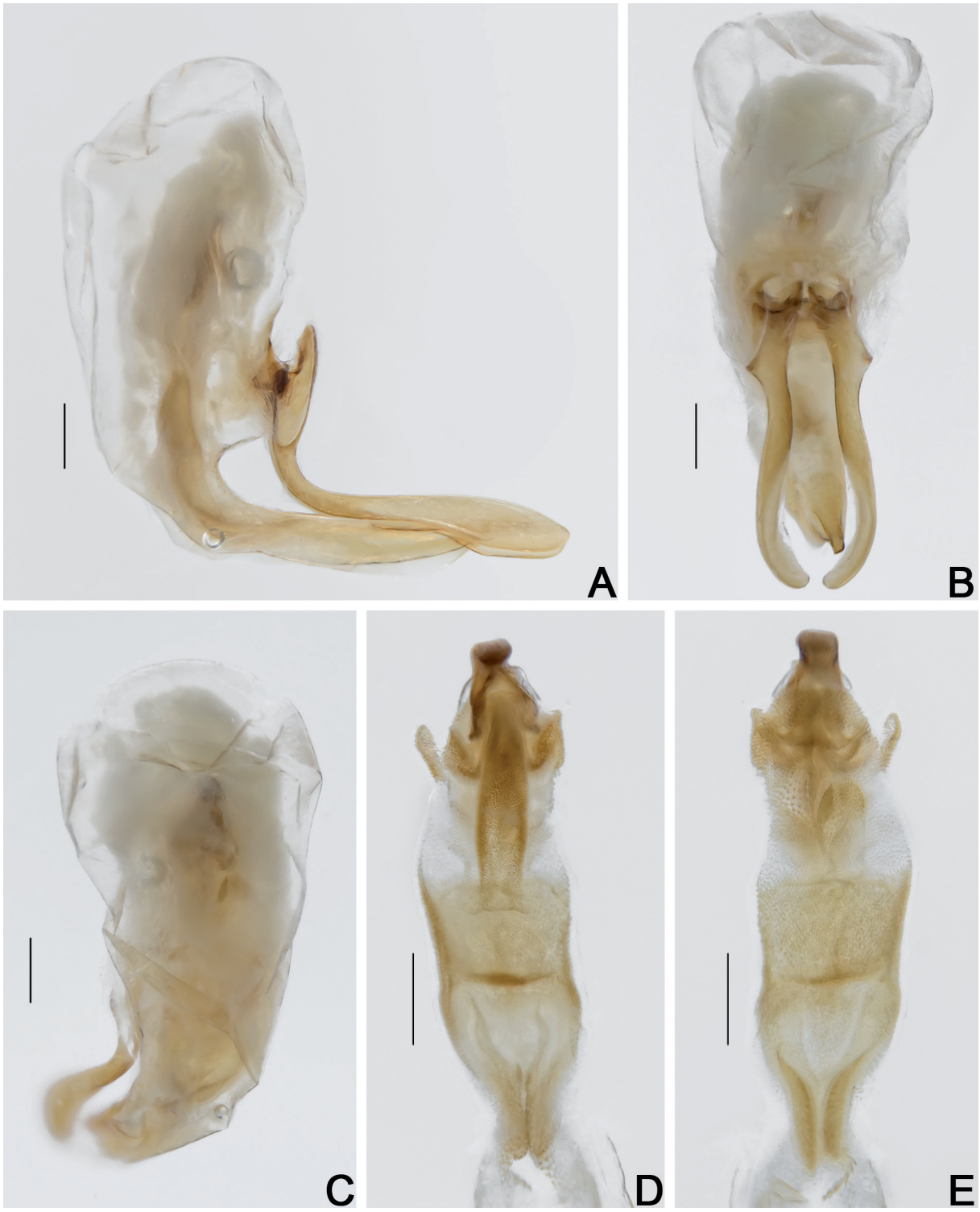

Fig. 62. *Cyparium oberthueri* Pic, 1956, ♂ (CELC). **A–C**. Aedeagus. **A**. Lateral view. **B**. Frontal view. **C**. Dorsal view. **D–E**. Internal sac. **D**. Frontal view. **E**. Dorsal view. Specimen collected at Mata da Biologia, Viçosa (MG, Brazil). Scale bars = 0.2 mm.

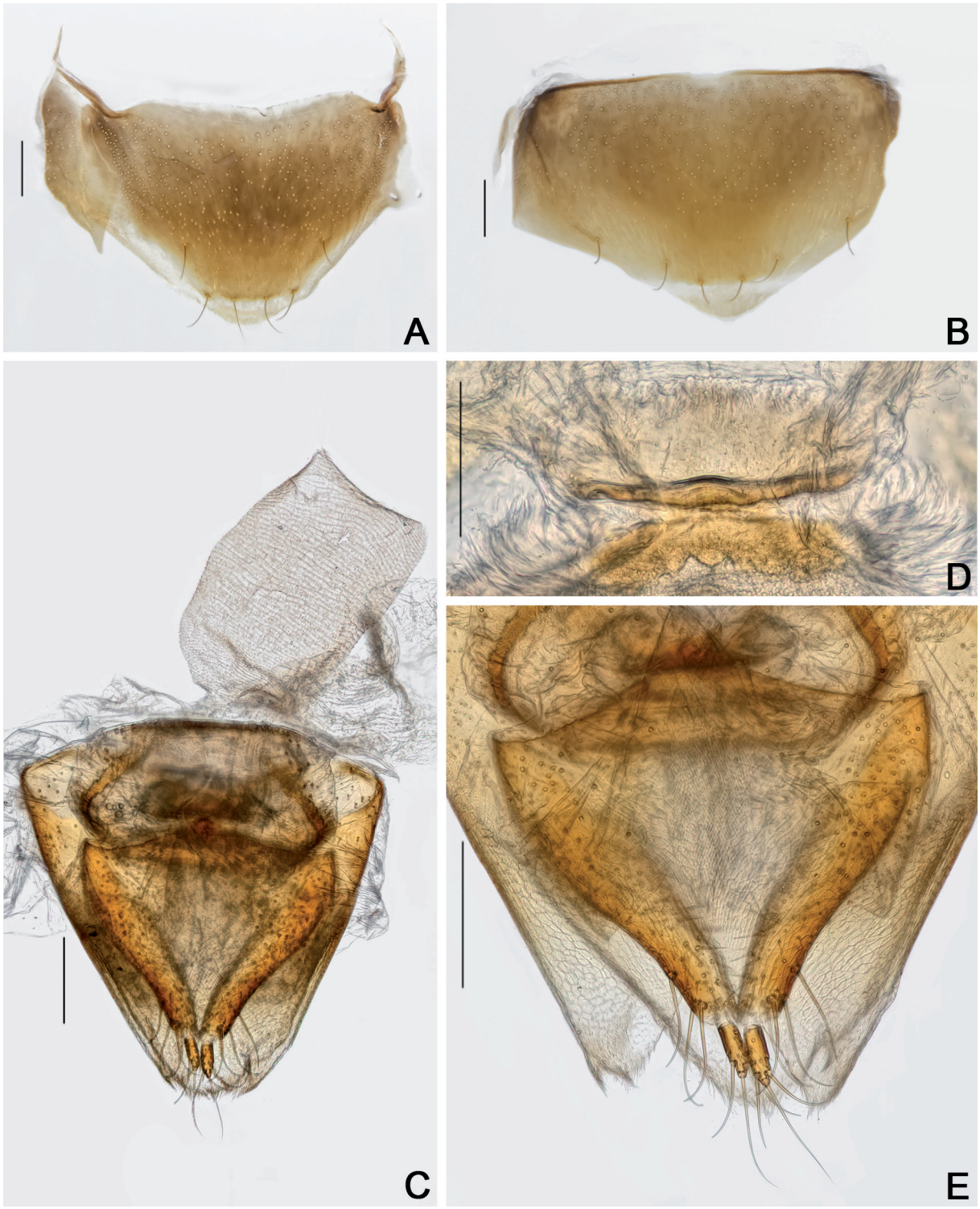

Fig. 63. *Cyparium oberthueri* Pic, 1956, ♀ (CELC). **A**. Tergite VIII. **B**. Sternite VIII. **C**. Terminalia. **D**. Sclerite of vaginal plate. **E**. Ovipositor. Specimen collected at Mata da Biologia, Viçosa (MG, Brazil). Scale bars: A–C, E = 0.2 mm; D = 0.1 mm.

original description and are morphologically similar to the available image of a syntype (Fig. 64A). At this moment, we prefer to call the specimens we have in hand as *C. oberthueri*, in the absence of any evidence to describe them as a new species.

Distribution

Known from "Prov. Matto Grosso", Midwest, Brazil (1886, P. Germain). New records from Viçosa, Minas Gerais, Southeast Brazil (Fig. 64C).

Fig. 64. *Cyparium oberthueri* Pic, 1956 (MNHN collection-Paris). **A**. Habitus. **B**. Labels. **C**. Distribution. Squares = P. Germain itinerary; circles = new records.

Discussion

There are two main problems in accurately identifying species of *Cyparium*. First, they are very similar to each other and morphological limits between species based on traditional characteristics (shape, size, colour pattern) are obscure. That is true for the species studied here and was previously pointed out by Leschen & Löbl (1995), who examined 48 species of the genus. Another important problem is that it is very common to observe intraspecific colour variation (e.g., in *C. lescheni* sp. nov., *C. newtoni* sp. nov., *C. oberthueri*; *C. terminale* as mentioned by Márquez (2007)), or species that were described based on teneral specimens like *C. palliatum* (as pointed out by Matthews (1888)). Therefore, the study of non-traditional characteristics, such as the morphology of mouthparts, meso- and metanotum, metendosternite, and male and female abdominal terminalia, among others, may help to circumvent these problems. Below we discuss some taxonomically important characteristics of *Cyparium* based on our results.

Cuticular microsculpture is shown to be very important for distinguishing species of *Cyparium*. It varies among the sclerites of the body, like the head and tergites (Table 1). This characteristic has not been very well studied in *Cyparium*, but it is well known in other genera, such as *Scaphisoma* Leach, 1815, *Brachynopus* Broun, 1881, and *Baeocera* Erichson, 1845 (Löbl & Leschen 2003; Löbl 2015, 2018b). For the species studied here, this microsculpture is imbricate or strigulate, and more or less separated; it covers the entire sclerite surface, or just a part of it. Most species of *Cyparium* studied here had different sets of cuticular microsculpture (Table 1), except for *C. loebli* sp. nov. and *C. pici* sp. nov. But even the latter two species showed some slight differences (microsculpture less spaced in *C. pici*).

Along with microsculpture, punctation also proved to be diagnostic. Elytron punctation is well known: it can have five to seven discal punctures (Ogawa *et al.* 2016). All species we studied here have six rows, but the latter two could be intermixed or not. Elytral apical punctation was also important, being more or less coarse and dense. The presence or absence of punctation on the metaventrite was diagnostic as well. Abdominal punctation was also diagnostic, like in the case of the coarse punctation on ventrite 1 in *C. pici*, and in tergite VII of *C. collare*.

Measurements of antennomeres are widely used to determine species in Scaphidiinae (Löbl & Leschen 2003; Ogawa & Sakai 2011; Ogawa *et al.* 2016; Löbl 2015, 2020; Löbl *et al.* 2021), and these were also taxonomically informative for the species of *Cyparium*. Measuring an entire antenna can be difficult, because it may be hidden, so we suggest focusing primarily on the last antennomere. The shape and colour (unicolorous/bicolored) of the last antennomere are quite variable between species, and it is usually easily visible even when the rest of the antenna is hidden.

Mouth parts are quite variable as well. The interspecific variation of the labrum shape came as a surprise, as can be seen, for instance, when comparing *C. achardi* sp. nov. and *C. loebli* (Figs 7G, 23D). The main differences in the remaining mouthparts are variations in proportions (length/width) and it is possible that noticing the structures alone, without others to compare, it would be difficult to describe them. The general shape of the mouthparts does not differ from that studied by Leschen & Löbl (1995, 2005) and Naomi (1988a, 1988b). Leschen & Löbl (1995) classified gular pores present in *Cyparium*, but the disposition and density of these pores were shown to be informative as well, as is the shape of the gula.

General pronotum shape is quite similar, but differences can be found in the proportions and shape of the anterior and posterior beads, and lateral areas. For example, in *C. achardi*, the anterior bead is less evident than in *C. pici*, and the shape of the former is also more squared, with the lateral areas less curved. We have not studied this structure in detail to separate species. However, it might be an interesting structure on which to conduct morphometric analysis. The same can be applied to the elytra, and also to the prosternal and mesoventral processes.

Table 1. Comparative morphology regarding the microsculpture of the various structures. Abbreviations: stri. = strigulate; imbr. = imbricate.

	Vertex	Hypomeron	Mesanepisternum	Metaventrite	Metanepisternum	Metepimeron	Ventrite 1
Cyparium achardi sp. nov.	–	–	–	–	imbr.	imbr.	stri.
Cyparium lescheni sp. nov.	–	stri.	stri.	stri.	imbr.	imbr.	stri.
Cyparium loebli sp. nov.	–	stri.	stri.	–	imbr.	imbr.	stri.
Cyparium newtoni sp. nov.	–	stri.	stri.	–	–	imbr.	stri.
Cyparium pici sp. nov.	–	stri.	stri.	–	imbr.	imbr.	stri.
Cyparium collare	–	imbr. (laterally)	imbr.	imbr. (laterally)	imbr.	imbr.	imbr.
Cyparium oberthueri	stri.	stri.	imbr.	–	imbr.	imbr.	stri.

The profurcae of scaphidiines are little studied. But comparing those of *Cyparium* to those of *Scaphisoma pandemum* von Groll & Lopes-Andrade, 2021 we noticed that the shape of the profurcae might be useful in generic diagnoses within Scaphidiinae. The profurcae of the seven species we studied were similar: short stalk and a longish apex (feather-shaped), but in *S. pandemum* the stalk is longer and the apex is rounded (von Groll & Lopes-Andrade 2021).

The sclerite between lateral area of mesanepisternum is considered to be a "not true mesepimeron" (Leschen *et al*. 1990). We consider this sclerite to be just a fold of the mesanepisternum (Fig. 3); on the other hand, the structure hidden by the elytra seems to be the mesepimeron (Fig. 9E). Nonetheless, we believe that this structure must be reviewed in *Cyparium*.

The metendosternite of Scaphidiinae has been illustrated for a few genera (Crowson 1938; Naomi 1989a; Leschen & Löbl 1995; von Groll & Lopes-Andrade 2021). Differences between genera are quite evident (e.g., arms longer and thinner, and stalk larger in *Scaphisoma* than in *Cyparium*), but among *Cyparium* species the differences are quite subtle: arms slightly curved, 'stalk ridge' occupying (or not) half of the stalk.

The metanotum of *S. pandemum* was illustrated and it is quite similar to those of the *Cyparium* species studied here. The metanotum studied here also presents a similar pattern as the metanotum of *Elodes pseudominuta* Klausnitzer, 1971 (Coleoptera, Scirtidae) (Friedrich & Beutel 2006): same alacrista, median membranous area and apodeme shapes. However, this structure is dissimilar to the reduced metanotum of the wingless *Trurlia* sp. (Staphylinidae, Scydmaeninae) (Jałoszyński 2009).

Venation of the hind wings was quite similar among species: CAS curved and smooth, MP_{1+2}, MSP, and RP_{3+4} well marked, and R_4 thin. Therefore, regarding the same genus they are not informative for diagnosis. Nonetheless, by comparing it with other genera it is possible to find differences. In *S. pandemum* the veins are more delicate and CAS less curved (von Groll & Lopes-Andrade 2021). The

venation of *Scaphidium* sp. and *Scaphium castanipes* Kirby, 1837 (Lawrence *et al.* 2021) differ from species of *Cyparium* mainly by the absence of MP_4, and MP_{1+2} and the straighter R_4.

The morphology of male aedeagus has been used in the taxonomy of Scaphidiinae (Leschen & Löbl 2005), as it is highly variable between species, but is quite similar within a species. Papers on *Cyparium* usually describe and illustrate it (Löbl 1984, 1999; Hwang & Ahn 2001; Fierros-López 2002; Márquez 2007; Ogawa & Sakai 2011; Ogawa *et al.* 2016). Although *Cyparium* have relatively homogeneous aedeagal characters (Leschen & Löbl 1995), there are numerous differences between the species that we have examined, like the morphologically similar *C. lescheni* and *C. newtoni*. Even the median lobe itself was enough to distinguish the species we have studied. Sometimes it is necessary to analyse the internal sac sclerites of scaphidiine beetles to search for diagnostic characteristics. We extracted and studied the internal sac of many *Cyparium* individuals, but did not find differences between the ones that had the same aedeagus shape, as in the case of specimens of *C. collare* from different localities. Although the ventral struts, sclerites VIII and IX, and tergite VIII are rarely illustrated, they were found to be very important for species delimitation, and may be diagnostic for some species, as in the case of *C. loebli* and *C. lescheni*.

Ogawa & Sakai (2011) emphasized that the vaginal plate is very useful to distinguish species of *Cyparium* and this is true for the species we have studied here. We found that the sclerite of the vaginal plate can be more or less developed; therefore, it cannot be analysed alone. The bursa copulatrix is a very variable structure, but some differences are only noticed when it is inflated. Unfortunately, we did not manage to keep the bursa inflated for the individuals we photographed for this work. But while we were testing techniques to dissect females on fresh collected specimens, we did manage to study inflated bursae, so it was possible to observe shape differences (e.g., *C. lescheni* Supp. file 2A and *C. collare* Supp. file 2B). Even though the spermatheca was not always detected, it does not mean that it does not exist; it is a very delicate and, usually, long structure that easily breaks. Every time it was observed, it was composed of a pair of filiform structures, similar to that of other species of *Cyparium* (Ogawa & Sakai 2011). We are working to improve techniques for dissecting females, but successful dissections seem to depend mostly on the degree of conservation of specimens. Distal gonocoxites and gonostyli are the best known structures of Scaphidiinae and are often illustrated (Ogawa & Sakai 2011; Ogawa & Löbl 2013, 2016; Ogawa *et al.* 2016). The main differences we found in these structures were the length in relation to width and the curvature, but sometimes the differences among species are more subtle than the ones regarding the vaginal plate. Therefore, we suggest studying all the female reproductive structures.

Specimens of *Cyparium* were collected from 39 different fungi: 36 Agaricales, one Hymenochaetales (*C. loebli* – probably incidental), one Polyporaceae (*C. collare*), and one unidentified mushroom ("*Lactarius*?", Russulales). The results corroborate with Newton (1984) and Kompantsev & Pototskaya (1987) who also mentioned species of *Cyparium* in Agaricales. *Cyparium lescheni*, *C. loebli*, and *C. newtoni* specimens were usually collected in large groups and sometimes cooccurring (especially the former and the latter); *C. oberthueri* beetles were also collected in groups, but apart from other species; *C. achardi* specimens were usually collected alone or in small groups, with four beetles each time at most; *C. collare* beetles were usually found alone or in small groups, but a few times they were found in large groups, usually with no other species; this is the most common species and seems to be the most generalist.

Conclusion

Cyparium now has 60 species; of these, 29 species are from the Neotropical region, thirteen from Brazil (Figs 4–5). Furthermore, by providing detailed morphological descriptions and redescriptions, along with illustrations, the morphology of *Cyparium* is somewhat better known now. Some of the structures and characteristics presented here can be used in future phylogenetic studies.

Acknowledgements

We thank the staff of Laboratório de Sistemática e Biologia de Coleoptera (UFV) for assistance in field collections at Viçosa. We also thank Luciano de A. Moura (MCNZ) and Fernando Z. Vaz-de-Mello (CEMT) for loaning specimens. We sincerely thank Azadeh Taghavian (MNHN) and Jiří Hájek (NMPC) for the images provided. We thank the doctoral qualifying committee (Angelico Asenjo, Andressa Paladini, Juares Fuhrmann and Igor de Souza Gonçalves), Dr Ivan Löbl, and the anonymous reviewer for the suggestions and corrections that helped to improve this manuscript. Financial support was provided by Conselho Nacional de Desenvolvimento Científico e Tecnológico (CNPq; research grant number 308432/2018-5 to the junior author), Fundação de Amparo à Pesquisa do Estado de Minas Gerais (FAPEMIG; Edital 02/2018—Programa Pesquisador Mineiro XII—PPM-00314-18) and Coordenação de Aperfeiçoamento de Pessoal de Nível Superior—Brasil (CAPES; Finance Code 001; doctorate degree grant to the senior author).

References

Achard J. 1921. Notes sur les Scaphidiidae du Musée de Leyde. *Zoologische Mededeelingen* 6: 84–91.

Achard J. 1922. Descriptions de scaphidides nouveaux (Col. Scaphidiidae). *Fragments entomologiques*: 35–45.

Ashe J.S. 1984. Description of the larva and pupa of *Scaphisoma terminatum* Melsh. and the larva of *Scaphium castanipes* Kirby with notes on their natural history (Coleoptera: Scaphidiidae). *The Coleopterists Bulletin* 38: 361–373.

Crowson R.A. 1938. The metendosternite in Coleoptera: a comparative study. *Transactions of the Royal Entomological Society of London* 87 (17): 397–415. https://doi.org/10.1111/j.1365-2311.1938.tb00723.x

Erichson W.F. 1845. *Naturgeschichte der Insecten Deutschlands. Erste Abteilung. Coleoptera. Dritter Band. Lieferung 1*. Nicolaische Buchhandlung, Berlin. https://doi.org/10.5962/bhl.title.8270

Fierros-López H.E. 2002. Descripción de dos especies nuevas de *Cyparium* Erichson 1845 (Coleoptera: Staphylinidae) de México. *Dugesiana* 9 (2): 7–14.

Friedrich F. & Beutel R.G. 2006. The pterothoracic skeletomuscular system of Scirtoidea (Coleoptera: Polyphaga) and its implications for the high-level phylogeny of beetles. *Journal of Zoological Systematics and Evolutionary Research* 44 (4): 290–315. https://doi.org/10.1111/j.1439-0469.2006.00369.x

Grebennikov V.V. & Newton A.F. 2012. Detecting the basal dichotomies in the monophylum of carrion and rove beetles (Insecta: Coleoptera: Silphidae and Staphylinidae) with emphasis on the oxyteline group of subfamilies. *Arthropod Systematics & Phylogeny* 70 (3): 133–165.

Harris R.A. 1979. A glossary of surface sculpturing. *Occasional Papers in Entomology* 28: 1-31.

Hübler N. & Klass K.D. 2013. The morphology of the metendosternite and the anterior abdominal venter in Chrysomelinae (Insecta: Coleoptera: Chrysomelidae). *Arthropod Systematics & Phylogeny* 71 (1): 3–41.

Hwang W. & Ahn K. 2001. New records of *Cyparium* Erichson and *Scaphidium* Olivier species in Korea (Coleoptera, Staphylinidae, Scaphidiinae). *Insecta Koreana* 18 (4): 369–372.

Jałoszyński P. 2009. *Trurlia*, a new Oriental genus of the tribe Cephenniini (Coleoptera: Scydmaenidae). *European Journal of Entomology* 106 (2): 261–274. https://doi.org/10.14411/eje.2009.034

Jałoszyński P. 2012. Taxonomy of '*Euconnus* complex'. Part I. Morphology of *Euconnus* s. str. and revision of *Euconnomorphus* Franz and *Venezolanoconnus* Franz (Coleoptera: Staphylinidae: Scydmaeninae). *Zootaxa* 3555 (1): 55–82. https://doi.org/10.11646/zootaxa.3555.1.3

Kirsch T. 1873. Beiträge zur Kenntniss der peruanischen Käferfauna auf Dr. Abendroth's Sammlungen basirt. *Berliner entomologische Zeitschrift* 17: 121–152.

Kompantsev A.V. & Pototskaya V.A. 1987. Novye dannye po lichikam zhukov-chelnovidok (Coleoptera, Scaphidiidae). *In*: Kompantsev A.V. & Pototskaya V.A. (eds) *Pototskaya Ekologiya i Morfologiya Nasekomychobyvateley Gribnych Substratov*: 87–100. Nauka, Mocow.

Lawrence J.F. & Newton Jr A.F. 1980. Coleoptera associated with the fruiting bodies of slime molds (Myxomycetes). *The Coleopterists' Bulletin* 34 (2): 129–143.

Lawrence J.F. & Ślipiński A. 2013. *Australian Beetles. Volume 1. Morphology, Classification and Keys*. CSIRO Publishing, Collingwood, Australia. https://doi.org/10.1071/9780643097292

Lawrence J.F., Zhou Y.-L., Lemann C., Sinclair B. & Ślipiński A. 2021. The hind wing of Coleoptera (Insecta): morphology, nomenclature and phylogenetic significance. Part 1. General discussion and Archostemata–Elateroidea. *Annales Zoologici* 71 (3): 421–606. https://doi.org/10.3161/00034541ANZ2021.71.3.001

Leschen R.A.B. 1994. Retreat-building by larval Scaphidiinae (Staphylinidae). *Mola* 4: 3–5.

Leschen R.A.B. & Löbl I. 1995. Phylogeny of Scaphidiinae with redefinition of tribal and generic limits (Coleoptera: Staphylinidae). *Revue suisse de Zoologie* 102 (2): 425–474. https://doi.org/10.5962/bhl.part.80472

Leschen R.A.B. & Löbl I. 2005. Phylogeny and classification of Scaphisomatini Staphylinidae: Scaphidiinae with notes on mycophagy, termitophily, and functional morphology. *Coleopterists Society Monographs* 3: 1–63. https://doi.org/10.1649/0010-065X(2005)059[0001:PACOSS]2.0.CO;2

Leschen R.A.B., Löbl I. & Stephan K. 1990. Review of the Ozark Highland *Scaphisoma* (Coleoptera: Scaphidiidae). *The Coleopterists' Bulletin* 44 (3): 274–294.

Löbl I. 1984. Les Scaphidiidae (Coleoptera) du nord-est de l'Inde et du Bhoutan I. *Revue suisse de Zoologie* 91(1): 57–107. https://doi.org/10.5962/bhl.part.81869

Löbl I. 1999. A review of the Scaphidiinae (Coleoptera: Staphylinidae) of the People's Republic of China, I. *Revue suisse de Zoologie* 106 (3): 691–744. https://doi.org/10.5962/bhl.part.80102

Löbl I. 2015. On the Scaphidiinae (Coleoptera: Staphylinidae) of the Lesser Sunda Islands. *Revue suisse de Zoologie* 122 (1): 75–120. Available from https://www.biodiversitylibrary.org/page/59078840 [accessed 5 Aug. 2022].

Löbl I. 2018a. *Coleoptera: Staphylinidae: Scaphidiinae*. World Catalogue of Insects, Vol. 16. Brill, Leiden, the Netherlands. https://doi.org/10.1163/9789004375956

Löbl I. 2018b. A review of Scaphisomatini from Sulawesi, with descriptions of ten new species (Coleoptera: Staphylinidae: Scaphidiinae). *Acta Entomologica Musei Nationalis Pragae* 58 (1): 151–165. https://doi.org/10.2478/aemnp-2018-0013

Löbl I. 2020. On the Scaphisomatini of Madagascar, and commentary on new trends in museums hampering taxonomic research. *Koleopterologische Rundschau* 90: 89–126.

Löbl I. & Leschen R.A.B. 2003. Scaphidiinae (Insecta: Coleoptera: Staphylinidae). *Fauna of New Zealand* 48: 1–94.

Löbl I. & Ogawa R. 2016. On the Scaphisomatini (Coleoptera, Staphylinidae, Scaphidiinae) of the Philippines, IV: the genera *Sapitia* Achard and *Scaphisoma* Leach. *Linzer biologische Beiträge* 48 (2): 1339–1492.

Löbl I., Leschen R.A.B & Warner W.B. 2021. Scaphisomatini of Arizona (Coleoptera, Staphylinidae, Scaphidiinae) collected by V-Flight Intercept traps. *Revue suisse de Zoologie* 128 (1): 173–185. https://doi.org/10.35929/RSZ.0043

Márquez J. 2007. Preliminary analysis of the colour variation in *Cyparium terminale* from Mexico, with comments on *C. palliatum*, and a new record for *C. yapalli* (Coleoptera: Staphylinidae, Scaphidiinae). *Entomological News* 118 (1): 1–10. https://doi.org/10.3157/0013-872X(2007)118[1:PAOTCV]2.0.CO;2

Matthews A. 1888. Fam. Scaphidiidae. *In*: *Biologia Centrali-Americana. Insecta, Coleoptera. Vol. 2, Part 1*: 158–181. [1887–1888]. Taylor & Francis, London. https://doi.org/10.5962/bhl.title.730

McKenna D.D., Farrell B.D., Caterino M.S., Farnum C.W., Hawks D.C., Maddison D.R., Seago A.E., Short A.E.Z., Newton A.F. & Thayer M.K. 2014. Phylogeny and evolution of Staphyliniformia and Scarabaeiformia: forest litter as a stepping stone for diversification of nonphytophagous beetles. *Systematic Entomology* 40 (1): 35–60. https://doi.org/10.1111/syen.12093

Naomi S. 1988a. Comparative morphology of the Staphylinidae and the allied groups (Coleoptera, Staphylinoidea): III. Antennae, labrum and mandibles. *Japanese Journal of Entomology* 56 (1): 67–77.

Naomi S. 1988b. Comparative morphology of the Staphylinidae and the allied groups (Coleoptera, Staphylinoidea): IV. Maxillae and labium. *Japanese Journal of Entomology* 56 (2): 241–250.

Naomi S. 1989a. Comparative morphology of the Staphylinidae and the allied groups (Coleoptera, Staphylinoidea): VII. Metendosternite and wings. *Japanese Journal of Entomology* 57 (1): 82–90.

Naomi S. 1989b. Comparative morphology of the Staphylinidae and the allied groups (Coleoptera, Staphylinoidea): X. Eighth and 10th segments of abdomen. *Japanese Journal of Entomology* 57 (4): 720–733.

Naomi S. 1990. Comparative morphology of the Staphylinidae and the allied groups (Coleoptera, Staphylinoidea): XI. Abdominal glands, male genitalia and female spermatheca. *Japanese Journal of Entomology* 58 (1): 16–23.

Newton A.F. Jr. 1984. Mycophagy in Staphylinoidea (Coleoptera). *In*: Wheeler Q. & Blackwell M. (eds) *Fungus/Insect Relationships. Perspectives in Ecology and Evolution*: 302–353. Columbia University Press, New York.

Newton A.F., Thayer M.K., Ashe J.S. & Chandler D.S. 2001. 22. Staphylinidae Latreille, 1802. *In*: Arnett R.H. Jr. & Thomas M.C. (eds) *American Beetles. Volume 1: Archostemata, Myxophaga, Adephaga, Polyphaga: Staphyliformia*: 272–418. CRC Press, Boca Raton, London, New York, Washington D.C.

Oberthür R. 1883. Scaphidiides nouveaux. *In*: *Coleopterorum Novitates. Recueil spécialement consacré à l'étude des coléoptères, Rennes* 1: 1–80. Available from https://www.biodiversitylibrary.org/page/60945290 [accessed 5 Aug. 2022].

Ogawa R. & Löbl I. 2013. A revision of the genus *Baeocera* in Japan, with a new genus of the tribe Scaphisomatini (Coleoptera, Staphylinidae, Scaphidiinae). *Zootaxa* 3652 (3): 301–326. https://doi.org/10.11646/zootaxa.3652.3.1

Ogawa R. & Löbl I. 2016. A review of the genus *Xotidium* Löbl, 1992 (Coleoptera, Staphylinidae, Scaphidiinae), with descriptions of five new species. *Deutsche entomologische Zeitschrift* 63 (1): 155–169. https://doi.org/10.3897/dez.63.8386

Ogawa R. & Sakai M. 2011. A review of the genus *Cyparium* Erichson (Coleoptera, Staphylinidae, Scaphidiinae) of Japan. *Japanese Journal of Systematic Entomology* 17: 129–136.

Ogawa R., Löbl I. & Maeto K. 2016. A new species of the genus *Cyparium* from northern Sulawesi, Indonesia (Coleoptera: Staphylinidae: Scaphidiinae). *Acta Entomologica Musei Nationalis Pragae* 56 (1): 195–201.

Omar M.B., Bolland L. & Heather W.A. 1979. A permanent mounting medium for fungi. *Bulletin of the British Mycological Society* 13 (1): 13–32. https://doi.org/10.1016/s0007-1528(79)80038-3

Papavero N. 1971. *Essays on the History of Neotropical Dipterology, with Special Reference to Collectors (1750–1905). Volume 1*. Museu de Zoologia, Universidade de São Paulo. https://doi.org/10.5962/bhl.title.101715

Pic M. 1916. Diagnoses spécifiques. *Mélanges exotico-entomologiques* 17: 8–20.

Pic M. 1920a. Nouveautés diverses. *Mélanges exotico-entomologiques* 32: 1–28.

Pic M. 1920b. Scaphidiides nouveaux de diverses origines. *Annali del Museo civico di Storia naturale di Genova* (3) 9: 93–97.

Pic M. 1931. Nouveautés diverses. *Mélanges exotico-entomologiques* 57: 1–36.

Pic M. 1947. [without tittle]. *Diversités entomologiques* 1: 1–16. https://doi.org/10.5962/bhl.title.107929

Pic M. 1956. Nouveaux coléoptères exotiques. *Bulletin de la Société entomologique de France* 60 [1955]: 173–175.

Reitter E. 1880. Die Gattungen und Arten der Coleopteren-Familie: Scaphidiidae meiner Sammlung. *Verhandlungen des naturforschenden Vereins in Brünn* 18 [1879]: 35–49.

Stephenson S.L., Wheeler Q.D., McHugh J. V. & Fraissinet P.R. 1994. New North American associations of Coleoptera with Myxomycetes. *Journal of Natural History* 28 (4): 921–936. https://doi.org/10.1080/00222939400770491

Tang L., Le L.Z. & He W.J. 2014. The genus *Scaphidium* in East China (Coleoptera, Staphylinidae, Scaphidiinae). *ZooKeys* 403: 47–96. https://doi.org/10.3897/zookeys.403.7220

von Groll E. & Lopes-Andrade C. 2021. *Scaphisoma pandemum* sp. nov. (Coleoptera: Staphylinidae: Scaphidiinae) from the Atlantic Forest of Southeast Brazil. *Zootaxa* 4999 (2): 143–156. https://doi.org/10.11646/zootaxa.4999.2.4

von Groll E., Aloquio S. & Lopes-Andrade C. 2021. A simple, low-cost device for collecting mushroom-dwelling Scaphidiinae (Coleoptera, Staphylinidae). *Zootaxa* 5071 (2): 296–298. https://doi.org/10.11646/zootaxa.5071.2.9

Zayas F. de 1988. *Entomofauna Cubana. Orden Coleoptera. Separata descripción de nuevas especies.* Editorial Cientifico-Técnica, La Habana.

Manuscript received: 28 December 2021
Manuscript accepted: 18 July 2022
Published on: 24 August 2022
Topic editor: Tony Robillard
Section editor: Max Barclay
Desk editor: Pepe Fernández

Brussels, Belgium; Natural History Museum of Denmark, Copenhagen, Denmark; Naturalis Biodiversity Center, Leiden, the Netherlands; Museo Nacional de Ciencias Naturales-CSIC, Madrid, Spain; Real Jardín Botánico de Madrid CSIC, Spain; Leibniz Institute for the Analysis of Biodiversity Change, Bonn – Hamburg, Germany; National Museum, Prague, Czech Republic.

Supplementary files

Supp. file 1. Holotypus labels. **A**. *Cyparium achardi* sp. nov. **B**. *C. lescheni* sp. nov. **C**. *C. loebli* sp. nov. **D**. *C. newtoni* sp. nov. **E**. *C. pici* sp. nov. https://doi.org/10.5852/ejt.2022.835.1909.7615

Supp. file 2. Female terminalia. **A**. *Cyparium lescheni* sp. nov. **B**. *C. collare* Pic, 1920. https://doi.org/10.5852/ejt.2022.835.1909.7617

Supp. file 3. Morphology of *Cyparium collare* Pic, 1920. https://doi.org/10.5852/ejt.2022.835.1909.7619
Fig 1. A–D. ♂ (SE, Areia Branca, MCN 166402). **A**. Dorsal view. **B**. Ventral view. **C**. Lateral view. **D**. Frontal view. **E–G**. ♂ (SE, Areia Branca, MCN 166403). **E**. Pronotum, dorsal view. **F**. Tergite VIII. **G**. Tergite IX. **H**. Sternite VIII. Scale bars: A–C = 1.0 mm; D, F–H = 0.2 mm; E = 0.5 mm.

Fig. 2. ♂ (SE, Areia Branca, MCN 166403), aedeagi. **A**. Lateral view. **B**. Frontal view. **C**. Dorsal view. Scale bars = 0.2 mm.

Fig. 3. A–F. ♂ (SE, Sta Luzia do Itanhi, MCN 166404). **A**. Dorsal view. **B**. Ventral view. **C**. Lateral view. **D**. Frontal view. **E**. Pronotum, dorsal view. **F**. Ventrite 1. **G**. ♂ (SE, Sta Luzia do Itanhi, MCN 166400), tergite VIII. Scale bars: A–C = 1.0 mm; D, F–G = 0.2 mm; E = 0.5 mm.

Fig. 4. ♂ (SE, Sta Luzia do Itanhi, MCN 166400). **A**. Terminalia. **B**. Tergite IX. **C**. Sternite VIII. **D–F**. Aedeagi. **D**. Lateral view. **E**. Frontal view. **F**. Dorsal view. **G–H**. Internal sac. **G**. Frontal view. **H**. Dorsal view. Scale bars = 0.2 in mm.